Analysis of *Arabidopsis* Histidine Kinase 1 dependent perception of and response to abiotic and biotic factors

Dissertation
der Mathematisch-Naturwissenschaftlichen Fakultät
der Eberhard Karls Universität Tübingen
zur Erlangung des Grades eines
Doktors der Naturwissenschaften
(Dr. rer. nat.)

vorgelegt von
Angela Melanie Fischer
aus Ratingen

Tübingen
2021

Gedruckt mit Genehmigung der Mathematisch-Naturwissenschaftlichen Fakultät der Eberhard Karls Universität Tübingen.

Tag der mündlichen Qualifikation:	27.04.2022
Dekan:	Prof. Dr. Thilo Stehle
1. Berichterstatter:	Prof. Dr. Klaus Harter
2. Berichterstatter:	Prof. Dr. Waltraud Schulze

Table of content

Table of content i

Figure List viii

Table List ix

Abbreviation List x

Summary xii

Zusammenfassung xiii

1 .... Introduction 1

1.1 Abiotic and biotic stress 1

1.1.1 Light signaling 1

1.1.2 ROS signaling and anthocyanin biosynthesis 3

1.1.3 Calcium signaling 5

1.2 Phytohormones 5

1.2.1 Salicylic acid and Jasmonic acid 5

1.2.2 Brassinosteroids 6

1.2.3 Ethylene 7

1.3 Multistep-Phosphorelay System 8

1.4 Serine/Threonine/Tyrosine Phosphorylation 9

1.4.1 Osmotic stress pathway 10

1.4.2 Immune response 12

1.4.3 Lipids 12

1.4.4 The plasma membrane 12

1.4.5 Lipid biosynthesis inhibitors 14

1.4.6 Phosphatidic acid (PA) 14
1.5 *Arabidopsis* Histidine Kinase 1 (AHK1) 15
1.6 AHK1's co-receptor BAK1 is standing at the beginning of many different signaling pathways 16
1.7 Lotus japonicus 17
1.7.1 Nodule formation and nitrogen fixation 17
1.8 Aim of this thesis 19
2Material and Methods 20
2.1 Molecular biology methods 20
2.1.1 Working with competent cells 20
2.1.1.1 Production of chemically competent E. coli cells 20
2.1.1.2 Production of electrically competent E. coli cells 20
2.1.1.3 Production of chemically competent Agrobacterium thumefaciens cells 20
2.1.1.4 Analysis of competence of competent cells 21
2.1.1.5 Transformation of competent cells Transformation of chemically competent E. coli 21
2.1.1.6 Transformation of electrically competent E. coli 21
2.1.1.7 Transformation of chemically competent A. thumefaciens 21
2.1.1.8 Verification of expression in A. thumefaciens 21
2.1.1.9 Storage of bacterial cells 21
2.1.2 Extraction of nucleic acids 22
2.1.2.1 Extraction of plasmid DNA 22
2.1.2.2 Extraction of RNA from A. thaliana 22
2.1.2.3 Extraction of genomic DNA from A. thaliana 23

2.1.2.4 Reverse transcription 23
2.1.2.5 Polymerase chain reaction (PCR) 23
2.1.2.6 Genotyping 23
2.1.2.7 Site-directed mutagenesis 23
2.1.2.8 RT-PCR 24
2.1.2.9 qRT-PCR 24
2.1.2.10 Dephosphorylation of DNA-fragments 24
2.1.2.11 Phosphorylation of DNA-fragments 24
2.1.2.12 Classical cloning 24
2.1.2.13 GatewayTM-Cloning 25
2.1.2.14 Agarose gel electrophoresis 25
2.1.2.15 Extraction of DNA-fragments from agarose gels 25
2.1.2.16 Measurement of DNA and RNA concentrations 25
2.1.2.17 DNA-sequencing 25
2.1.3 Cell-biological methods 26
2.1.3.1 Cultivation of E. coli 26
2.1.3.2 Cultivation of A. thumefaciens 26
2.2 Physiological methods 26
2.2.1 Seed surface sterilization with EtOH 26
2.2.2 Cultivation of *A. thaliana* 26
2.2.3 Cultivation of *A. thaliana* on soil 26
2.2.4 Cultivation of *A. thaliana* on ½ MS-Agar plates 27
2.2.5 Cultivation of *A. thaliana* on filter paper 27
2.2.6 Cultivation of Nicotiana benthamiana 27
2.2.7 Lotus japonicus and *Mesorhizobium loti* resources 27

2.2.7.1 Plant growth and infection of L. japonicus 27
2.2.8 Crossing of *A. thaliana* lines 28
2.2.9 Gravitropism assay 28
2.2.10 Infiltration of *N. benthamiana* 28
2.2.11 Activation with ß-estradiol 28
2.3 Biochemical methods 28
2.3.1 Native extraction of 6xHis-tagged proteins from *E. coli* 28
2.3.2 Purification of 6xHis-tagged proteins under native conditions 29
2.3.3 Cleaning and reusage of Ni-NTA Superflow columns 29
2.3.4 SDS-PAGE 29
2.3.5 Western Blot 29
2.3.6 Coomassie staining 30
2.3.7 Immunoprecipitation of MBP-Fusion Proteins using MBP-Trap_A 30
2.3.8 Amidoblack 10B protein concentration measurement 30
2.3.9 PIP Strip™ membrane-type 31
2.3.10 Immunodetection 31
2.3.11 Ethylene Assay 31
2.3.12 *N. benthamiana* RD29b-promotor-Assay 32
2.3.13 Light-reaction tests 32
2.3.13.1 FR-light–associated high-irradiance responses (HIR persistence) 32
2.3.13.2 HY5, CHS and very low fluence response (VLFR) pre-qPCR treatment 32
2.3.14 Massspectrometry LC-MS-MS 32
2.4 Lipid extraction from leaf tissue 32
2.5 Materials 34
2.5.1 Strains and Plantlines 34

2.6 DNA 36
2.6.1 Vectors....36
2.6.1.1 Vectors, already supplied for this Ph.D. thesis....36
2.6.1.2 Vectors, that were created during this Ph.D. thesis....36
2.7 General chemicals and solutions....36
2.7.1 Chemicals....36
2.7.1.1 Antibiotics....36
2.7.1.2 Hormones and inhibitors....36
2.7.1.3 Elicitors (PAMPs)....37
2.7.1.4 Enzymes and commercial kits....37
2.7.1.5 Ladders....38
2.7.2 Antibodies....38
2.8 Solutions, media, and buffers....38
2.8.1 Media, buffers, and solutions for bacteria....39
2.8.1.1 Growth media....39
2.8.1.2 Media for producing chemically competent cells....39
2.8.2 Media, buffers, and solutions for plant work....39
2.8.2.1 Growth media and Seed sterilization....39
2.8.2.2 Transformation solutions for plants....39
2.8.3 Solutions for RNA work and Polymerase Chain Reaction....40
2.8.4 Buffers and solutions for DNA work....40
2.8.5 Buffers and solution for Proteinwork....40
2.8.5.1 Buffers for native extraction and purification of 6x His-tagged proteins....40
2.8.5.2 Amidoblack B solutions....40
2.8.5.3 Loading buffers....40

2.8.5.3.1 SDS gel and Western blot solutions 41
2.9 Plant Growth Conditions 41
2.10 Machines 42
2.11 Software 42
2.11.1 Webpages 42
2.12 External devices 43
3 .... Results 44
3.1 Physiological analysis of *Arabidopsis* mutants carrying different ahk1 alleles 44
3.1.1 AHK1 and the light signaling pathway 46
3.1.2 HY5 qPCR and Anthocyanin pathway 48
3.1.3 Lighting up the phenotype on an evolutionary basis in dicotyledons 49
3.2 "Fishing" for an AHK1 ligand 53
3.2.1 Ligand identification with the *E. coli* expressed AHK1 ectodomain ($AHK1^{ED}$) 53
3.2.2 Mass spectrometry 54
3.2.3 Approach to identifying a putative AHK1 ligand by an ethylene assay 55
3.2.4 AHK1 dependent promotor-induced Assay 56
4 .... Discussion 61
4.1 Looking for AHK1's main pathway with ahk1 alleles 61
4.2 Ligand fishing 66
4.3 Evaluating assays for delving into putative ligands 69
4.4 Outlook 78
5 .... References 82

6 .... Appendix 121

6.1 Oligonucleotides 122

6.1.1 Genotyping of *A. thaliana* mutant lines 122

6.1.2 Oligonucleotides for the detection of T-DNAs in stably transformed *Arabidopsis thaliana* lines 122

6.2 Vectors provided for this PhD thesis 122

6.2.1 Entry vectors 122

6.2.2 Plant and *E. coli* vectors 122

6.2.3 Vectors which have been generated during the Ph.D. thesis 123

6.2.4 Vector maps 124

7 .... Erklärung 125

8 .... Acknowledgements 126

Figure List

Figure 1-1: *A) The Multistep Phosphorelay System (MSP) in plants which derived from the B) Two Component System (TCS) in bacteria.* 8

Figure 1-2: *Phosphatidic acid (PA) production during the phosphatidylinositol (PI)- cycle.* 13

Figure 1-3: *The structure of Arabidobsis Histidine Kinases (AHK) based on PFAM analysis.* 15

Figure 1-4: *Pathways influenced by AHK1 after 15 min 100 mM mannitol treatment in an unlabeled phosphoproteomic study.* 16

Figure 2-1: *Protein and DNA ladders.* 38

Figure 3-1: *Root length of different ahk1-alleles and double mutant lines of Arabidopsis thaliana.* 44

Figure 3-2: *Hypocotyl length of A. thaliana ahk1 mutant seedlings show a wt-like dose response to different light treatments.* 47

Figure 3-3: *The ahk1 mutants show a reduced sensitivity to FR light.* 49

Figure 3-4: *Highlighting AHK1 gene homologues in Lotus japonicus and nodule formation in the lhk4a mutant.* 51

Figure 3-5: *$AHK1^{ED}$ purification.* 54

Figure 3-6: *Ethylene assay with ahk1-plant lines.* 56

Figure 3-7: *An activator/reporter gene assay suggests a lipid-dependent regulation of gene expression by AHK1 in N. benthamiana cells.* 59

Figure 4-1: *What is left to be explored for AHK1's ligand?* 67

Figure 4-2: *A proposed signaling cascade for ligand binding activation of AHK1.* 77

Figure 8-1: *$AHK1^{ED}$ ligand specification.* 121

Table List

Table 2-1: qRT-PCR Settings. 24

Table 2-2: E. coli and A. thumefaciens strains 34

Amplification of plasmids for cLSM or ROS-Assays in planta. 34

Table 2-3: A. thaliana lines which were used for the Ph.D. thesis. 34

Table 2-4: Antibiotics. 36

Table 2-5: Hormones, elicitors and inhibitors. 36

Table 2-6: Enzymes and commercial biology kits. 37

Table 7-1: Results from the third repetition of ligand fishing with the LC-MS. Performed by Dr. Mark Stahl. 121

Abbreviation List

AHK=*Arabidopsis* HISTIDINE KINASE

AWF= apoplastic washfluid

BAK1=BRI1 ASSOCIATED KINASE1

BIK= BOTRYTIS INDUCED KINASE1

BIN2= BRASSINOSTEROID-INSENSITIVE2

BIR2= BAK1-INTERACTING RECEPTOR-LIKE KINASE2

BL= blue light

BR= brassinosteroid

BRI1= BRASSINOSTEROID INSENSITIVE1

BSU1=BRI1 SUPPRESSOR 1

BZR1=BRASSINAZOLE RESISTENT1

CDS- CDP-DG synthase

COP1=CONSTITUTIVE PHOTOMORPHOGENIC 1

CPK= CALCIUM DEPENDENT PROTEIN KINASE

CRY= CRYPTOCHROME

DAG= diacylglycerol

DGK=DIACYLGLYCEROL KINASE

ER= endoplasmic reticulum

FA= fatty acid

FHY3=FAR-RED ELONGATED HYPOCOTYL 3

flg22= flagellin22

FLS2= FLAGELLIN INSENSITIVE2

FR= far-red light

G-3-P=glycerol-3-phosphate

GA= gibberiline

GPAT=Glycerol phosphate acyl transferase

HY5= ELONGATED HYPOCOTYL 5

IQD= IQ67 DOMAIN

IP3- inositol (1,4,5) triphosphate

NPC= NON-SPECIFIC PHOSPHOLIPASE C

NPH3=NON-PHOTOTROPIC HYPOCOTYL3

MSP= multistep phosphorelay system

MAPK=MITOGEN-ACTIVATED PROTEIN KINASE

PA= phosphatidic acid

PAAT= lysoPA acyl transferase

PE= phosphatidylethanolamin

PEN= extract from *Penicillium chrysogenum*

PHOT=PHOTOTROPIN

PI= phosphatidylinositol

PI4P= PI 4-phosphate

$PI(4,5)P_2$= phosphatidylinositol (4-5) bisphosphate

PITPs= phosphatidylinositol transfer proteins

PIS= PI-synthase

PLA= PHOSPHOLIPASE A

PLC= PHOSPHOLIPASE C

PLD= PHOSPHOLIPASE D

PP2A/C=SERINE/THREONINE PROTEIN PHOSPHATASE 2A/C

PM= plasma membrane

RBOH=*Arabidopsis thaliana* RESPIRATORY BURST OXIDASE HOMOLOG

RLCK=RECEPTOR-LIKE CYTOPLASMIC KINASE

ROS= reactive oxygen species

SA= salicylic acid

SPA= suppressor of phyA-105

TCS= two component system

TF= transcription factor

Wortmannin, U73122, *n*-butanol and R59022- inhibitors of the PA pathway

Summary

The *Arabidopsis thaliana* Histidine Kinase 1 (AHK1) is part of the multistep phosphorelay system and stands at the beginning of a signaling cascade. Phylogenetic analysis showed that AHK1 and also its ecto-domain (ED) is highly conserved in dicot plants, like *A. thaliana* and *Lotus japonicus*. A homology-based structural model revealed that the $AHK1^{ED}$ might comprise a Per-Arnt-Sim (PAS) domain. A PAS-domain is known for binding low molecular weight ligands. It is similar to PAS-like CACHE domains that other AHK's carry, and which is associated with the phytohormone cytokinin. In this study we tried to identify the ligand of AHK1. For identification of the AHK1 ligand, the ED of AHK1 is expressed in *E. coli*, purified and used for ligand-fishing via LC-MS. In addition, we used a microscopic approach in which we expressed transiently full-length AHK1 in plant leaves. The plant leaves were than treated with our candidates or with the inhibitors of our candidates. As shown by a quantitative phosphoproteomics approach, the activation of AHK1 led to the rapid phosphorylation of many proteins. The identified proteins were involved in, for instance, stress and light signaling. Therefore, we pursued to characterize the main pathway of AHK1. We executed phenotypic analyses using *Arabidopsis* seedlings carrying different *ahk1* mutant alleles based on the findings. Hereby we applied different environmental cues e.g. irradiation with light of different intensity and wavelengths, application of different stress conditions, which are linked to proteins differentially phosphorylated by AHK1.

In conclusion, our analysis will help to understand the molecular process underlying the activation of AHK1. Furthermore, we could describe two homologs of AHK1 in *L. japonicus*, which we called LHK4-1 and LHK4-2. In their alleles we could find similarities and differences to *ahk1*. Our phenotypic analysis in *Arabidopsis* could further elucidate the signaling network in which AHK1 is embedded. Our data indicate that AHK1 is involved in lipid signaling but we were not able to identify a lipid as AHK1's signal.

Zusammenfassung

Die *Arabidopsis thaliana* Histidin Kinase 1 (AHK1) ist Teil des Multistep Phosphorelay Systems und sie steht am Anfang einer Signalkaskade. Phylogenetische Analysen der Ektodomäne (ED) von AHK1 zeigten, dass sie hochkonserviert in Dikots, wie *A. thaliana* und *Lotus japonicus* (*L. japonicus*) ist. Ein Homologie-basiertes strukturelles Model zeigte, dass die AHK1^{ED} eine Per-Arnt-Sim (PAS) Domäne beinhalten könnte. Eine PAS Domäne ist bekannt dafür molekular leichte Liganden zu binden. Sie ähnelt strukturell der PAS-ähnlichen CACHE Domäne, die AHK's tragen und mit dem Pflanzenhormon Cytokinin assoziiert. In dieser Studie haben wir versucht den Liganden von AHK1 zu identifizieren. Um den Liganden von AHK1 zu identifizieren, exprimierten wir die ED von AHK1 in *E. coli* purifizierten und nutzten es für Ligandenfischen. Zusätzlich nutzten wir einen mikroskopischen Ansatz, in welchem wir die AHK1 in Gesamtlänge transient in Pflanze exprimierten. Danach wurden die Pflanzenblätter mit unseren Kandidaten, oder den Inhibitoren unserer Kandidaten behandelt. Wie im quantitativen Phosphoproteomik Ansatz gezeigt wurde, führt die Aktivierung von AHK1 zu einer schnellen Phosphorylierung von vielen Proteinen. Die identifizierten Proteine waren z.B. involviert in Stress und Licht Signalwegen. Aufgrund dieser Resultate führten wir phänotypische Analysen mit *Arabidopsis* Samen, die unterschiedliche *ahk1* Allele trugen, durch. Hierbei behandelten wir mit unterschiedlichen umweltlichen Signalen z. B. Bestrahlung mit Licht in unterschiedlichen Intensitäten und Wellenlänge oder durch Anwendung von verschiedenen Stresskonditionen, die verbunden sind mit Proteinen, die von AHK1 unterschiedlich phosphoryliert wurden.

Abschließend kann unsere Analyse helfen, den molekularen Prozess, der die Aktivierung von AHK1 unterliegt, zu verstehen. Des Weiteren konnten wir 2 Homologe von AHK1 in *L. japonicus* identifizieren. Diese nannten wir LHK4-1 und LHK4-2. In ihren Allelen konnten wir Gemeinsamkeiten und Unterschiede zu *ahk1* finden. Unsere phänotypischen Analysen konnten das Signalnetzwerk in welchem AHK1 agiert weiter erläutern. Unsere Daten weisen darauf hin, dass AHK1 im Lipid Signalweg involviert ist, aber wir konnten nicht den Liganden von AHK1 identifizieren.

1 Introduction

Histidine kinases (HK's) are well conserved proteins in prokaryotes like in *Escherichia coli* and in some eukaryotes like plants and yeast (Capra and Laub, 2012; Cheung and Hendrickson, 2008; Janiak-Spens et al., 1999; Pekarova et al., 2016). Standing at the beginning of signaling cascades they serve as receptors in e. g. abiotic and biotic pathways. HK's are standing at the beginning of signaling pathways that react upon abiotic and biotic stressors which have a constant impact on plants (McLean et al., 2019; Osakabe et al., 2013; Tanigawa et al., 2012). Hence, as plants evolved, they adapted to biotic and abiotic conditions through adjusting their metabolism and growth to improve their reaction to the different kinds of stress (Pekarova et al., 2016; Suzuki, 2016). This thesis addresses the question which role the *Arabidopsis* HISTIDINE KINASE 1 (AHK1) plays in response to abiotic and biotic stressors.

1.1 Abiotic and biotic stress

Abiotic stress is defined as non-living factors and biotic stress as living factors that have a negative impact on organisms (Beck et al., 2014; Khare et al., 2020). Abiotic stress are factors like light, drought or humidity. Biotic factors are bacteria, fungi, and other organisms (Beck et al., 2014; Khare et al., 2020). The extend of abiotic and biotic factors are influenced by climate change and/or changes regarding the habitat and growth conditions which makes it necessary to understand how plants react to these stressors.

Abiotic and biotic stress factors influence plant development and growth and can even cause death of a plant if it cannot react to these factors adequately. Therefore, plants had to develop quick responses to those factors. They did this via highly specific perception systems and signaling pathways (Beck et al., 2014; Cortleven et al., 2019; Kollist et al., 2019).

1.1.1 Light signaling

Light can serve as a source of energy for plants or signals in developmental processes such as photomorphogenesis (Han et al., 2020a; Yadav et al., 2020; Zhang et al., 2019; Zoulias et al., 2020). Photomorphogenesis regards the growth and development of plants in light. It affects several stages of the development of the plants. There are several characteristics of *Arabidopsis* grown under light like hypocotyl shortening, de-etiolation of the apical hook, anthocyanin accumulation and cotyledons with more photosynthetic activity (Arsovski et al., 2012; Podolec and Ulm, 2018; Ponnu et al., 2019; Wang et al., 2014). To respond to light adequately, plants evolved the ability to sense it through

specified photoreceptors e.g. for parts of for humans visible and invisible spectrum of light: ultraviolet light (UV-B, ca. 280-315 nm, UV-A, ca.315-400 nm), blue (BL, ca. 420-500 nm), red (R, ca. 600-700 nm) and far red (FR, ca. 700-800 nm) (Han et al., 2020a; Ouzounis et al., 2015; Pattison et al., 2018). Different light receptors sometimes have overlaps in the wavelength they react to different pathways in sensing light which are mediating signal transduction. In *Arabidopsis*, as in other plant species, there is not necessarily one receptor for the perception of one wavelength range. CRYPTOCHROME1 and CRYPTOCHROME2 (CRY) are able to sense blue light (BL), but CRYs can also sense UV-A (Hoffman et al., 1996; Ohgishi et al., 2004; Tissot and Ulm, 2020). The UV-B light receptor is UVR8 (Favory et al., 2009; Kliebenstein et al., 2002), PHOTOTROPIN1 and PHOTOTROPIN 2 (PHOT) are also able to sense BL alike the CRYs (Briggs and Christie, 2002; Lin et al., 1995; Ohgishi et al., 2004). There are five more receptors in *A. thaliana*, PHYTOCHROMEs (PHY), PHYA which responds mainly to FR, but also BL, PHYB-E, which primarily respond to R and FR light (Li et al., 2011). PHYs have an non-active P_r- and an active P_{fr}-state (Mancinelli, 1994). PHYs are synthesized in the P_r-state and absorb R light with a maximum at 665 nm, while in their active P_{fr}-state they absorb FR light with a maximum at 730 nm. This photochemical reaction is reversible and is called photoconversion (Eichenberg et al., 2000; Mancinelli, 1994). After being activated, PHYs relocate from the cytosol to the nucleus to induce cellular responses (Chen et al., 2012; Hisada et al., 2000; Kim et al., 2000; Kircher et al., 1999). A central protein, which suppresses light signaling in the dark, is the RING E3 ligase CONSTITUTIVE MORPHOGENESIS1 (COP1). It does so by interacting with the positive regulator of photomorphogenesis, ELONGATED HYPOCOTYL 5 (HY5), a basic region/leucine zipper motif (bZIP) transcription factor (Ma et al., 2002; Osterlund et al., 2000; Saijo et al., 2003; Seo et al., 2003). COP1 regulates several light-signaling pathways in the nucleus. COP1s responses are also dependent on its interaction partner SUPPRESSOR OF PHYA-105 (SPA) with whom it forms a complex which represses light responses of the cell (Laubinger et al., 2004; Ordonez-Herrera et al., 2015). Hence, COP1 acts as key regulator in dark-light transitions (Sanchez-Barcelo et al., 2016). After blue light perception, activated phytochromes CRY1 and CRY2 inhibit COP1-SPA association directly, thereby stabilizing blue light photoreceptors, transcription factors and causing photomorphogenesis (Hiltbrunner, 2019; Hoecker, 2017; Holtkotte et al., 2017; Laubinger et al., 2004; Leivar et al., 2008; Ordonez-Herrera et al., 2015; Zuo et al., 2011).

Downstream of CRY1 acts BRASSINAZOLE-RESISTANT1, which also links BL with brassinosteroid (BR) signaling. Downstream of PHOT1/2 acts the protein NON-PHOTOTROPIC

HYPOCOTYL3 (NPH3) (Galen et al., 2004; He et al., 2019; Ibanez et al., 2018; Inada et al., 2004; Zhao et al., 2018). CRY1 and CRY2 can bind to PHYTOCHROME INTERACTING FACTORs (PIFs), not only to induce a reaction to blue light signaling alone. For plant growth in shade conditions, CRY1 and CRY2 are reacting to changes in low BL through interacting with PIF4 and PIF5 (Ma et al., 2016; Pedmale et al., 2016; Wang et al., 2017).

Additionally, key players of the light signaling pathway have been shown to connect it to a broad range of other pathways. The two antagonists COP1 and HY5 have been shown to perform in other pathways besides light signaling. HY5 and BZR1 have been shown to induce cotyledon opening in a BR dependent manner. HY5 and COP1 are of functional importance for thermomorphogenesis (Delker et al., 2014; Li and He, 2016; Zhang et al., 2019). In addition, HY5 plays a role in light independent stomatal development (Zoulias et al., 2020). CRYs have been shown to release and synthesize ROS after excitation by blue light, based on the reduction of the flavin adenine dinucleotide (FAD) cofactor *in planta* (Consentino et al., 2015; El-Esawi et al., 2017; Jourdan et al., 2015). Furthermore, HY5 have also been shown to link light signaling to ROS by binding directly to the promotor region of ROS related genes and regulating them (Chen et al., 2013; Krasensky-Wrzaczek and Kangasjärvi, 2018).

1.1.2 ROS signaling and anthocyanin biosynthesis

Anthocyanins are secondary metabolites found in plants and fungi, which belong to the flavonoids. Depending on the pH, they are responsible for the red to blue color of plant organs. They are water soluble phenolic pigments that help the plant to react to abiotic and biotic stress, but also help to attract animals for pollination or seed dispersal (Khalid et al., 2019; Quattrocchio et al., 2006; Thoma et al., 2020). Around 600 anthocyanins have been identified in nature (Liu et al., 2018). CRY1 and CRY2, PHYA, PHYB and UVR8 seem to influence anthocyanin through gene expression adjustment *via* HY5 leading to the synthesis of central metabolic enzymes. Anthocyanins are synthesized in the cytoplasm and the endoplasmic reticulum. In the cytoplasm, anthocyanins are produced from phenylalanine and mainly accumulate in the vacuole (Ahmad et al., 1998; Giliberto et al., 2005; Lin et al., 1998; Thoma et al., 2020). They have a higher antioxidant activity than regular flavonoids, therefore also serving as efficient antioxidants (Ahmed et al., 2014; Chalker-Scott, 1999; Hoballah et al., 2007; Khoo et al., 2017; Liu et al., 2018; Quattrocchio et al., 2006). Anthocyanins protect the plant against high intensity UV (and blue) light (Bieza and Lois, 2001; Li et al., 2014b; Lorenc-Kukula et al., 2005). In most plant species UV light leads to an enhanced accumulation of anthocyanins (Brazaityte et al.,

2015; Goto et al., 2016; Rodriguez et al., 2014; Vastakaite et al., 2015), whilst their production is completely suppressed by COP1 activity. Therefore, COP1 and HY5 are also part of this light dependent pathway (Jiang et al., 2016; Maier et al., 2013). To measure whether a gene is involved in anthocyanin biosynthesis, usually the quantification of the expression of the enzyme CHALCONE SYNTHASE (CHS) is used (Zhou et al., 2013). The CHS is an enzyme which acts in one of the major steps for anthocyanin biosynthesis and is a well characterized reporter gene (Deikman and Hammer, 1995). Due to anthocyanin involvement in abiotic and biotic signaling, a dependency on phytohormones like abscisic acid (ABA) under drought or jasmonate under e.g. cold stress was also shown (Gonzalez-Villagra et al., 2017; Li et al., 2020; Wingler et al., 2020). Under FR light, jasmonic acid (JA) can promote anthocyanin production in a PHYA-dependent manner (Li et al., 2014b).

Reactive oxygen species (ROS) are part of plant signaling during growth and developmental processes and adaptations to environmental cues. One of the most common and stable form of ROS is H_2O_2. ROS are produced upon abiotic and biotic stress in different cellular compartments of plants (Kadota et al., 2014b; Kawasaki et al., 2017; Tian et al., 2018; Waszczak et al., 2018). ROS serve amongst others as second messenger, where they can help the plant cell to adjust to stressors. They are involved in the signaling pathways of programmed cell death (PCD) and the cell cycle (Huang et al., 2019a; Huang et al., 2019b). Apoplastic ROS is mainly produced by NADPH oxidases RESPIRATORY BURST OXIDASE HOMOLOGs (RBOHs) at the cell wall/plasma membrane (PM) interface (Bolwell et al., 2002). Recently, the sensor for apoplastic H_2O_2 has been identified to be the LRR-RK HYDROGEN PEROXIDE INDUCED Ca^{2+} INCREASES 1 (HPCA1) (Wu et al., 2020), although it might not be the only sensor. RBOHD is also known to interact with cytoplasmic AHK5 (Drechsler, unpublished), which also seem to signal upon H_2O_2 perception (Heunemann, 2016). RBOHs link H_2O_2 production to miscellaneous pathways, from phosphatidic acid (PA), calcium (Ca^{2+}) and pH, to phytohormones like BRs (Jasso-Robles et al., 2020; Lv et al., 2018; Ma et al., 2012; Tian et al., 2018; Wu et al., 2020). Upon binding of BR to its receptor BRASSINOSTEROID INSENSITIVE1 (BRI1) cellular levels of H_2O_2 increase. Downstream of BRI1 acts the transcription factor BZR1, which is modified by H_2O_2 leading to BZR1 binding to PIF4 and the AUXIN RESPONSE FACTOR 6 (ARF6) which promotes several BR and ethylene linked processes (Lv et al., 2018; Tian et al., 2018).

1.1.3 Calcium signaling

Calcium (Ca^{2+}) has many functions in the cell. It acts as co-factor for hydrolysis of ATP or phospholipids, is needed upon cell division for the mitotic spindle or in the cell wall where it is stored and released from when needed as second messenger. At the inner leaflet of the plasma membrane (PM) Ca^{2+} can bind to Ca^{2+}-sensors, if different stimuli initiate a rise in cytosolic Ca^{2+} levels. A signaling cascade is activated leading to gene regulation or Ca^{2+} influx/efflux proteins are activated which leads to Ca^{2+} acting as second messenger (Taiz, 2006; Tuteja and Mahajan, 2007). Ca^{2+} can also function as second messenger bound to calmodulin and Ca^{2+}-binding proteins (Li et al., 2017a; Marhavy et al., 2019). Ca^{2+} levels effect many different pathways in the plant. Ca^{2+} signaling also seems to act upstream of SA and JA signaling (Bonaventure et al., 2007; Du et al., 2009; Wasternack and Hause, 2013).

1.2 Phytohormones

1.2.1 Salicylic acid and Jasmonic acid

Salicylic acid (SA) is acting as a phytohormone in plant defense signaling. SA can enhance the tolerance against various biotic and abiotic stress factors, like cold or osmotic stress (An and Mou, 2011b; Mikolajczyk et al., 2000; Ryals et al., 1994; Saleem et al., 2020). Exogenous SA can trigger immune responses in plants (An and Mou, 2011a). SA is a β-hydroxy phenolic acid derivate, synthesized through two pathways, the shikimic acid/iso-chorismate pathway, which produces 90 % of SA in plastids and the cytosol, and the phenylalanine ammonia-lyase pathway, which produces 10 % of SA in the cytosol (Ding and Ding, 2020). The first identified protein binding SA was NONEXPRESSOR of PR GENE1 (NPR1). By now three classes of SA binding proteins with six receptors were identified. Class I consist of NPR1 and 2, class II of NPR3 and 4 and class III of BLADE ON PETIOLE1 (BOP1) and 2 (Backer et al., 2015; Cao et al., 1994). NPR1-4 can bind SA with higher affinity than BOP1 and 2 (Castello et al., 2018; Manohar et al., 2015). In addition to their role as receptors, NPR1 and NPR2 have been demonstrated to positively regulate downstream targets of SA signaling. NPR3 and NPR4 seem to act as their antagonists (Castello et al., 2018; Ding et al., 2018). For NPR1/3/4 the downstream targets are proteins of the TGA family of bZIP transcription factors to whom they directly bind. This regulates SA gene expression in the nucleus (Despres et al., 2000; Zhang et al., 2006; Zhang et al., 1999; Zhou et al., 2000). Not all downstream targets of the pathways after SA binding to its receptors are yet identified (Ding and Ding, 2020; Ding et al., 2018).

SA functions as antagonist of Jasmonate (JA) (Phuong et al., 2020; Robert-Seilaniantz et al., 2011). It was shown, that if insects lay eggs on plants, SA accumulates, thereby inhibiting JA signaling and triggering SAR (Bruessow et al., 2010; Hilfiker et al., 2014).

JA is a phytohormone which bioactive form is JA-Isoleucin (JA-Ile) (Wasternack and Strnad, 2016). It is based upon synthesis from C_{18} fatty acids in plastids and peroxisomes and accumulates upon abiotic and biotic stresses like drought, high light, wounding, necrotrophic pathogens but also during developmental processes (Bali et al., 2018; Salvi et al.; Sharma et al., 2018; Wasternack and Hause, 2013; Wingler et al., 2020). For instance, JA-Ile promotes anthocyanin production under FR light in *Arabidopsis* but also inhibits microbial infections, leading to a decrease of nodulation in *Lotus japonicus* (*L. japonicus*) (Li et al., 2014b; Nakagawa and Kawaguchi, 2006; Wasternack and Hause, 2013). The JA-Ile receptor complex consists of the F-box protein CORONATINE INSENSITIVE 1 (COI1), JASMONATE ZIM DOMAIN (JAZ) proteins and the co-factor inositol pentakisphosphate (Sheard et al., 2010). COI1 has a binding pocket where it recognizes JA-Ile, initiating a signaling pathway. (Blazquez et al., 2020; Sheard et al., 2010). It has been shown that COI also regulates the expression of the *YUCCA9* gene, which is also part of the auxin biosynthesis (Hentrich et al., 2013).

1.2.2 Brassinosteroids

Brassinosteroids (BR) are steroidal phytohormones, their most important receptor is the PM-localized leucine rich repeat receptor kinase (LRR-RK) BRI1. BR binds to BRI1 and its co-receptor BRI1-ASSOCIATED KINASE 1 (BAK1) (Albrecht et al., 2012; Li et al., 2002; Nam and Li, 2002).

BRI1-KINASE INHIBITOR1 (BIK1) usually maintains BRI1 in its inactive form and thereby blocks BAK1 (Wang and Chory, 2006). When BR binds to the BRI1- BAK1 heterodimer, it is leading to inactivation of BIK1 and induction of BR signaling cascade (Li et al., 2002; Oh et al., 2009a; Wang et al., 2008a). BRI1 and BAK1 are deactivated by PROTEIN PHOSPHATASE 2A (PP2A) through dephosphorylation (Guo et al., 2013; He et al., 2002; Kim et al., 2011; Kim et al., 2009; Mora-Garcia et al., 2004; Segonzac et al., 2014b; Tang et al., 2008; Tang et al., 2011; Wang et al., 2016a).

BR signaling regulates plant development, cell elongation and division, growth, photomorphogenesis and other cell processes. It also enables the cell to adjust to abiotic and biotic stress, (Belkhadir and Chory, 2006). It is connected to other phytohormone pathways like ethylene and fast response pathways linked to Ca^{2+} and H_2O_2, to promote specific responses (Divi et al., 2010; Du and Poovaiah,

2005; Kadota et al., 2014b; Planas-Riverola et al., 2019). Ethylene signaling is activated by BR in response to abiotic stress factors (Divi et al., 2010; Shi et al., 2015).

1.2.3 Ethylene

Ethylene is the first identified gaseous plant hormone that is perceived by five receptors in *Arabidopsis thaliana* (*A. thaliana*): ETHYLENE RESPONSE1 (ETR1), ETR2, ETHYLENE RESPONSE SENSOR (ERS1), ERS2, and ETHYLENE INSENSITIVE 4 (EIN4) (Bleecker et al., 1988; Bleecker and Kende, 2000; Chang et al., 1993b; Hua and Meyerowitz, 1998; Hua et al., 1998; Merchante et al., 2013; Pekarova et al., 2016; Sakai et al., 1998b). Through the signal transduction initiated by these receptors it regulates flowering time, fruit ripening, growth, and senescence of flowers and leaves and other developmental processes (Chang et al., 1993a; Giovannoni, 2004; Iqbal et al., 2017; Lutts et al., 1996; Pierik et al., 2006). Abiotic and biotic stress factors influence the production of ethylene. So far salinity, cold, drought, flooding, and some bacteria have been identified to influence ethylene biosynthesis (Lutts et al., 1996; Marhavy et al., 2019; Masood et al., 2012; Nazar et al., 2014). Ethylene is also an essential signaling component during rhizobial symbiosis (Lin et al., 2020). A specific phenotype, the triple response, has been used for screens to identify proteins that are part of the ethylene pathway. The triple response is seen in etiolated seedlings. The triple response phenotype is altered in mutants of proteins that are part of ethylene perception and signaling. In the meantime, it is also possible to measure changed ethylene production in mutants (Felix et al., 1991). This helps to evaluate ethylene responses more accurately and can be used to identify elicitors which trigger ethylene responses. This is useful for identifying a ligand of a protein which regulates the ethylene response in some way.

Ethylene can be synthesized in most parts of the plant. It is derived in three steps from the L-amino acid methionine, or it is derived of L-methionine, 5'-Methylthioadenosine, is recycled via the Yang cycle (Taiz, 2006; Wang et al., 2002). Due to its gaseous nature, ethylene diffuses through membranes into intracellular space and outside the plant to where the plant needs it, elsewise it is transported outside the cell (Taiz, 2006).

The triple response-derived ethylene perception and signaling pathway starts with ligand binding to ER membrane-bound ETR1, ERS1, ETR2, ERS2 and/or EIN4 (Chang et al., 1993b; Grefen et al., 2008; Hua et al., 1998; Sakai et al., 1998a). Thereupon, the Raf-like Ser/Thr kinase CONSTITUTIVE TRIPLE RESPONSE 1 (CTR1) is deactivated. After deactivation of CTR1, ETHYLENE INSENSETIVE2 (EIN2) is phosphorylated and interacts with the receptors at the ER membrane.

Thereafter it transfers into the nucleus where it stabilizes and interacts with the transcription factors EIN3 and EIN3-LIKE1 to activate the ethylene response genes (Alonso et al., 1999; An et al., 2010; Bisson and Groth, 2010; Hall and Bleecker, 2003; Hua and Meyerowitz, 1998; Ju et al., 2012; Kieber et al., 1993; Qiao et al., 2012; Solano et al., 1998; Wen et al., 2012).

ETR1 and ERS1 function as active histidine kinases (Chang et al., 1993a; Desikan et al., 2006a; Pekarova et al., 2016). ETR1 histidine kinase (HK) activity leads to stomatal closure. ETR1 HK activity also can also regulate ethylene responses independent of CTR1 (Desikan et al., 2006b; Hall et al., 2012). After ethylene had bound to ETR1 and ERS1, the receptor autophosphorylates and starts a multistep phosphorelay by transferring the phosphate to an AHP which in return transfers it to ARR's (see chapter 1.3). The same signaling cascade mechanism is activated by AHK's (**Figure 1-1** A)) that bind cytokinin (Hass et al., 2004; Scharein and Groth, 2011; Street et al., 2015). Although kinase activity is controlled by ethylene, the multistep phosphorelay system is not the main ethylene signaling pathway in *Arabidopsis*, at least not with respect to the regulation of the triple response (Pekarova et al., 2016; Wang et al., 2003).

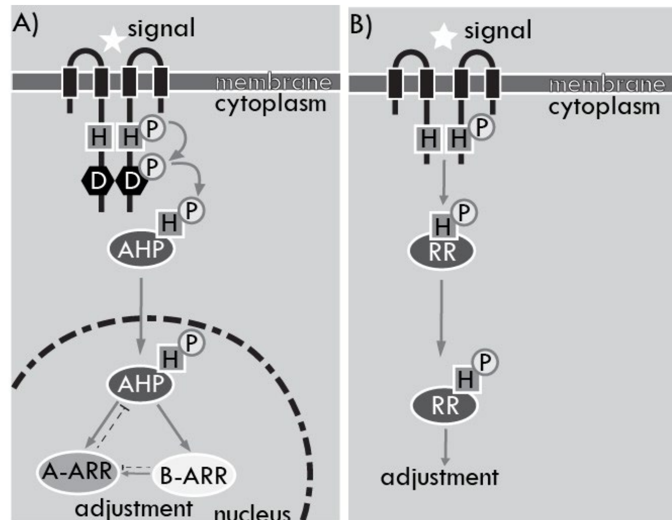

Figure 1-1: A) The Multistep Phosphorelay System (MSP) in plants which derived from the B) Two Component System (TCS) in bacteria.

A) The MSP system in plants evolved from the TCS. It is activated when a signal binds to the ectodomain of a histidine kinase and induces autophosphorylation at a histidine (H) in the cytoplasmic end of an AHK. The phosphate (P) is transferred from the H to the aspartate (D) in the protein. The P thereafter binds to an H of the ARABIDOPSIS HISTIDINE PHOSPHOTRANSFER PROTEIN (AHP), which brings the P to the nucleus and induces cellular adjustment upon binding to type A or type B ARABIDOPSIS RESPONSE REGULATORs (ARRs).

B) The TCS is based on the same principal but less elaborated. Upon signal binding, autophosphorylation at an H is induced and the P is transferred to an H of a RR, which transduces into the nucleus to lead to adjustment upon the signal.

Figure is based on (West and Stock, 2001).

1.3 Multistep-Phosphorelay System

Plant kinases are subdivided by the amino acid that they phosphorylate, although some HK's might also act as phosphatases, like AHK4 (Mahonen et al., 2006) and AHK1 (Hofmann, Müller, Drechsler et al., 2020). In general, AHK's are known to be part of the

multistep phosphorelay system (MSP) (**Figure 1-1** A)), which is in plants a signal transduction pathway that evolved from the bacterial two component system (TCS) (**Figure 1-1** B; the figure is based on (West and Stock, 2001)). The MSP is well described for the perception and signal transduction of the phytohormones CK and ET in plants. The CK MSP pathway will be described in more detail below (Pekarova et al., 2016). The receptors identified for MSP are six AHK's, three of them are CK receptors (AHK2, AHK3 and AHK4) and two (ETR1 and ERS1) of the five ET receptors. AHK's are activated upon ligand binding, they autophosphorylate at a histidine (H) residue by the transfer of a phosphoryl group from ATP (Hanks et al., 1988; Mahonen et al., 2006). After that, the phosphate is transferred to an aspartate (D) of the AHK and passed to *Arabidopsis* histidine phosphotransfer proteins (AHPs). In turn, AHPs (Hutchison and Kieber, 2007; Pekarova et al., 2016; Suzuki et al., 2000) transfer the phosphate to either a type A or type B *Arabidopsis* response regulators (ARRs). Type B-ARR are responsible for the regulation cytokinin response genes and able to bind to type A ARR, which can in return inhibit type B-ARR and act as negative regulators of cytokinin signaling (D'Agostino et al., 2000; Hwang and Sheen, 2001; Mason et al., 2005; Pekarova et al., 2016; To et al., 2004).

The TCS (**Figure 1-1** B)) on the other hand, is the precursor of the MSP. The TCS is found in e.g. bacteria and yeast. It needs a histidine kinase (HK) that associates to a signal, autophosphorylates and activates a response regulator (RR) which initiates a response (Lohrmann and Harter, 2002). Due to this, HK's are activating usually very specifically their RR (Kalantari et al., 2015; Laub and Goulian, 2007). The MSP and the TCS initiate signal transduction responses, but there are additional, even more prominent phosphorylation systems *in planta* (Alberts B, 2002).

1.4 Serine/Threonine/Tyrosine Phosphorylation

Plants can phosphorylate different amino acids. This reversible post translational modification can not only be executed on histidine but also on the amino acids serine (Ser), threonine (Thr) and tyrosine (Tyr) (Huber, 2007; Lohrmann and Harter, 2002; Oh et al., 2011). The amino acids Ser, Thr and Tyr can build O-phosphomonoesters (Klumpp and Krieglstein, 2002; Matthews, 1995). Among these three amino acids Ser and Thr are more common to be phosphorylated than Tyr (Ghelis, 2011). These phosphorylations are more stable than the phosphorylated histidine or aspartate, which makes them easier to study and also the longest studied phosphorylated amino acids (Dautel, 2016; Duclos et al., 1991; Janiak-Spens et al., 1999; Wei and Matthews, 1991).

Alike HK's, in plants Ser/Thr/Tyr phosphorylation often have receptor kinases standing at the beginning of signaling cascades that regulate divers processes, like microtubule organization, stress-, hormone-, Ca^{2+}- or immune signaling (Bender et al., 2017; Clark, 2001; Lee and Ellis, 2007; Monroe-Augustus et al., 2003; Naoi and Hashimoto, 2004). Tyr and Ser/Thr kinases have been identified in *Arabidopsis*. Tyr kinases are e. g. part of ABA signaling and stomatal closure like RAB18. Not much is known about these kinases due to their rather late discovery in the 2000s (Ghelis, 2011; Ghelis et al., 2008).

Signal transduction within Ser/Thr phosphorylation cascades is in general executed by Ser/Thr kinases. Some Ser/Thr kinases are also able to phosphorylate Tyr, like BRI1 and BAK1, who autophosphorylate Tyr (Afzal et al., 2008; Goring and Walker, 2004; Macho et al., 2015; Oh et al., 2012a; Oh et al., 2009b; Oh et al., 2011). BR signaling is an example of the Ser/Thr/Tyr signaling cascade in plants (Ghelis, 2011; Oh et al., 2009b).

Ser/Thr kinases are protein kinases which are able to transfer a phosphate of an ATP to an OH-group of a serine or threonine. Often these kinases are regulated by specific stimuli and stand at the beginning of a signaling cascade. The stimuli can be e.g. phosphorylation or dephosphorylation. Both are posttranslational protein regulation, which can act antagonistically to the same specific stimulus. Downstream of kinases can act protein phosphatases which are further regulating target proteins by dephosphorylating a protein, leading to transducing reversibly the phosphate to other proteins, e.g a TF. When a kinase or a protein is dephosphorylated by Ser/Thr phosphatases, it thereby can be inactivated. (He et al., 2002; Sun et al., 2013a; Tang et al., 2008; Wang et al., 2016a; Wang et al., 2008b).

Ser/Thr/Tyr phosphorylation have also been studied in organisms other than plants. As a result, direct interaction of Ser/Thr kinases with components of the TCS has been first shown in bacteria (Kalantari et al., 2015). With the interaction of CTR1 and EDS1/ETR1 (Ju et al., 2012; Scharein and Groth, 2011) and AHK1 with the Ser/Thr kinase BAK1 (Dautel, 2016), this is also the case in plants.

1.4.1 Osmotic stress pathway

Osmotic stress in plant cells is induced through many abiotic cues such as drought, low humidity, osmotic molecules, such as NaCl. Further, the activation of osmotic stress responses can be induced by oxidative damage, temperature stress, wind, and solar irradiance (Borsani et al., 2001; Gujjar and Supaibulwatana, 2019; Maruyama et al., 2014; Nishiyama et al., 2011; Werner and Finkelstein, 1995; Xiong et al., 2001; Zhao et al., 2020).

Introduction

Different phytohormones are responsible for reacting to osmotic stress. The main hormone is abscisic acid (ABA), although cytokinin, SA, JA, auxin, ethylene and gibberellins (GA) have been demonstrated to be also involved in the osmotic stress responses (Borsani et al., 2001; Jung et al., 2007; Jung et al., 2008; Kranz et al., 1998; Maruyama et al., 2014; Skirycz et al., 2010; Xiong et al., 2001; Yanhui et al., 2006). In addition to the phytohormones, lipid and Ca^{2+}- signaling seem to be part of osmotic signal transduction, although this pathway is not very well investigated yet (Mikolajczyk et al., 2000; Munnik et al., 2000; Takahashi et al., 2001).

Currently, literature indicates an osmotic pathway which acts independently of ABA as well. This signaling pathway seems to be dependent of the SNF1-RELATED KINASE2 s(SnRK2) SnRK2.4 and SnRK2.10 and the PHOSPHOLIPASE C (PLC), PHOSPHOLIPASE D (PLD) and DIACYLGLYCEROL KINASE (DGK) (Klimecka et al., 2020; Maszkowska et al., 2019; Munnik et al., 2000; Munnik and Vermeer, 2010; Soma et al., 2017). Osmotic stress supresses ROS levels in *A. thaliana* and increases PLD levels in barley. The PLD-inhibitor *n*-butanol decreases also ABA and GA levels (Blum et al., 2001; Hong et al., 2008; Meringer et al., 2016; Zhao et al., 2020).

The ABA dependent pathway starts when ABA binds to its receptor family PYRABACTIN RESISTANCE1 (PYR)/PYR-LIKE (PYL)/REGULATORY COMPONENTS of ABA RECEPTORS (RCAR). Binding of the hormone to its receptors deactivates PP2C and activates ABA-responding SnRK2s (Finkelstein et al., 2002; Fujii and Zhu, 2012; Ma et al., 2009). SnRKs activate transcription factors regulating the ABA dependent osmotic response at gene activity level. These TFs belong to the ABSCISIC ACID-RESPONSIVE ELEMENT (ABRE) BINDING PROTEINs (AREBs)/ABRE BINDING FACTOR (ABFs) family (Fujita et al., 2005; Joshi et al., 2016; Yoshida et al., 2015; Yoshida et al., 2010). SnRK2 can also phosphorylate the A-type response regulator ARR5 thereby acting antagonistically to CK signaling in response to drought stress (Zubo and Schaller, 2020). In return the B-type response regulators ARRs1, 11 and 12 can inhibit SnRK2 (Huang et al., 2018).

In yeast, the so-called high-osmolarity glycerol response (HOG) pathway is activated through osmotic stress. The membrane-bound hybrid sensor kinase SLN1, a HK, initiates a TCS phosphorelay upon osmotic stress (Janiak-Spens et al., 1999; Tran et al., 2007). In addition to SLN1, lipids have also been shown to play a role in the reaction of yeast to osmotic stress (Tanigawa et al., 2012). In *Arabidopsis* AHK1 has been suggested to be an ortholog of SLN1 acting in the ABA dependent osmotic pathway (Tran et al., 2007). However, this has been hinted to be treated with caution (Kumar et al., 2013) and disproved (Dautel et al., 2016; Sussmilch et al., 2017; Urao et al., 1999).

1.4.2 Immune response

Plants sense intruders through identifying specific pathogen-associated molecular patterns (PAMPs), which are recognized by pattern recognition receptors (PRRs) of receptor kinases (RK) and receptor-like kinases (RLKs) (Macho and Zipfel, 2014). The text focuses on PAMP triggered immunity (PTI) although effector triggered immunity (ETI) is also part of the innate immune response of plants.

The LEUCINE RICH REPEAT Receptor Kinase (LRR-RK) FLAGELLIN SENSITIVE2 (FLS2) is a PRR located in the plasma membrane. Its ligand, flagellin22 (flg22), a PAMP, acts as "molecular glue" on FLS2 and its co-receptor BAK1, whereupon both proteins are phosphorylated, and a signal transduction cascade is initiated (Chinchilla et al., 2007; Heese et al., 2007; Koller and Bent, 2014; Roux et al., 2011; Schulze et al., 2010; Schwessinger et al., 2011; Sun et al., 2013b). Downstream targets including RBOHD are phosphorylated and ROS production and signaling activated by RBOHD. In the nucleus transcriptional adaptation leads to the induction of immunity-related genes (Kadota et al., 2014a; Macho and Zipfel, 2014; Schwessinger et al., 2011). FLS2 and BRI1 both interact with BAK1. Although BAK1 and FLS2 interaction is linked to flg22 triggered ROS signaling, BL was shown to not trigger ROS production (Albrecht et al., 2012; Gomez-Gomez et al., 2001b; Koller and Bent, 2014; Li et al., 2014a; Sun et al., 2013b).

1.4.3 Lipids

Lipids are alongside carbohydrates, proteins, nucleic acids, and other important macromolecules building blocks for living systems. In lipid bilayers, such as the PM, they form structural units or cell structures due to their partially inner hydrophobic and outer hydrophilic part. The plasma membrane contains different kinds of lipids (phospholipids, glycolipids, sphingolipids, sterols, phosphoinositides etc.) and is suggested to have also a different composition in its outside and inside layers. Inside and outside the lipid bilayer proteins are integrated or attached (Cassim et al., 2019). Lipids were also shown to function as cofactors, electron carriers, anchors for proteins based on their hydrophobic feature and signaling molecules (Best et al., 2019; Cassim et al., 2019; Li et al., 2019) in prokaryotic and eukaryotic organisms (Nelson, 2008; Taiz, 2006).

1.4.4 The plasma membrane

The plasma membrane (PM) separates the cytosol with pH 7.5 from the apoplast with more acidic pH between 5.0 and 6.5. It is a matrix made of lipids and proteins, in *Nicotiana benthamiana* (*N. benthamiana*) in a ratio of 1.3 ± 0,07 (Cacas et al., 2016; Gao et al., 2004; Geilfus, 2017). The membrane consists of

two leaflets made of approx. 30 % phospholipids; the percentage is depending on the plant species and whether it is the inner or outer leaflet. The main phospholipids are phosphatidylcholine (PC) and phosphatidylethanolamine (PE). Phosphatidic acid (PA), PI- phosphatidylinositol (PI), phosphatidylglycerol (PG) and phosphatidylserine (PS) are lesser represented in the PM (Bohn et al., 2001; Cacas et al., 2016; Uemura et al., 1995; Uemura and Steponkus, 1994). In addition to phospholipids, sphingolipids, sterols and phosphoinositides are intrinsic components of the PM. The

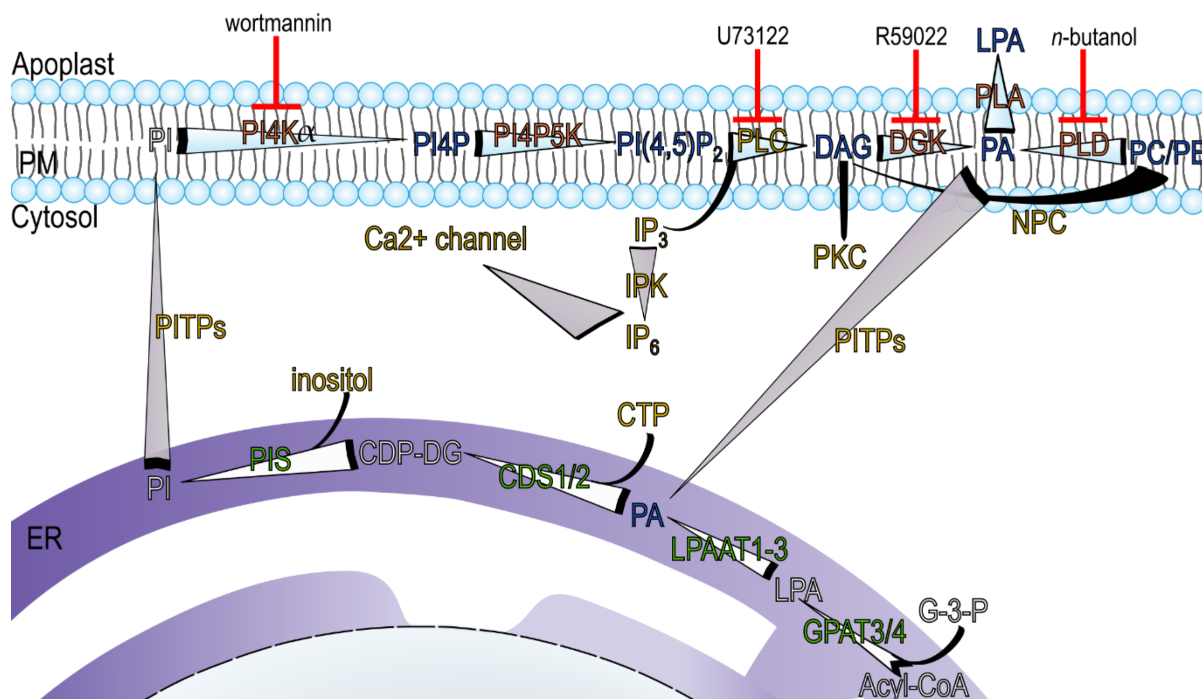

Figure 1-2: Phosphatidic acid (PA) production during the phosphatidylinositol (PI)- cycle.

PA can be synthesized by acylation of the *lyso*-PA by LPAAT mostly, via phosphorylation from DAG by DGK or by hydrolysis of PC by PLD. During this cycle PI is also de novo synthesized: G-3-P is acylated at the ER by GPAT to *lyso*-PA, Lyso-PA is acylated by LPAAT to PA. PA and CTP are catalysed by CDS to form CDP-DG. CDP-DG reacts with inositol, via catalysation from PIS, into PI. PI is a minor phospholipid, that can be transported from the ER to the PM, or the other way around, from PITPs. At the PM PI can be resynthesized, PIK's transform PI to PI(4,5)P_2 in two steps. PI(4,5)P_2 is hydrolysed by PLC into the second messenger IP3, which influences Ca^{2+}-channels and DAG which is further phosphorylated by DGK into PA. It is also possible, that PC or PE are synthesized by PLD into PA at the PM. The PA can then be retransferred via PITP's to the ER where the cycle begins again.

Abbreviations: CDS- CDP-DG synthase; DG- diacylglycerol; ER- endoplasmic reticulum; G-3-P- glycerol-3-phosphate; GPAT- Glycerol phosphate acyl transferase; IP3- inositol (1,4,5) triphosphate; PA- phosphatidic acid; PAAT- LysoPA acyl transferase; PE- phosphatidylethanolamine; PI- phosphatidylinositol; PI4P- PI 4-phosphate; PI(4,5)P_2- phosphatidylinositol (4-5) bisphosphate; PITPs- phosphatidylinositol transfer proteins; PIS- PI-synthase; PLC- phospholipase C; PLD- phospholipase D; PM-plasma membrane. Wortmannin, U73122, n-butanol and R59022- inhibitors of the pathway

lipid composition can change upon stress initiation (Grison et al., 2015; Markham et al., 2006; Wewer et al., 2011; Yu et al., 2018).

1.4.5 Lipid biosynthesis inhibitors

Investigation of lipids and their role in plants are very rudimental. To understand their role in the cell and especially in signaling, inhibitors of their biosynthesis are of importance. There are different inhibitors for the PA biosynthesis available, with different degrees in specificity (**Figure 1-2**) (Cassim et al., 2019).

Wortmannin inhibits PI4Kα but acts rather unspecific, as it inhibits more than one pathway (Walker et al., 2000). Neomycin is an antibiotic, which is an unspecific inhibitor of PA synthesis. It segregates phosphatidylinositol 4,5-diphosphate ($PI(4,5)P_2$), the substrate of phosphatidylinositol phospholipase C (PLC), leading to its inhibition. PLC regulates also inositol triphosphate (IP_3). Upon its inhibition, Ca^{2+} -channels are blocked causing hyperosmotic stress (Schacht, 1978; Takahashi et al., 2001). Another more specific inhibitor of PLC activity are the aminosteroid U73122, which inhibits the activity of some PI-PLCs, the mechanism remains unclear (Klein et al., 2011; Staxen et al., 1999). U73122 is the active form, whereas U73343 the inactive analog of U73122 (Cassim et al., 2019; Staxén et al., 1999). U73122 also inhibits IP_3 production and thereby Ca^{2+} channels (Parre et al., 2007).

n-butanol/1-butanol is a competitive inhibitor of phospholipase D (PLD). As its inactive form its isomer, *sec*-butanol, can be used. (Munnik, 2001; Munnik et al., 1995).

R59022 (DGKI) is a direct inhibitor of DIACYL GLYCEROL KINASEs (DGKs), which is one of the two possible PA biosynthesis pathways besides PHOSPHOLIPASE D (PLD), in the phosphoinositol pathway (Figure 1-2) (Cacas et al., 2017; Gomez-Merino et al., 2004).

1.4.6 Phosphatidic acid (PA)

PA is a phospholipid that acts as a signaling molecule and is part of the PM as a minor compound. Its level rises during plant development, upon wounding and osmotic stress (Li et al., 2006; Testerink and Munnik, 2011; Wang et al., 2006; Wang et al., 2016b).

PA has two biosynthesis pathways (**Figure 1-2**). One is *via* phosphorylating diacylglycerol (DAG), produced by PLC from phosphatidyl inositol (PI), through DIACYLGLYCEROL KINASE (DGK). The other depends on hydrolyzation of PC and PE through PLD (Arisz et al., 2009; Barneda et al., 2019; Pappan et al., 1998). There are seven DGKs and twelve PLDs in *Arabidopsis*, DGK3s and

DGK6s gene expression have been shown to be altered upon BR treatment in wild type plants and their phosphorylation are affected in an *ahk1* mutant when treated with mannitol (Dautel, 2016). DGKs and PLDs gene expression seem to be generally affected by BR according to published data (Dautel, 2016; Gully et al., 2019; Wu et al., 2014).

It is known, that PA is linked closely to Ca^{2+} signaling (Kuppe et al., 2008). It has been shown that PA and Ca^{2+} function together in osmotic stress responses (Blum et al., 2001).

PA is interacting with a number of proteins which are acting in different pathways, like in H_2O_2 signaling through RBOHD/F, ethylene signaling through CTR1, or through SnRK2.1/2.4 in osmotic stress signaling independent of ABA. PA can also bind to CPK1 which is involved in PA- and in Ca^{2+}-signaling (D'Ambrosio et al., 2017; Jakubowicz et al., 2010; Ma et al., 2012; McLoughlin et al., 2013; Testerink et al., 2004; Zhang et al., 2009). In addition, Ca^{2+} is necessary for some PLD activation which in return catalyzes a key step in PA production (Li et al., 2009)

1.5 *Arabidopsis* Histidine Kinase 1 (AHK1)

The *Arabidopsis* Histidine Kinase 1 (AHK1) is one of six histidine kinases in *A. thaliana*. It has two transmembrane domains alike the other AHK's with the exception of soluble AHK5 (**Figure 1-3** A) and B)). In contrast to AHK2, 3 and 4, AHK1 is missing the so-called CHASE- (cyclases/histidine kinases associated sensing extracellular) domain which binds cytokinin (Mougel and Zhulin, 2001;

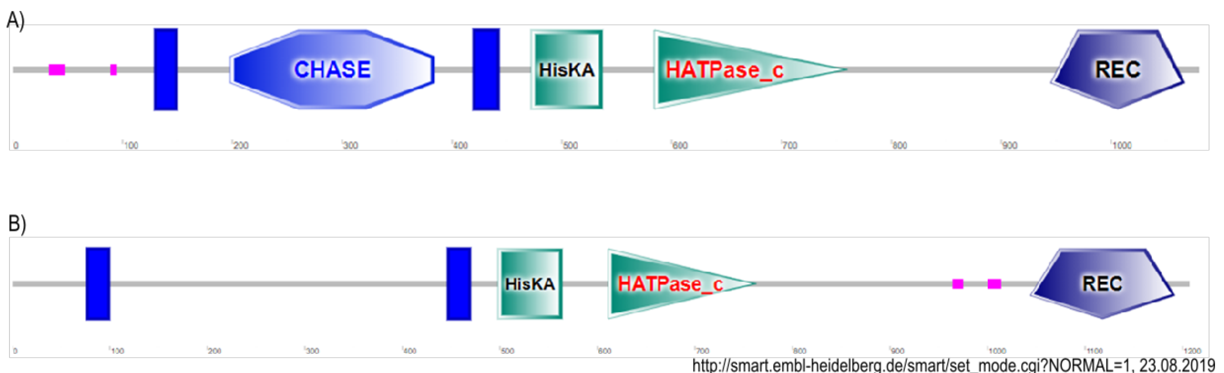

Figure 1-3: The structure of *Arabidobsis* Histidine Kinases (AHK) based on PFAM analysis.

A) AHK4 consists of two transmembrane domains (TD) in a blue rectangle, in between the **cyclases/histidine kinases associated sensing extracellular** (CHASE) domain in blue with a gradient, followed by the Histidine Kinase (HisKA, green square), H-ATPase (green triangle) and Receiver (REC) domain, a purple pentagon. B) AHK1 with almost the same protein domain structure, but without the CHASE-domain. In between the two TD domains a Per-Arnt-Synt (PAS) domain was identified by Dautel, 2016. Source: http://smart.embl-heidelberg.de/smart/set_mode.cgi?NORMAL=1

Pekarova et al., 2016; Upadhyay et al., 2016). In contrast, AHK1 has a regular PAS- domain located in the ectodomain (ED) in between its two transmembrane domains reaching out into the apoplastic space (Dautel, 2016; Upadhyay et al., 2016). (Dautel, 2016). PAS-domains are known to bind small molecules of any kind. The cytoplasmic part of AHK1 has, like every other histidine kinase, a histidine kinase domain, an H-ATPase domain and a receiver domain (**Figure 1-4**) (Dautel, 2016; Pekarova et al., 2016).Similar to other HK's, AHK1 is able to form homodimers as well as to stay monomeric. AHK1 can interact with AHP2 and BAK1 (Hofmann et al., 2020).

A phosphoproteomic analysis after mannitol treatment of *Arabidopsis* seedlings was executed by (Dautel, 2016), which revealed AHK1's influence on many different pathways (**Figure 1-4**). The gene ontology (GO) terms of proteins which were differentially phosphorylated in *ahk1* mutants were analysed. However, many of these differentially phosphorylated proteins have still unknown functions (Dautel, 2016).

AHK1 was shown to react to different stimuli. Up till now AHK1 was shown to react to drought, heat and osmotic stress (Dautel, 2016; de Vries et al., 2020; Kumar et al., 2013). Although AHK1 was proposed to be an osmosensor (Hao et al., 2004; Urao et al., 1999), repetition of these osmotic phenotyping experiments of (Tran et al., 2007; Wohlbach et al., 2008) could not confirm this function (Dautel, unpublished).

Figure 1-4: Pathways influenced by AHK1 after 15 min 100 mM mannitol treatment in an unlabeled phosphoproteomic study.

The 310 proteins with unknown function were labeled as unknown. The size of the word is relative to how often it came up in the study.

Experiment was executed by Dautel, 2016.

Wordcloud rendered with Spyder (Python 3.7).

1.6 AHK1's co-receptor BAK1 is standing at the beginning of many different signaling pathways

BAK1 is an LRR-RK that functions as co-receptor for many ligand-binding LRR kinases including FLS2 and BRI1 (Ladwig et al., 2015; Li et al., 2002). BAK1 has been shown to interact with AHK1 as well (Caesar et al., 2011a; Dautel, 2016). Thus, FLS2 and BRI1 function might be

expected to be directly or indirectly affected by AHK1 (Chinchilla et al., 2007; Dautel, 2016; Nam and Li, 2002).

1.7 *Lotus japonicus*

Most Fabaceae, a plant family with species found globally, are able to form symbiosis with nitrogen fixing bacteria (Doyle and Luckow, 2003). In this symbiosis rhizobial bacteria live inside specialized root organs, so called nodules. While the rhizobia supply the plant with ammonia, fixed from aerial nitrogen, the plant supplies the bacteria with carbohydrates and other nutrients (Canfield et al., 2010). In general, plants access nitrogen through soluble nitrate or ammonium salts that are presented inly in insufficient amounts in the soil, therefore nitrogen can become a growth limiting factor for plants (Masclaux-Daubresse et al., 2010; Zahran, 1999). Most Fabaceae can, in addition to the rhizobial symbiosis, also form arbuscular mycorrhiza with Glomeromycetes fungi, another kind of symbiosis. Glomeromycetes do not provide the plant with nitrogen and ammonia, but with phosphate, other essential nutrients and water (Parniske, 2008). For agriculture legumes are important because of their ability to form these two different symbioses, which makes them able to grow on soil of mediocre nutritional value. They are able to improve the nutritional composition of the soil, as previous-crop and thereby reduce the need of additional fertilization, thus being a good alternative for environmental and ecological reasons (Canfield et al., 2010; Sutton et al., 2011).

Medicago truncatula and *Lotus japonicus* are used as model organisms for legumes, based on their ability to establish the above-mentioned symbioses, having a relatively small genome and being easy to cultivate and transform (Márquez, 2006; Roy et al., 2020). Here we focus on *L. japonicus*. By now, two *Lotus* ecotype genomes are sequenced and annotated (Kamal et al., 2020a; Mun et al., 2016; Sato et al., 2008), and there is a database for retrotransposon mutant lines. Currently CRISPR/Cas9 lines of *Lotus* are also in progress (Fukai et al., 2012; Malolepszy et al., 2016; Roy et al., 2020; Urbanski et al., 2012). Hence, research on *L. japonicus* could lead to improving the understanding of nitrogen fixation and thereby increasing yield (Roy et al., 2020).

1.7.1 Nodule formation and nitrogen fixation

Nodulation is induced when in nitrogen insufficient soil, *L. japonicus* and other legumes spread flavonoids as signaling molecules for their rhizobial symbionts (Peters et al., 1986; Redmond et al., 1986). Rhizobial species, e.g. *Mesorhizobium lotii*, respond to these flavonoids by secreting nodulation (nod) factors. The rhizobial nod factors are perceived directly by the LysM domain of *Lotus* NOD-

FACTOR RECEPTOR1 (NFR1) and NOD-FACTOR RECEPTOR5 (NFR5), which both are localized in the PM (Broghammer et al., 2012a; Madsen et al., 2011; Radutoiu et al., 2007). NFR1 and NFR5 associate with SYMBIOSIS RECEPTOR KINASE (SYMRK) and 3-hydroxy-3-methylglutaryl CoA reductase 1 (HMGR1), to form a complex (Antolín-Llovera et al., 2014; Kevei et al., 2007; Stracke et al., 2002). The recognition of nod factors is acquainted by calcium spiking, induced through CYCLIC NUCLEOTIDE-GATED CHANNEL15 (CNGC15). CNGC15 releases Ca^{2+} from the nuclear envelope activating thereby other Ca^{2+} pumps like *M. truncatula* Ca^{2+} ATPase 8 (MCA8) leading to PLC dependent Ca^{2+} spiking (Charpentier et al., 2016; Engstrom et al., 2002). Ca^{2+} spiking leads to the stimulation of Ca^{2+}/CALMODULIN-DEPENDENT PROTEIN KINASE (CCaMK) which regulates transcription factors such as NODULATION SIGNALING PATHWAY 1 (NSP1), NSP2 and NIN, which in turn initiate the formation of symbiosis (Hayashi et al., 2010; Oldroyd, 2013; Poovaiah et al., 2013; Shimoda et al., 2012). Ca^{2+} spiking is thereafter inhibited by ET, when compatible nod factors were recognized (Denarie and Cullimore, 1993; Roy et al., 2020). The recognition of nod factors by their receptors and rhizobial infection are also negatively regulated by gibberellins (GA) and JA.

After the recognition, infection thread formation starts, allowing the rhizobia to enter the root and start with forming the nodule, a new root organ (Broghammer et al., 2012b; Haney et al., 2011; Liu et al., 2019a; Moling et al., 2014; Truchet et al., 1991). By this means, JA can positively affect early stages of nodulation like infection thread and nodule formation (Suzuki et al., 2011). The formation of the nodule primordium is also positively regulated by cytokinin (CK) and auxin and negatively by ET, JA and GA (Huo et al., 2006; Nizampatnam et al., 2015; Plet et al., 2011; Roy et al., 2017; Wang et al., 2015). During nodule organogenesis, the phytohormones CK and AUX play crucial roles (Lin et al., 2020). Furthermore, BR and its receptor BRI1 seem to be required for the establishment of functional nodules as well (Chen et al., 2014; Cheng et al., 2017; Grunewald et al., 2009; Mortier et al., 2014; Reid et al., 2016). The determinated nodule is finally established through interaction of auxin, strigolactones, CK and JA (Kim et al., 2013).

Beneficial ammonia uptake and the cost of symbiosis formation need to be balanced by the plant. This balancing is achieved in a systemic feedback loop called the Autoregulation of Nodulation (AON) (Kinkema et al., 2006).

1.8 Aim of this thesis

AHK1 was suggested to be an osmosensor in plants (Tran et al., 2007; Urao et al., 1999). It has also been shown, that AHK1 is involved in the response to other environmental cues such as drought stress and heat, which could be linked to osmotic stress, through the initiation of differential gene expression (Dautel, 2016; de Vries et al., 2020; Kumar et al., 2013). AHK1's role in osmotic stress signaling is yet unclear, as it has been shown to act independent of the abscisic acid (ABA) dependent osmotic stress response pathway and its main pathway still needs to be found. Whether it acts instead in an ABA independent, pathway alike inositol 1,4,5-trisphosphate ($InsP_3$) a product of PLC has yet to be investigated (Munnik and Vermeer, 2010; Sussmilch et al., 2017; Takahashi et al., 2001).

However, our studies could not confirm the published results that are also discussed contradictory in the plant community (Dautel, 2016). It could not be shown, that AHK1 is significantly influenced by mannitol or other osmotic compounds. Therefore, I wanted to elucidate the role of AHK1 from its beginning based on available Ser/Thr/Tyr phosphorylation phosphoproteomic datasets provided by Dautel (2016) and to search for AHK1's main signal-response pathway. Furthermore, nothing was known about the implications of the AHK1/BAK1 interaction in the HK's functional output.

To elucidate AHK1's main pathway we tested *ahk1* mutants and *ahk1*/*bak1* double mutants for, compared to wild type (Ws-2 accession), aberrant growth phenotypes under different temperature, phytohormone and light regimes.

Another approach was to elucidate AHK1's putative ligand, which could give a hint on the main signal-response pathway. The aim was to at least narrow down putative ligands to some candidate groups and thereby trying to identify compound families, which might initiate the AHK1 signaling cascade.

2 Material and Methods

2.1 Molecular biology methods

2.1.1 Working with competent cells

2.1.1.1 Production of chemically competent E. coli *cells*

Cells from the *Escherichia coli* (*E. coli*) strains NEB5α and TOP10 were streaked out on a selection-free LB-plate and grown over night at 37 °C. 5mL LB-liquid medium was inoculated with a colony and grown over night at 28°C in an incubator. Two 200 mL SOB-media were inoculated in 2 L flasks with 0,1 mL of the LB-preculture and shook at 25 °C to OD_{600} 0,45 to 0,55. Afterwards the cultures were incubated on ice for 15 min, then centrifugated at 4 °C 2500 g for 10 min. The supernatant was discarded, the pellet resuspended in 4 °C cold 5 mL RF1 and incubated for one hour on ice. Centrifugation was repeated with the same conditions; the pellet was resuspended in 4 °C cold 4 mL RF2 and incubated on ice for 15 min. Aliquots of 50 µl were immediately frozen in liquid nitrogen and stored at -80 °C. Testing of the cells for resistance and competence was executed on the day of production and two weeks later. For the analysis were streaked out on Ampicillin-, Kanamycin-, Spectinomycin- and Gentamycin-selection.

2.1.1.2 Production of electrically competent E. coli *cells*

Cells from a glycerol-stock of CopyCutter Epi4000 were distributed on LB-Streptinomycin-plate and grown over night at 37 °C. A 5 mL LB-liquidculture was inoculated with a colony and grown over night at 37 °C while shaking. 100 mL mainculture were diluted with the over-night preculture to an OD_{600}=0,01. Cells grow until OD_{600} 0,5 was reached. Liquid culture was pelletized by centrifugation at 4 °C with 4000 rpm for 15 min. The cells were washed twice with precooled 80 mL sterile water and once with precooled 40 mL sterile 10 % glycerol. Subsequently the cells were resuspended in 1 mL sterile 10 % glycerol. Aliquots of 100 µL were directly frozen in liquid nitrogen and stored at -80 °C.

2.1.1.3 Production of chemically competent Agrobacterium thumefaciens *cells*

Strain GV3101 was streaked out on LB-media with the antibiotics Rifampicin and Gentamycin as selection using a glycerol stock of the *Agrobacterium thumefaciens* (*A. thumefaciens*). The antibiotics were used in all cultures. The plates were incubated for two days at 28° C. A 5 mL LB-preculture was inoculated with a colony and incubated overnight at 28 °C while shaking. 22,5 mL LB-medium were inoculated with 2,5 mL of preculture and grown overnight at 28 °C while shaking. 250 mL LB-medium was diluted with the 25 mL overnight culture. The main culture was grown up to an OD600 of 0,5 – 0,8. Thereafter, the culture was incubated on ice for 15 min and subsequently pelletized by centrifugation at 4 °C with 4000 g for 5 min. The cell pellet was resuspended in 50 mL of precooled 150 mM CaCl2-solution. The cells were again pelletized by centrifugation at 4 °C with 4000 g for 5 min. The cell pellet was resuspended in 10 mL of precooled 20 mM CaCl2-solution. Aliquots of 100 µL were immediately frozen in liquid nitrogen and stored at -80°C. For the analysis of resistance, it was checked that the cells do not grow on Kanamycin- and Spectinomycin-selection.

2.1.1.4 Analysis of competence of competent cells

For the test of the competence of *E. coli* cells a transformation of 50 µL competent cells was executed with 1 µL of 10 pg/µL pUC19. For the one hour recovering after heatshock at 37 °C just 300 µL LB were used. After the recovering 20 µL, 50 µL and 80 µL of the transformed cells were distributed on LB medium with Ampicillin selection and grown over night at 37 °C. The grown colonies were counted for the calculation of competence. The transformation efficiency (TE) is defined as TE = Colonies/µg DNA/dilution. Therefore, as the number of colonies forming units per 1 µg of plasmid.

2.1.1.5 Transformation of competent cells Transformation of chemically competent E. coli

Chemically competent *E. coli* cell strains (NEB5α, One Shot TOP10, Origami-2 (DE3)) were thawed on ice. 0,1-1 µg of vector-DNA was added and the mixt by flicking against the reaction tube followed by an incubation on ice for 5-30 min. A heat shock of 42°C for 30-50 s was executed, transferred on ice, 1 mL LB-medium was added, and the cells were incubated at 37 °C for 1 h while shaking. The cells were pelletized by centrifugation at 4000 rpm for 4 min, plated on LB-plates with respective antibiotic selection and grown over night at 37°C.

2.1.1.6 Transformation of electrically competent E. coli

Electrically competent *E. coli* cells (CopyCutterTM EPI400TM) were thawed on ice. 0,1-1 µg of DNA was added to the thawn cells and left on ice for 5-30 min. The DNA had to be in water or in very low salt buffer. After the incubation on ice the 100 µL culture was filled into precooled electroporation cuvettes, thereafter electroporated with 1,8 kV. The mixture was then again placed on ice. 1 mL LB-medium was added, and the cells were transferred to a 1,5 mL tube and incubated at 37 °C for 1 h while shaking. The cells were centrifugated at 4000 rpm for 4 min, plated on LB-plates with the respective selection and grown over night at 37 °C.

2.1.1.7 Transformation of chemically competent A. thumefaciens

An aliquot of chemically competent *A. thumefaciens* was thawed on ice. 1-5 µg of vector DNA were added, incubated for 15 min on ice, and for 5 min at 37 °C. Then 1 mL LB-medium was added on ice. The cell culture then was shaken at 28 °C for 2 h. The cells were pelletized with 4000 rpm for 4 min and plated on LB-plates with Rifampicin-, Gentamycin- and the vector-specific selection and then cultivated at 28 °C for 2-3 d.

2.1.1.8 Verification of expression in A. thumefaciens

To verify the correctness of the nucleotide sequence of the respective expression construct transformed in *A. thumefaciens*, a digestion on extracted DNA was executed. Therefore, the plasmids were extracted by an Alkaline Lysis and digested with a restriction enzyme.

2.1.1.9 Storage of bacterial cells

For long-term storage of *E. coli* and *A. thumefaciens* glycerol -stocks were generated. For glycerol-stocks 750 µL of the respective over-night culture were mixed with 750 µL autoclaved glycerol, incubated at room temperature for 5-10 min, frozen in liquid nitrogen and stored at -80 °C.

2.1.2 Extraction of nucleic acids

2.1.2.1 Extraction of plasmid DNA

The Alkaline Lysis was executed according to Sambrook *et al.* 1989. 4 mL LB-medium with an appropriate antibiotic were inoculated with a single *E. coli* colony and incubated over night at 37 °C shaking. The cells were pelletized by centrifugation at room temperature with 6000 rpm for 2 min. The cells were resuspended in 250 µL of Mini I-solution. The lysis was executed with the addition of 250 µL of Mini II-solution and incubation at room temperature for 1 min. The neutralization was obtained with the addition of 300 µL Mini III-solution via inverting. Cell fragments and the drop out were removed by centrifugation at 4 °C with 13000 rpm for 20 min. 750 µL 2-propanol was mixed with 750 µL of the supernatant, the mixture was left for at least 1 h at -20 °C. The vector-DNA was pelletized by centrifugation at 4 °C with 13000 rpm for 20-30 min, washed with 70 % and 100 % ethanol (EtOH) and dissolved in 55 µL sterile and autoclaved water after the EtOH evaporated. For the inactivation of DNases the samples were heated up to 65°C for 10 min.

Midi Preps for plasmid DNA in higher concentrations and of higher purity were executed using the NucleoBond Xtra Midi (50) Kit (Macherey-Nagel) according to the manual.

2.1.2.2 Extraction of RNA from A. thaliana

For the RT-PCR the extraction of RNA from A*rabidopsis thaliana* (*A. thaliana)* was executed using the RNAesy Kit from Qiagen according to the extended manual and with DTT.

For qPCR RNA extraction was performed with Concert Plant RNA Reagent (Invitrogen #12322): 40-100 mg of frozen plant tissue was grinded with 3 times 10 s with Silamat® with glass beads. 500 µL Plant RNA Reagent was added to the grinded tissue and mixed by vortexing and flicking until sample was resuspended. The reaction tube was incubated horizontally for 5 min at room temperature (RT). The mixture was centrifuged for 2 min at 12000 g in a microcentrifuge at RT. Thereafter, the 400-450 µL supernatant was transferred to an RNase-free tube and 100 µL 5 M NaCl was added. Mixing of the clarified extract followed by tapping the tube. 300 µL chloroform was added, sample inverted and centrifuged for 10 min at 4° C an 12000 g for separating the phases. Next, the upper, 400-450 µL aqueous phase was transferred into a new RNase-free tube with 450 µL 2-propanol. After mixing, it stood at RT for 10 min. Subsequently, it was centrifuged at 4 °C, 12000 g for 10 min. Then, the supernatant was discarded by pipetting. 75 % EtOH to the pellet, which was difficult to see. The liquid is centrifuged at RT for 1min at 12000 g. Hereafter, the supernatant was carefully removed off. The RNA dried under a hood for 10-30 min. 87,5 µL RNase-free water was added and the RNA dissolved by pipetting. Here the RNA could be stored at -80 °C., if not, 10 µL DNase buffer and 2,5 µL DNase I was added and incubated for 20 min at RT.

The following RNA clean up and on column DNase digest was performed with the RNeasy Kit (Qiagen) with slight differences: To the RNA with DNase I, 350 µL RLY buffer was added and thoroughly mixed. Thereafter, 250 µL 100 % EtOH was added, the mixture was pipetted up and down for transferring them into a RNeasy Mini spin column (blue) and centrifuged for 15 s at 8000 g. The supernatant was discarded. 80 µL of DNase I incubation mix was pipetted directly on the RNeasy spin column and incubated at RT for 30 min. Afterwards, 350 µL RW1 buffer was added, whereupon the column was centrifuged at 8000 g for 15 s. The supernatant was discarded and 500 µL RPE buffer was pipetted to the column, centrifuged for 2 min at 8000 g. Thereon, the tube was placed upon a new 2 mL reaction tube. The membrane dried through centrifugation at full speed for 2 min. Again,

the column was placed into a new 1,5 mL reaction tube. 40 µL RNase free water was pipetted on the membrane and centrifuged at 8000 g for 1 min. With a platereader, the RNA concentration was specified. The amount of RNA needed for cDNA synthesis was calculated.

2.1.2.3 Extraction of genomic DNA from A. thaliana

A small, in liquid nitrogen, frozen young leave was grinded with the Silamat® S6 through addition of around 100 µL glass beads at 4500 rpm for 10 s. Thereafter, 350 µL Edward's buffer (see 2.8.4) was added, the mixture was left at RT until the frozen material was thawed, whereupon the samples were incubated at 65 °C for 10 min. After centrifugation at 13000 rpm for 15-30 min at 4 °C the liquid phase was transferred into a new reaction tube with an equal volume of 2-propanol and left for at least 30 min at 20 °C. The genomic DNA was pelletized by centrifugation at 13000 rpm for 20-30 min. The pellet was washed with 70 % EtOH and 100 % EtOH and dissolved in 55 µL ddH_2O. For inactivation of DNases the reaction tube was left on 65 °C for 10 min. The genomic DNA was stored at -20 °C.

2.1.2.4 Reverse transcription

For the reverse transcription the protocol of the RevertAidTM H Minus Reverse Transcriptase was followed using total RNA as template RNA and Oligo(dT)18 (ThermoFisher Scientific) as primer. For cDNA synthesis in Freiburg for qPCR-cDNA MultiScribe™ Reverse Transcriptase (ThermoFisher Scientific) was used according to protocol. The reverse transcription program was performed in three steps: 10 min at 25 °C, 120 min at 37 °C and 5 min at 85 °C.

2.1.2.5 Polymerase chain reaction (PCR)

The Polymerase chain reaction (PCR) was used to identify homozygous plants and for amplification of new genes. *Taq* DNA Polymerase from NewEngland Biolabs was used for amplification of genomic DNA PCRs, Phusion® High Fidelity DNA Polymerase from Thermo Scientific was used for amplification of DNA-fragments, needed for cloning.
Taqman ROX Master Mix (2X) from Bioscience was used for quantitative real time PCR. With probes from IDT. The PCRs with the different DNA polymerases were executed according to the respective manual.

2.1.2.6 Genotyping

A. thaliana and *L. japonicus* lines were genotyped. To confirm the T-DNA insertion and transposons being homozygous, PCRs were executed on genomic DNA with *Taq* DNA Polymerase (New England Biolabs) and two pairs of primers. One pair to detect putative wildtype alleles and one to detect the T-DNA insertion or transposon. Amplification of only the wildtype shows wildtype plant, amplification of both primer pairs shows heterozygosity and a homozygous plant just amplifies the T-DNA specific primers. For each genotyping reaction a negative- and positive control was added. The amplicons were detected with agarose gel electrophoresis.

2.1.2.7 Site-directed mutagenesis

For site-directed mutagenesis, specific primers that are modified at the bases to be changed were designed and used. This base pair change should have a new cleavage site, if possible. Two PCR reaction setups, with either forward or reverse primer of 25 µL each were pipetted according to the

manual of *Phusion* DNA Polymerase (ThermoFisher). After 10 cycles both setups were mixed. Additional 30 cycles were performed. Either the template vector was erased from the reaction setup by the addition of 1µL of the restriction endonuclease DpnI, or the amplified sequence was eluated from a DNA gel. DpnI was inactivated at 85°C for 10 min. 5 µL of the reaction setup were then transformed into *E. coli* cells.

2.1.2.8 RT-PCR

RT-PCR was performed with *Phusion* DNA Polymerase (ThermoFisher) and with Ahk1-specific primers over two exons amplifying round about 500 bp (table in appendix 1.27).

2.1.2.9 qRT-PCR

Was performed with Taqman probes mastermix. For the qRT-PCR Reaction performed with Taqman-probes the following protocol was used:

Table 2-1: qRT-PCR Settings.

Step	Degrees (°C)	Time	Repetition
1	50	2 min	1
	95	10 min	
2	95	15 sec	35-45
3	60	1 min	

2.1.2.10 Dephosphorylation of DNA-fragments

The dephosphorylation of DNA-fragments avoids the reattachment of sticky or blunt ends. It reduces that the amplified DNA is ligated back into the former vector. For the dephosphorylation the Shrimp Alkaline Phosphatase (Thermo Scientific) was used according to manual.

2.1.2.11 Phosphorylation of DNA-fragments

The phosphorylation of DNA-fragments facilitates the directed attachment of phosphorylated DNA-fragments with dephosphorylated DNA-fragments in ligations. T4 Polynucleotide Kinase (Thermo Scientific) was used according to manual, for the phosphorylation.

2.1.2.12 Classical cloning

Gene was cleaved out from a former vector, extracted from an agarose gel, de- and phosphorylated, the DNA-fragment was ligated with T4 DNA Ligase (Thermo Scientific) according to manual. DNA-fragment and new vector-backbone were ligated with following ratio of their DNA-amount: 1fragment:4plasmid-backbone.

2.1.2.13 GatewayTM-Cloning

In the GatewayTM system of Thermo Scientific/Invitrogen the gene-of-interest is amplified with specific *att*L attachment sites into the *entry* clone (BP reaction). BP-reactions were executed using the respective expression clone and the *Donor* vector *pDONR207* in the concentration of 150 ng/µL. 0,5 µL of the expression clone, *pDONR207*, TE-buffer pH 8.0 and BP Clonase Enzyme Mix was mixed, incubated for at least 2 h at RT or 16 °C overnight and transformed into *E. coli*.

The entry clone serves as donor of the gene of interest for different *destination* vectors. In d*estination* vectors, the GatewayTM cassette is flanked by *att*R sequences, that recombinates with the *entry* clone (LR-reaction). Destination vectors have different features for protein expression, like different fluorophores. 150 ng *Entry* clone, 150 ng *Destination* vector, TE-buffer pH 8.0 and LR Clonase Enzyme Mix were added to 5 µL. The LR-mix was incubated for at least 1 h at RT. Subsequently, 0,5 µL Proteinase K was added and incubated for 20 min at 37°C. Heat inactivation was performed over 10 min at 75 °C, the LR reaction setup was transformed into *E. coli*.

An *in vitro* recombination between the expression clone and a *Donor* vector with the GatewayTM cassette flanked by *att*P sites (BP-reaction) generates an *entry* clone and a *destination* vector.

2.1.2.14 Agarose gel electrophoresis

Agarose gel electrophoresis was used to separate DNA fragments by size through using an electric field. Therefore, the agarose was heated in 1x TAE buffer. Agarose concentration varied based on the analyzed DNA fragments between 1 - 3 % (w/v). To make DNA visible, Midori green Advanced DNA Stain (Nippon Genetics Europe) was added in a 0,03 % (v/v) concentration. The gel was run in 1x TAE buffer in gel chambers with 50-120 V. DNA loading buffer was used in a 1:5 ratio.

2.1.2.15 Extraction of DNA-fragments from agarose gels

DNA fragments were separated with gelelectrophoresis, so that the wanted DNA-fragments could be cut out and further procedure was executed with the use of the Quick Gel Extraction Kit (invitrogen) and Gel Extraction Kit (genaxxon) according to the manuals.

2.1.2.16 Measurement of DNA and RNA concentrations

DNA was dissolved in ddH_2O and RNA in RNase free ddH_2O. The amount of nucleic acids was measured with a NanoDrop1000 Spectrophotometer (Thermo Scientific). For RNA, the measurement was repeated three times. Also, a platereader was used to determine the amount of RNA. Here, the measurement was repeated twice.

2.1.2.17 DNA-sequencing

The sequencing of DNA fragments and plasmids was executed by GATC Biotech AG and eurofins by sanger sequencing.

2.1.3 Cell-biological methods

2.1.3.1 Cultivation of E. coli

Plasmid transformed *E. coli* were poured and distributed on LB-agar with suitable antibiotics. LB-agar plates were incubated overnight at 37 °C and stored for up to one month at 4 °C.

5 mL liquid cultures of *E. coli* with suitable antibiotic were inoculated with a single *E. coli* colony from LB-agar and grown overnight at 37 °C while shaking. These cultures were used for the extraction of plasmid DNA (Alkaline Lysis) or used further like for production of competent cells or Midi Preps. Cultures of bigger volume were needed here and the 5 mL overnight-culture was used to inoculate the bigger culture. These cultures were grown according to the respective protocols.

CopyCutterTM EPI400TM cells were inoculated in 5 mL LB-medium with suitable antibiotic overnight. 4 mL liquid culture were mixed with 1 mL overnight culture and shaken at 37 °C for 4 h. CopyCutterTM Induction Solution was added in a dilution from 1:1000 (5 µL) to induce plasmid amplification. The culture was used for extraction of plasmid DNA (Alkaline Lysis).

For proteinexpression in Origami-2 (DE3) and BL21 (DE3) cells, 5 mL LB-medium with suitable antibiotic were inoculated with a colony of the transformed cells. It was grown over night shaking at 37 °C. The liquid culture was diluted into the main autoinduction medium culture with suitable antibiotic to an OD_{600}=0,1 or 0,05 for the induction of expression. The culture was cultivated for 72 h shaking at 20 °C and then harvested.

2.1.3.2 Cultivation of A. thumefaciens

A. thumefaciens with rifampicin and gentamycin resistance, was cultivated on LB with suitable antibiotics. For the cultivation on plates, transformed cells were distributed using sterile glass beads. Dilution streaking from glycerol stocks were performed on LB as well. LB plates were left for 2-3 d at 28 °C or at RT. Storage in fridge at 4 °C followed for up to one month. 5 mL liquid culture was inoculated with a single colony and grown overnight at 28 °C while shaking.

2.2 Physiological methods

2.2.1 Seed surface sterilization with EtOH

Around 50 mg of *A. thaliana* seeds were surface sterilized with 1 mL 70 % EtOH solution with 0,01 % triton-x-100 and shaken overhead for 15 min. EtOH was discarded and 250 µL 100 % EtOH was pipetted on the seeds, which were shaken overhead for 2 min. EtOH was discarded and ddH_2O was pipetted the seeds so that they could be transferred on sterile filter paper, dried and used immediately or until 2 days later.

2.2.2 Cultivation of *A. thaliana*

For all physiological experiments seeds from plants which were contemporaneously grown in the greenhouse were used. Seeds were before cultivation stored for 2 d at -20 °C, sterilized and stratified.

2.2.3 Cultivation of *A. thaliana* on soil

To synchronize germination of seeds, sterilized *A. thaliana* seeds were stratified on wet soil at 4 °C for around 24 h. The trays were covered by a hood for the first week. Depending on the purpose the

plants were grown in the greenhouse or phytochambers. Under either continuos light or if not stated otherwise 16 h light/8 h dark conditions.

2.2.4 Cultivation of *A. thaliana* on ½ MS-Agar plates

A. thaliana seeds were sterilized with EtOH and with autoclaved toothpicks isolated on ½ MS-Agar plates with or without supplemented with different substances. Stratification followed at 4 °C for 2-4 d.

2.2.5 Cultivation of *A. thaliana* on filter paper

For light signaling experiments, sterilized *A. thaliana* seeds were distributed on filter paper sucked with 4 mL ddH_2O inside of round petri dishes and stratified for 2 d at 4 °C.

2.2.6 Cultivation of Nicotiana benthamiana

The seeds of *Nicotiana benthamiana (N. benthamiana)* were sown on GS90 soil. Two weeks old seedlings were singularized into pots with GS90 with confidor and grown for additional two to three weeks, at 23 °C/20 °C (day/night), 12 h light and 60 % humidity.

2.2.7 Lotus japonicus and *Mesorhizobium loti* resources

Plants for analysis of infection with *M. loti* were *L. japonicus* ecotype Gifu B-129 wild type, two AHK1 homologues were identified: *LHK4A* (LotjaGi2g1v0379900) and *LHK4B* (LotjaGi4g1v0129800). Of one we cultivated a mutant line *lhk4a-1* (plantline ID: 30010661).

Plants were inoculated using *M. loti* MAFF303099 expressing *DsRED*.

2.2.7.1 Plant growth and infection of L. japonicus

L. japonicus seeds were sterilized using sodium-hypochloride solution with 10 g/l chloride and swallowed in Conserve solution (Producer, City) for at least one hour at RT. Thereafter the seeds were transferred onto a sterile plate with soaked filter paper and stratified for 3 d at 4 °C. After stratification seeds were kept in darkness at 22 °C to germinate for 3 d following the protocol for the ecotype Gifu. Plants were grown on plates, for which seedlings were transferred to 12 cm square plastic petri dishes containing 50 mL quarter-strength Broughton and Dilworth medium (B&D) each (Broughton and Dilworth, 1971). Plants growth condition are 21 °C in light and 17 °C in darkness (16 h light, 8 h dark).

For infection with *Mesorhizobium loti* (*M. loti*), liquid cultures were grown for 2 d at 28 °C in YMB media, subsequently harvested by centrifuging for 10 min at 3000 g. The bacterial pellet was washed twice and resuspended in quarter-strength B&D medium. For inoculations, the optical density at λ=600 was adjusted to 0,01 and 50 µl bacterial suspension were applied to each root. Roots of control plants were mock-treated with 50 µl of sterile medium. Inoculations took place right after transfer to plates.

For measurements of nodulation plates were scanned at 400 dpi resolution respectively one day, 7 d, 10 d, 13 days and 16 d after transfer to plates. Infected plants were grown for 4 weeks. Plants were scanned after 3 weeks and after 4 weeks post inoculation.

For seed reproduction seedlings were transferred to pots containing GS90 soil and grown at 22 °C (16 h light, 8 h dark) at high light and over 70 % humidity conditions.

2.2.8 Crossing of *A. thaliana* lines

A. thaliana lines were cultivated as described until flowering. For crossing of *A. thaliana*, sepals, petals and stamen were removed from the flowers that were slightly opening. The stigma of the carpel was pollinated with pollen of the desired line. All flowers which were not pollinated got removed, the fertilized stigma was put in a small seedbag. The seeds which resulted from this pollination were cultivated and genotyped. Analysis could show if both alleles were present. The plant lines were propagated until homozygous plant lines could be identified.

2.2.9 Gravitropism assay

Sterilized seeds were placed on ½ MS-agar and ½ MS-agar supplemented with enough space left in between seeds. Up to 30 seeds were placed on one plate, that were stratified at 4 °C for 3 d and grown in constant light conditions at 20 °C for 7 d in an upright position. Thereafter, the plates were turned for 135° to the left. After 2 d of additional growth the plates were scanned for analysis. Using ImageJ the growth angle (α) of the root towards the applied gravitropic stimulus in reference to the original direction of gravity was analyzed.

2.2.10 Infiltration of *N. benthamiana*

For infiltration of *N. benthamiana* plants, constructs were transformed into *A. thumefaciens*. Liquid cultures were grown overnight at 28 °C (2.1.2.3). Their OD was measured, the cultures were centrifugated and diluted to an OD of 0,7-0,8 with infiltration medium, that consists of 10 mM MES, 200 nM acetosyringon, 10 mM $MgCl_2$ and ddH_2O. To ease infiltration, *N. benthamiana* plants were watered a few hours before infiltration and left with a hood on the tray. Constructs were always mixed 1:1 with p19 and then infiltrated into young *N. benthamiana* leaves.

Overnight the plants were left with hoods. Afterwards the protein expression was inducted with ß-estradiol (see 2.2.11).

2.2.11 Activation with ß-estradiol

20 µM ß-estradiol was mixed in water with 0,1 % triton-x-100, The mix was applied on the lower half of the *N. benthamiana* leaves with a brush until the leave was covered. The stock of 10mM ß-estradiol was dissolved in EtOH.

2.3 Biochemical methods

2.3.1 Native extraction of 6xHis-tagged proteins from *E. coli*

For native protein extraction, cells from a 150-250 mL culture were harvested via centrifugation at 2000 *g* for 5 min at 4°C in a swing-out centrifuge. Cells were resuspended in NPI-10 (see 2.8.5.1, 10:1 in comparison to cell culture) with freshly added PMSF to 1 mM PMSF. After cell suspension, the liquid was transferred to 2 mL safelock reaction tubes containing autoclaved and well dried 100 µl glass beads (0,25 – 0,5 mm). The reaction tubes were vortexed at 8 °C for 10 min. The cell lysate was centrifuged at 4 °C for 40-70 min at 15000 *g*. The cleared protein liquid was either directly transferred to purification columns, Ni-NTA Superflow Columns, or shock-frosted in liquid nitrogen.

2.3.2 Purification of 6xHis-tagged proteins under native conditions

Ni-NTA columns were equilibrated with 10 mL NPI-10 buffer. Columns work by gravity flow. Thereafter, cleared protein lysate was pipetted onto the columns. Then, two washing steps followed each 10 mL with the NPI-20 buffer. Elution of the purified protein was performed three times by sealing first the purification column and incubating with 1 mL NPI-250 for 30 min, then collecting eluted protein. 5 min for the additional two elution's with 1 mL elution buffer NPI-250 each. For buffers used, see 2.8.5.1.

2.3.3 Cleaning and reusage of Ni-NTA Superflow columns

Ni-NTA columns were cleaned after purification with two 10 mL of 0,5 M NaOH washing steps. The cleaned column was stored upright at 4 °C. The upper part of the column was covered with 5 mL 30 % EtOH to prevent microbial growth. The column was reused for purification of the same protein.

Ni-NTA resin was recharged according to Novex Ni-NTA Purification manual, if the blue resin turned white or yellow after purification. Therefore, columns containing 1,5 mL of Ni-NTA resin, were washed twice with 10 mL of 50 mM EDTA stripping off chelated nickel ions. Next, the column was washed twice with 10 mL 0,5 M NaOH and twice with 10 mL ddH_2O. Recharging was performed by applying twice 10 mL $NiCl_2$ hexahydrate solution (5 mg/mL). Residues of $NiCl_2$ hexahydrate were washed off twice with 10 mL ddH_2O. 5 mL 30 % EtOH was applied onto the column, sealed, and stored at 4 °C.

2.3.4 SDS-PAGE

Proteins were analyzed and separated via SDS-PAGE. It was performed with hand cast gels using the equipment of Hoefer Scientific Instruments.

For the SDS-gel, first a running gel was poured and covered with 100 % isopropanol. After this part was polymerized, the isopropanol removed and cleared with VE-water, a second stacking gel phase was added. Solutions are listed in chapter 2.8.5.3.1.

SDS-gels were wedged to a running chamber, the cavities were filled with SDS running buffer (2.8.5.3), protein samples were loaded into gel-pockets. Additionally, the SpectraTM Multicolor Broad Range Protein Ladder (Thermo Scientific) was added. Gel electrophoresis was executed at 20–25 mA per gel for the stacking gel. When proteins reached the running gel, the amperage was raised to 30-35 mA per gel until the dye front enters the SDS running buffer.

2.3.5 Western Blot

Protein transfer from SDS-GEL onto PVDF membrane (Millipore) was performed using wet blot system. Therefore, PVDF membrane was activated for 1 min in 100 % MeOH prior to usage. Two sponges and Whatman-paper (GE healthcare) were pretreated with SDS running buffer. Sponge, Whatman-paper, gel, PVDF membrane, Whatman-paper and sponge were clapped into a bubble-free sandwich, starting from the lowest. Protein transfer was performed for 90 min at 4 °C at 300 mA per sandwich. A magnetic stir bar was put into SDS running buffer. Alternatively, the transfer was conducted overnight at 30 mA per sandwich at 4 °C.

Thereafter, the PVDF membrane was rinsed with TBS-T and blocked 2 h (RT) to overnight at 4 °C. Washing steps were repeated three times à 10 min each, and were always performed in between the following steps. First or combined first and second antibodies were incubated for 1 to 3 h at RT,

followed by the washing steps with TBS-T. If a second antibody incubation step was necessary it was always executed for 1 h. Whereupon, the membrane was again.

Immunodetection was carried out by incubation of the PVDF membrane in a chemical staining solution (see 2.8.5.3.1) until the bands were clearly visible or with chemiluminescence. Detection was performed with horseradish peroxidase.

2.3.6 Coomassie staining

Coomassie staining were always executed after SDS-PAGE (2.3.4). To confirm that all proteins were transferred to the PVDF membrane or for checking, whether the protein-purification was successful, a SDS-gel was incubated shaking for 1-4 h in Coomassie staining solution, after SDS-PAGE (2.3.4). Next, the staining solution was poured back into the flask for reusage and the destainer solution was poured on the gels. Destaining time varied and destaining was performed while shaking until protein bands were clearly visible. Stained SDS-gels were kept between two cellophane (Roth) foils that were wetted with 10 % glycerol, dried over 2-3 d and scanned.

2.3.7 Immunoprecipitation of MBP-Fusion Proteins using MBP-Trap_A

For immunoprecipitation 25 µL MBP-traps from chromotek were used per sample, MBP-traps were always pipetted using cut tips. Ahead of IP, beads were equilibrated in three steps, by successive change of buffer. First MBP-traps were suspended in 500 µL 100 % MeOH once, then twice with 500 µL 50 % MeOH and finally three times with 500 µL washing buffer. Buffers were ice cold beads were resuspended by pipetting and supernatant was removed carefully after 2 min centrifugation at 4 °C at 2500 g.

Native protein was thawed. 200 µL native-purified protein (MBP or MBP-AHK1^{ED}) was diluted with washing buffer to 500 µL and added to the equilibrated traps. The mixture was left rotating at 4 rpm for 1 h at 4°C. Unspecific bound protein was removed by washing five times with 500 µL washing buffer. Than 300 µL apoplastic washfluid (AWF) with or without mannitol treatment, extracted by Prof. C. Zörb, University of Hohenheim, or 100 µL of 2 mL lipid extracts from *Arabidopsis* plants (extracted from: Ws-2, *ahk1-4*, *bak1-1*, *bri1-5*) was added and further diluted to 500 µL using washing buffer.

The mix was left rotating at 4 rpm for 1 h at 4°C. Afterwards it was again washed five times in 500 µL washing buffer and resuspended in 50 µL glycine at pH 2.5. Then the reaction tubes were heated to 95 °C for 10 min, placed on ice instantly and centrifuged at 4 °C 14,000 rpm for 40 min. The supernatant was sent into LC-MS performed by Dr. M. Stahl. The pellet was kept as a control.

2.3.8 Amidoblack 10B protein concentration measurement

10 µL protein was mixed with 30 µL ddH_2O and 160 µL coloring solution (90 % MeOH, 10 % acetic acid and 0,05 % amidoblack 10B). After 15 min incubation at RT, the mix was centrifuged at maximum speed (22.000 g) for 10 min. The supernatant was discarded, the tube was filled with 200 µL decoloring solution (90 % MeOH, 10 % acetic acid) and vortexed. Next, the reaction tubes were centrifuged at maximum speed for 10 min and the supernatant was discarded. The pellet was dissolved in measuring solution (0,2 M NaOH) and the OD_{600} was specified with a photometer. For comparison, a BSA standard curve from 0,1 mg/mL to 1 mg/mL BSA was used. For each protein-extraction, concentration was measured in three technical replicates.

2.3.9 PIP Strip™ membrane-type

The PIP strip membrane was covered with 5 mL of PBS-T with 0,1 % Tween-20 and 3 % BSA blocking solution. If harsher washing was needed, TBS-T was used instead of PBS-T. The membrane was blocked overnight at 4 °C. Thereafter, at least 0,5 mg of the native protein were added in 5 mL PBS-T 3 % BSA. Incubation was done at RT for 1 h. Subsequently, the membrane was washed three times with 5 mL PBS-T for five to ten minutes. Hereafter, the tag-specific antibody (anti-MBP mouse, monoclonal and anti-GST mouse) was added to the membrane, diluted in PBS-T 3 % BSA. Dilution was done according to the manual. The antibody was incubated for 1 h at RT, following three washing steps with PBS-T for 5-10 min at RT. Then, the second antibody, anti-mouse horseradish peroxidase (HRP), also diluted in PBS-T 3 % BSA, was added to the membrane and incubated for 1 h at RT. After it, the membrane was again washed three times à five to ten minutes in PBS-T.

Subsequently, the washing buffer was discarded, and the interaction detected with chemiluminescence. For buffers see 2.8.5. Every step was performed with gloves so that no lipids could come onto the membrane.

2.3.10 Immunodetection

The proteins which were transferred and immobilized on the PVDF-membrane were detected with specific antibodies. After the western wet blot, the PVDF-membrane with the bound proteins was incubated in blocking solution for at least 1 h at room temperature or overnight at 4 °C. Subsequently to three washing steps with TBS-Tween for 10 min each the first antibody was added and incubated for at least 2 h at room temperature or overnight at 4 °C. The first antibody binds specifically to the protein which should be detected. Excessive antibody was removed in three washing steps with TBS-T for 10 min each. The second antibody which binds onto the first antibody, and which is fused to a tag, generally the Alkaline Phosphatase (AP), was added and incubated for at least 1 h at RT. Excessive antibody was again removed by three washing steps with TBS-Tween for 10 min each. Subsequently to the equilibration of the PVDF-membrane in staining buffer for 5 min the staining with the staining solution was executed. The staining solution contains 5-Bromo-4-chloro-3-indolyl phosphate (BCIP) and nitro blue tetrazolium chloride (NBT) (2.8.5). BCIP is oxidized by the AP to a blue indigo-dye whereas the BCIP oxidation leads to the reduction of NBT and therefore to the generation of a blue formazan-dye. The staining reaction was stopped by washing with MilliQ water as soon as clear bands were visible. For documentation the PVDF-membrane was dried and scanned. Alternatively, to the use of two antibodies just one antibody was applied when it was specifically binding to the tag and already fused to the AP.

2.3.11 Ethylene Assay

For the ethylene assay plants were grown under short-day conditions as described before (see 2.2.1.2). When the *Arabidopsis* plants were around 30 d old, the leaves were cut in small squares (3x3 mm or 2x3 mm), left overnight in a petri dish at RT. Next, three leavediscs were transferred in one glass tube filled with 1 mL ddH_2O, three tubes per plantline per treatment. Then, an elicitor was given to the leavediscs like PEN, flg22 or AWF with or without mannitol. The glass tubes were closed with gum closures and placed on a shaker that shook at 200 rpm for 3 h at RT.

Subsequently, the ethylene levels were measured by gas-chromatography.

2.3.12 *N. benthamiana* RD29b-promotor-Assay

Tobacco plants were co-transformed by infiltration as previously described (2.2.10), using the two plasmids: p35S::AHK1:GFP and pRD29b::NLS:mCherry. Fluorescence intensity of mCherry-NLS was measured by confocal microscopy, using a Leica SP8 microscope and LAS-X software.

Prior of measurement leaves were infiltrated with either water or 80 mM Mannitol. Additionally, *N. benthamiana* leaves were left for 15 min in 0,05 % *n*- and *sec*-butanol and DGKI, 1:1000 neomycin and 1:1000 PAO for 2 h.

2.3.13 Light-reaction tests

Sterilized *Arabidopsis* seeds were sown on filter paper as described (see 2.2.5). Then a white light induction was performed for 8 h at 20 °C, whereupon the petri dishes were transferred into black boxes and left there until the next day, where the seeds were put under their light treatment (red light R, far-red light FR, blue light B, and dark D).

2.3.13.1 FR-light–associated high-irradiance responses (HIR persistence)

Plant seeds were sown on four filter papers with 4 mL ddH_2O in a petri dish. Left for 2 d at 4 °C. Light induction was performed for 8 h at 20 °C, transferred into dark boxes for another 16 h and then left under 2.5 min FR light followed by different lengths of dark turns. Either completely dark, or for 4 min, 8 min, 12 min, or 20 min cycle. Plants were grown for 4 d according to (Buche et al., 2000). Afterwards the hypocotyl length was estimated.

2.3.13.2 HY5, CHS and very low fluence response (VLFR) pre-qPCR treatment

Plant seeds were sown on four filter papers with 4 mL ddH_2O in a petri dish. Left for 2 d at 4 °C. Light induction was performed for 8 h at 20 °C, the petri dishes were transferred into dark boxes for 16 h and 3 d more, thereafter, they were transferred to be treated with FR light. 1 h or 4 h, or none for HY5 and CHS qPCR. For the qPCR on the reportergene for very low fluence rate (VLFR) PRR9 the FR light treatment was 0 min, 40 min, 80 min, 120 min, and 160 min long. The FR light intensity was 15 $\mu mol/m^2*sec$

2.3.14 Massspectrometry LC-MS-MS

Mass spectrometry was done by Mark Stahl by using LC-MS/MS Synapt G2-Si mass spectrometer and analysed with the program MassLynx MS-software.

2.4 Lipid extraction from leaf tissue

Dry weights of 5 to 30 mg of *Arabidopsis* leaves lead to get the best results. Up to six *Arabidopsis* leaves were immersed in 3 mL 0,01 % butylated hydroxytoluene (BHT) in isopropanol preheated to 75 °C for 15-30 min. Therefore, a glass tube with a metal screw cap was used. 1,5 mL chloroform and 0,6 mL ddH_2O were added separately, the liquid was vortexed and shaken on an incubator at RT for 1 h. 4 mL chloroform/methanol (MeOH) (2:1) with 0,01 % BHT were added and shaken for 30 min- overnight. This extraction-step was repeated on all samples until the leaves became white. For this, up to three extractions were necessary.

Subsequently, 1 mL 1 M KCl was pipetted to the extracts, the liquids were vortexed, and centrifuged at 3000 rpm for 5 min at RT, the upper phase was discarded. 2 mL water were added, shaken and

centrifuged again. The upper phase was discarded again carefully, so there was no rest of water. The purification with water was repeated several times.

For evaporation of the organic phase tubes were opened in the fume hood and flushed with gaseous nitrogen until the liquid was evaporated. If too much water was left in the chloroform-MeOH mix, the evaporation process took a lot longer. The glass tubes with dried out lipid extracts were stored in a freezer at -20 °C. When needed the solvent was resolved in MeOH.

The extracted leaves were dried overnight at 105 °C and weighed afterwards.

2.5 Materials

2.5.1 Strains and Plantlines

Table 2-2: E. coli and A. thumefaciens strains

Strain (company)	Genotype	Function
NEB®5α (New England Biolabs)	*fhuA2 Δ(argF-lacZ) U169 phoA glnV44 Φ80 Δ(lacZ)M15 gyrA96 recA1 relA1 endA1 thi-1 hsdR17*	Cloning and amplification of vectors
One Shot®TOP10 (invitrogen)	*F- mcrA Δ(mrr-hsdRMS-mcrBC) Φ80ΔlacM15 ΔlacX74 nupG recA1 araD139 Δ(ara-leu)7697 galE15 galK16 rpsL (StrR) endA1 λ-*	Cloning and amplification of vectors
CopyCutterTM EPI400TM (Epicentre, USA)	*F- mcrA Δ(mrr-hsdRMS-mcrBC) Φ80dlacZΔM15 ΔlacX74 recA1 endA1 araD139 Δ(ara, leu)7697 galU galK λ- rpsL (StrR) nupG trfA tonA pcnB4 dhfr*	Cloning and amplification of coding sequences which are toxic to *E. coli*
Origami-2 (DE3) (Merck, D)	*Δ(ara-leu)7697 ΔlacX74 ΔphoA PvuII phoR araD139 ahpC galE galK rpsL F' [lac+ lacIq pro] (DE3) gor 522::Tn 10 trxB (StrR, TetR)*	Protein expression
BL21 (DE3) (Merck, D)	*Δ(ara-leu)7697 ΔlacX74 ΔphoA PvuII phoR araD139 ahpC galE galK rpsL F' [lac+ lacIq pro] (DE3) gor 522::Tn 10 trxB (StrR, TetR)*	Protein expression
DB3.1TM (invitrogen)	*F-gyr*A462 *end*A1 Δ(sr1-*rec*A) *mcr*B *mrr hsd*S20(rB–, mB–) *sup*E44 *ara-* 14 *gal*K2 *lac*Y1 *pro*A2*rps*L20(SmR) *xyl*-5 λ– *leu mtl*1	Amplification of *Donor* and *Destination* vectors with *ccdB* cassettes
A. thumefaciens GV3101:pMP90 (Koncz and Schell, 1986)	*Rif*^{R}, pTiC58 Δ*traC,* pMP90, *Gent*^{R},	*Amplification of plasmids for cLSM or ROS-Assays in planta*

Table 2-3: A. thaliana lines which were used for the Ph.D. thesis.

Plantline (NASC)	Ecotype	Description	Source
Nos-0	Nos-0	Wildtype (WT)	Paul Verslues
ahk1-1	Nos-0	Kumar *et al.* (2013)	Paul Verslues

Ws-2	Ws-2	WT	Katharina Caesar
ahk1-3	Ws-2	Wohlbach *et al.* (2008)	Katharina Caesar
ahk1-4	Ws-2	Wohlbach *et al.* (2008)	Katharina Caesar
ahk1-3/35S::AHK1-GFP	Ws-2	*pH7FWG2-AHK1* (vector #1168) in *ahk1-3*, homozygous	Katharina Caesar
bri1-5	Ws-2	Noguchi *et al.* (1999)	Peter Huppenberger
bak1-1 (N6125)	Ws-2	Li *et al.* (2002)	NASC
bri1-5 ahk1-3	Ws-2	Homozygus	Rebecca Dautel
bak1-1 ahk1-3	Ws-2	Homozygous	Rebecca Dautel
bak1-1 ahk1-4	Ws-2	Homozygous	Rebecca Dautel
Col-0	Col-0	Wildtype	Paul Verslues
ahk1-5	Col-0	Kumar *et al.* (2013)	Paul Verslues
ahk1-6	Col-0	Kumar *et al.* (2013)	Paul Verslues
AHK1 ox	Col-0	*pUBQ10::AHK1-GFP* (vector #1708)	Katharina Caesar
bri1-201 (N9532)	Col-0	Domagalska *et al.* (2007)	Sacco de Vries
bri1-301	Col-0	Kang *et al.* (2010)	Sacco de Vries

2.6 DNA

2.6.1 Vectors

2.6.1.1 Vectors, already supplied for this Ph.D. thesis

Vectors which were needed but not generated for studies during this Ph.D. thesis, are included in the appendix (1.28), alike their maps (1.28.4).

2.6.1.2 Vectors, that were created during this Ph.D. thesis

Vectors being generated during this Ph.D. thesis are included in the appendix (1237.2.3), alike their maps (7.2.4).

2.7 General chemicals and solutions

2.7.1 Chemicals

Unless otherwise noted, all used chemicals were ordered analytically pure from Sigma-Aldrich (Steinheim, D) and Roth (Karlsruhe, D).

2.7.1.1 Antibiotics

Table 2-4: Antibiotics.

Antibiotic	Selection *E. coli*	Selection *A. thumefaciens*	Selection *A. thaliana*	Solvent	Company
Ampicillin	100 µg/mL	-	-	70 % EtOH	Roth®
Chloramphenicol	30 µg/mL	30 µg/mL	-	EtOH	
Gentamycin	10 µg/mL	40 µg/mL	-	H_2O	Duchefa
Hygromycin	-	-	25 µg/mL	H_2O	Sigma-Aldrich
Kanamycin	50 µg/mL	50 µg/mL	50 µg/mL	H_2O	Roth®
Neomycin	25 µg/mL	40 µg/mL	100 µM	H_2O	
Spectinomycin	50 µg/mL	100 µg/mL	-	H_2O	AppliChem
Streptomycin	25 µg/mL	300 µg/mL	-	H_2O	
Rifampicin	-	100 µg/mL	-	DMSO	Sigma-Aldrich

2.7.1.2 Hormones and inhibitors

Table 2-5: Hormones, elicitors and inhibitors.

Hormone/elicitor/inhibitor	Doseage	Solvent	Impact	Company
Brassinolide	1 nM	EtOH	Brassinosteroid pathway	Sigma-Aldrich
n-butanol	0,1-0,5 %	Max 10 % in H_2O	Alternative substrate for PLD	Thermo Fisher Scientific

sec-butanol	0,1-0,5 %	Max 10 % in H_2O	Negative control to *n*-butanol	Thermo Fisher Scientific
Phenylarsine oxide (PAO)	60 µM	DMSO	PI(4)K inhibitor	
lyso-phosphatidic acid	12.5 µM	Max. **5 mg/mL in H_2O** (with sonification), or 0,5 mg/mL in DMSO	Elicitor	Enzo Life Science
Salicylic acid (SA)	100-300 µM	EtOH	SA pathway	Sigma-Aldrich
β-estradiol	20 µM	EtOH	For induction	Sigma-Aldrich

2.7.1.3 Elicitors (PAMPs)

The pathogen-associated molecular pattern flagellin22 was provided by Farid el Kasmi (ZMBP, Biochemistry).

2.7.1.4 Enzymes and commercial kits

Table 2-6: Enzymes and commercial biology kits.

Enzyme or commercial kit	Company
Taq DNA Polymerase	New England Biolabs
Phusion® High Fidelity DNA Polymerase	Thermo Scientific
T4-DNA-Polymerase	Thermo Scientific
Gateway® LR Clonase enzyme mix	Thermo Scientific
Gateway® BP Clonase enzyme mix	Thermo Scientific
restriction endonucleases	Thermo Scientific and New England Biolabs
Shrimp Alkaline Phosphatase, SAP	Thermo Scientific
T4 Polynucleotide Kinase, PNK	Thermo Scientific
T4 DNA Ligase	Thermo Scientific
RevertAidTM H Minus Reverse Transcriptase	Thermo Scientific
PureLinkTM Quick Gel Extraction Kit	Invitrogen
Gel Extraction Kit	genaxxon
EURx GeneMATRIX Universal RNA Purification Kit	roboklon
NucleoBond Xtra Midi (50)	Macherey-Nagel
Maxima® SYBR Green qPCR Master Mix (2X)	Thermo Scientific

2.7.1.5 *Ladders*

SpectraTM Multicolor Broad Range Protein Ladder (Thermo Scientific) was used for protein work and self-made PstI digested λ-DNA, λ-PstI DNA size marker was used for DNA work (Figure 2-1).

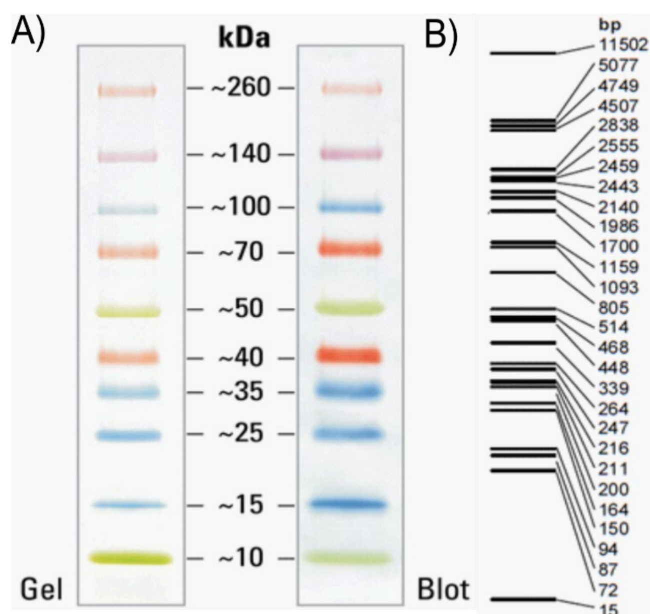

Figure 2-5: Protein and DNA ladders.

A) Proteinladder PageRuler™ Prestained Protein Ladder from Thermofisher and B) lambda-DNA ladder. Source for A): Thermofisher, for B) Ape.

2.7.2 Antibodies

Table 2-7: Antibodies

Antibody	Clonality	Organism	Dilution	Company
α-AHK1	polyclonal	rabbit	1:1.000	Roche
α-MBP	monoclonal	mouse	1:4.000	Sigma
α-mouse-AP	polyclonal	goat	1:5.000	BioRad
α-rat-AP	polyclonal	goat	1:10,000	Sigma
α-rabbit-AP	polyclonal	goat	1:7.000	Bio-Rad
α-His-AP	monoclonal	mouse	1:2.500	antibodies-online
α-mouse-HRP	monoclonal	goat	1:10,000	Sigma

2.8 Solutions, media, and buffers

<u>10X TE-buffer pH 8.0</u>

100 mM Tris/HCl pH 8,0

10 mM EDTA pH 8,0

2.8.1 Media, buffers, and solutions for bacteria

2.8.1.1 Growth media

Luria-Bertani broth (LB)
1,5 % agar for plates
1 % (w/v) Bacto-Peptone
0,5 % (w/v) Yeast extract
1 % (w/v) NaCl

Autoinduction medium
ZY medium
10 g Tryptone (casein)
5 g Yeast extract
to 920 mL with H_2O
Autoclave

25x 5025 (1L)
125 g Glycerol
12.5 g Glucose
50 g Lactose
Autoclave

25x M (1L)
88,8 g Na_2HPO_4
85 g KH_2PO_4
67 g NH_4Cl
40,27 g $Na_2SO_4 \cdot 10xH_2O$
Autoclave

Autoinduction medium
ready to use (1 L)
920 mL ZY medium
40 mL 25x 5025
40 mL 25x M
2 mL 1 M MgSO4

2.8.1.2 Media for producing chemically competent cells

RF1
100 mM RbCl
50 mM $MnCl_2$
30 mM potassium acetate
10 mM $CaCl_2$
15 % (v/v) glycerol
Adjust to pH 5,8 with acetic acid
Sterilize by filtration

RF2
10 mM MOPS
10 mM RbCl
75 mM CaCl2
15 % (v/v) glycerol
Adjust to pH 6,1 – 6,4 with KOH and HCl
Sterilize by filtration

2.8.2 Media, buffers, and solutions for plant work

2.8.2.1 Growth media and Seed sterilization

½ MS-agar
2,15 g/L Murashige and Skoog basal salt mixture (Sigma-Aldrich)
0,039 % (w/v) MES
Adjust to pH 5,7 with KOH
1-1,5 % (w/v) phytoagar (Duchefa)

Hormones were added to autoclaved ½ MS-agar at 60 °C

EtOH seed sterilization solution
70 % (v/v) EtOH
0,01 % (v/v) triton-x-100

2.8.2.2 Transformation solutions for plants

Stable transformation solution for *Arabidopsis*
5 % sucrose
0,01 % Silwet L-77
200 µM Acetosyringon
10 mM MgSO4

Transformation solution for *N. benthamiana*
1 % (v/v) 1 M MES/KOH pH 5,6
0,1 % (v/v) 200 mM Acetosyringon
0,33 % (v/v) 3 M $MgCl_2$

ß-estradiol induction solution
20 µM β-estradiol
0,1 % (v/v) triton-x-100

2.8.3 Solutions for RNA work and Polymerase Chain Reaction

<u>RNA dNTP mix</u>
10 mM dATP
10 mM dGTP
10 mM dCTP
10 mM dTTP
Dissolve in RNase free water

<u>PCR dNTP mix</u>
10 mM dATP
10 mM dGTP
10 mM dCTP
10 mM dTTP
Dissolve in ddH_2O

2.8.4 Buffers and solutions for DNA work

<u>MiniI</u>
50 mM Tris/HCl pH 8,0
10 mM EDTA
Autoclave
Add 20 mg/mL RNase

<u>MiniII</u>
1 % (v/v) SDS
0,2 M NaOH

<u>MiniIII</u>
29,44 % (w/v) KCH_3COO
11,44 % (v/v) acetic acid glacial
Adjust to pH 5,5

<u>Edwards buffer</u>
for genDNA extraction
200 mM Tris/HCl pH7.5
250 mM NaCl
0,5 % (v/v) SDS

<u>50x TAE buffer</u> (2 L)
1,2 L MQ water
484 g TRIS base
Dissolve
37,24 g EDTA
114 mL glacial acetic acid (17,4 M)
Fill up to 2 L with MQwater

2.8.5 Buffers and solution for Proteinwork

2.8.5.1 Buffers for native extraction and purification of 6x His-tagged proteins

<u>NPI-10</u> (500 mL)
50 mM $NaH_2PO_4 \cdot H_2O$
300 mM NaCl
10 mM Imidazole
To 450 mL with MQwater
Adjust to pH 8,0 with NaOH
To 500 mL with MQwater
1 mM PMSF and 300 units Benzonase added immediately before use

<u>NPI-20</u> (500 mL)
50 mM $NaH_2PO_4 \cdot H_2O$
300 mM NaCl
20 mM Imidazole
To 450 mL with MQwater
Adjust to pH 8,0 with NaOH
To 500 mL with MQwater

<u>NPI-250</u>
50 mM $NaH_2PO_4 \cdot H_2O$
300 mM NaCl
250 mM Imidazole
To 450 mL with MQwater
Adjust to pH 8,0 with NaOH
To 500 mL with MQwater

2.8.5.2 Amidoblack B solutions

<u>Coloring solution</u> (20 mL)
90 % Methanol
10 % Acetic acid
0,05 % Amido black 10B

<u>Decoloring solution</u> (20 mL)
90 % Methanol
10 % Acetic acid

<u>Measuring solution</u> (100 mL)
0,2 M NaOH

2.8.5.3 Loading buffers

<u>2x Urea Lyse and Load buffer (denaturating)</u>
50 mM Tris HCl pH 6,8
100 mM DTT
7 M Urea
0,04 % Bromophenol blue
2 % SDS
30 % Glycerol
stored at -20 °C

5x LaemmLi buffer
300 mM Tris Base
10 % SDS
50 % Glycerol
Adjust to pH 6,8
3 % ß-mercaptoethanol 0,05 %
Bromophenol blue

2.8.5.3.1 SDS gel and Western blot solutions

SDS PAGE gels were always poured four at once at 10 % for the running gel
SDS PAGE gels were always poured four at once at 4.5 % for the stacking gel

Bottom buffer mix for running gel
1 M Tris HCl pH 8,0
0,27 % (v/v) SDS

Upper buffer mix for stacking gel
0,25 M Tris HCl pH 6,8
0,2 % (v/v) SDS

30 % acrylamide	ddH_2O	Bottom buffer	10 % APS	TEMED
8 mL	6.8 mL	9 mL	200 µL	16 µL

30 % acrylamide	ddH_2O	Upper buffer	10 % APS	TEMED
1,2 mL	2,8 mL	4 mL	40 µL	8 µL

10x SDS-Running buffer (1 L)
30 g Tris BASE
144 g Glycine
15 g SDS
Adjust to pH 8,3

Coomassie solutions
Staining solution (1 L),
0,05 % (w/v) Bromophenol blue
25 % (v/v) Isopropanol
10 % (v/v) Acetic acid
Fill up to 1 L with MQwater

Destaining solution
10 % Acetic acid
Fill up with MQwater

Transfer buffer (1 L/chamber)
14,3 g Glycine
3,9 g Tris BASE
20 % EtOH
Fill up to 1 L with MQwater

5x TBS buffer
250 mM Tris HCl
50 mM Tris BASE
750 mM NaCl
Adjust to pH 7.5 with HCl
1x TBS was used with 0,2 % Tween-20

10x PBS buffer
1.37 M NaCl
25 mM KCl
100 mM Na_2HPO_4
18 mM KH_2PO_4
Adjust to pH 7.4-7.5
1xPBS was used with 0,1 % Tween-20

Blocking solution
1x PBS/TBS
5 % milkpowder

Staining buffer A
100 mM Tris BASE
100 mM NaCl
10 mM $MgCl_2$

Nitro blue tetrazolium chloride (NBT) solution
5 % (w/v) in 70 % DMF

5-Bromo-4-chloro-3-indolyl phosphate (BCIP) solution
5 % (w/v) in 100 % DMF

Staining solution
99 % Staining buffer A
0,66 % NBT solution
0,33 % BCIP solution

2.9 Plant Growth Conditions

Longday chamber
16 h light – 8 h dark
light tubes: 33 % 6500 K, 550 Lumen, 70-79 Ra
66% 4000 K, 1.350 Lumen, 80-89 Ra
20 °C day – 18 °C night
50 % humidity

Shortday chamber
8 h light – 16 h dark
light tubes: 50% 6500 K, 550 Lumen, 70-79 Ra
50% 4000 K, 1.350 Lumen, 80-89 Ra
21 °C day – 20 °C night
50 % humidity

Longday chamber *N. benthamiana*
12 h light – 12 h dark
light tubes: 50% 6500 K, 550 Lumen, 70-79 Ra
50% 4000 K, 1.350 Lumen, 80-89 Ra
22 °C day – 20 °C night
60 % humidity

Constant light Percival	Greenhouse *A. thaliana*	20 °C day – 18 °C night
24 h light 89µmol m^{-2} s^{-1}	16 h light – 8 h dark	55-60 % humidity
20 °C or 24 °C		

2.10 Machines

Agarose gel-electrophoresis chambers: Peqlab PerfectBlue™ Gelsystem

Beckmann J2-21M induction drive centrifuge

clean benches: Microflow Biological Safety cabinet, ASTEC

cLSM TCS SP8, Leica Microsystems GmbH

Eppendorf Centrifuges 5417R, 5417C, 5810R

incubators: HettCube 600 R, Hettrich; Inova 44, Eppendorf

Labnet Power Station 300 Plus

Mini Trans-Blot Electrophoretic Transfer Cell, BioRad

NanoDrop photometer ND-1000, NanoDrop products

PCR-Thermocycler PeqStar96 Universal gradient, Peqlab

Platereaders: Berthold Tech TriStar2S, BertholdTech

PowerPac™ High-Current Power Supply, BioRad

qPCR-machines: ABI3000,

Roth Micro Centrifuge

Scanner: Expression 1600, Epson

SDS-PAGE chambers: Hoefer Scientific Instruments, Mighty Small II SE250

Silamat® S6, Ivoclar Vivadent

Sherwood flame photometer Model 410

Thermomixer 5436, Eppendorf

Vortex-Genie™, Bender & Hobein AG

2.11 Software

Adobe Illustrator CS5 (Adobe Systems Software Ireland Limited)

Adobe Photoshop CS5 (Adobe Systems Software Ireland Limited)

Adobe Reader IX & 2017 Pro (Adobe Systems Software Ireland Limited)

ApE - A plasmid editor (by M. Wayne Davis)

Gimp 2.10,12 (The Gimp Team)

ImageJ (Wayne Rasband, National Institutes of Health)

Inkscape 0,92.4 (Inkscape.org)

jalview version 2.11.1.0

Leica Application Suite X (Leica Microsystems GmbH)

Leica Application Suite AF Lite (Leica Microsystems GmbH)

MEGA-X version 10,1.8 phylogenetic tool (Kumar et al., 2018)

Microsoft Office 2010 (Microsoft Corporation)

RStudio (RStudio, Inc.)

Spyder (Python 3.7) (The Scientific Python Development)

2.11.1 Webpages

Arabidopsis lines and sequences http://arabidopsis.org/

https://www.arabidopsis.org

Arabidopsis eFP browser http://bar.utoronto.ca/efp/cgi-bin/efpWeb.cgi

Pub Med and BLAST https://www.ncbi.nlm.nih.gov

prediction of protein domains www.elm.eu.org

http://smart.embl-heidelberg.de

apps.webofknowledge.com

2.12 External devices

GATC-Biotech (D) later eurofins (USA)

3 Results

3.1 Physiological analysis of *Arabidopsis* mutants carrying different ahk1 alleles

ARABIDOPSIS HISTIDINE KINASE 1 (AHK1) was suggested to function as an osmosensor in response to osmotic stress, caused by different osmotically active substances. However, osmotically active substances were not the only variable that was changed in the published papers. The plants were grown under different conditions of light intensities and day length but compared to each other (Kumar et al., 2013; Lu et al., 2013; Tran et al., 2007). R. Dautel tried to reproduce the published results, without success. The results of her experimental repetitions of the analyses hinted that the altered osmotic phenotype of the *ahk1* mutants was highly dependent on the only identified AHK1 interaction partner so far, BRASSINOSTEROID INSENSITIVE 1-associated receptor kinase 1 (BAK1) (Dautel, 2016).

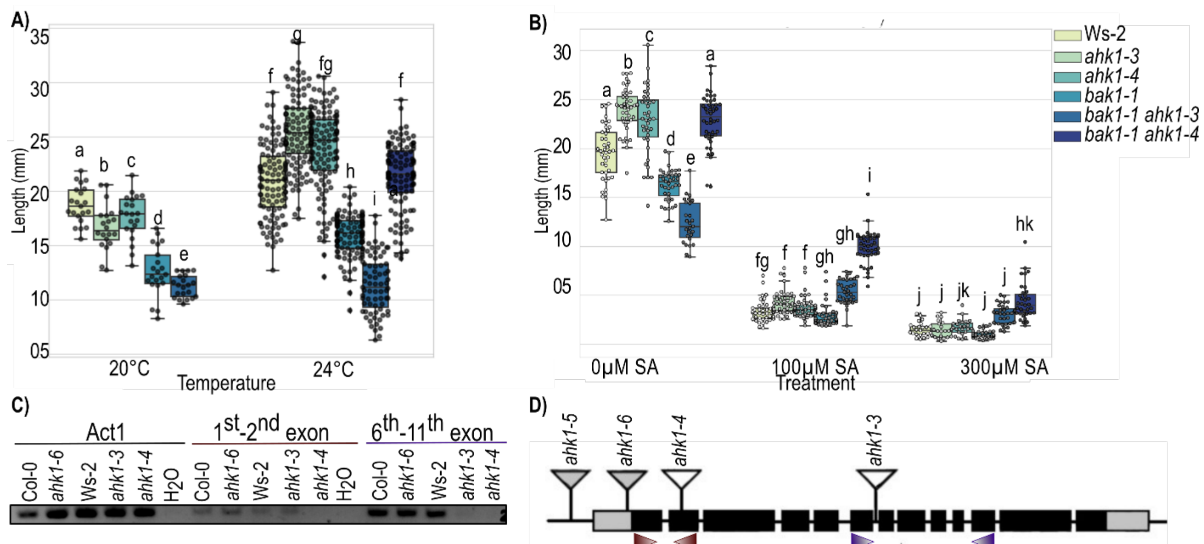

Figure 3-6: Root length of different *ahk1*-alleles and double mutant lines of *Arabidopsis thaliana*. A) Root length of seedlings grown for 9 days at 20 °C under continuous light and at 24°C under 16 h light and 8 h dark regime. B) Root length of seedlings grown for 7 days under 16 h light and 8 h dark regime, in the absence of SA or presence of SA at the indicated concentrations. C) Reverse transcriptase (RT)-PCR on *ahk1*- mutants *ahk1-3*, *ahk1-4* in Ws-2 background and *ahk1-6* in Col-0 background. Amplified gene length is 500 base pairs (bp) long. D) Shows the AHK1 gene with its T-DNA insertion lines and where they do have their T-DNA insertion. Red triangles show the first pair of primers and purple the second, used for RT-PCR.
Data is represented by box plots, middle lines of boxes indicate the median; box limits embody the 25th and 75th percentiles as determined by Python Seaborn software; whiskers extend 1.5 times the interquartile range from the 25th and 75th percentiles, data points are shown as points. One-way ANOVA was performed ($p<0,05$) followed by Tukey HSD post-hoc test. Different characters indicate statistical differences, $p<0,05$.

Results

Despite the fact, that the published results concerning AHK1's involvement in osmosensing under constant light and temperature conditions, were not reproduced in the study of Dautel, 2016 (Dautel, 2016; Dautel, unpublished; (**Figure 3-1** A)), it indicated differences between mutants carrying different *ahk1* alleles (**Figure 3-1** A)). By showing significantly different root length compared to wt at 20 °C and 24 °C *ahk1-3* is significantly different from wt, but *ahk1-4* is neither significantly different to wt nor *ahk1-3*. Hence, under different tested conditions, the root length showed different phenotypes between the *ahk1-3* and *ahk1-4* mutant. Additionally, at 20 °C the roots of the *ahk1* mutants are shorter and at 24 °C longer compared to wt, due to the different light and temperature conditions used before (Kumar et al., 2013; Lu et al., 2013; Urao et al., 1999; Wohlbach et al., 2008). The differences in between *ahk1* mutants seem to be even stronger in the double mutants, with AHK1's interaction partner BAK1. This led to the assumption that at least one of the *ahk1* mutants, proposed in the literature to carry a loss-of-function (LOF) allele, might not be a complete gene knock-out (Wohlbach et al., 2008).

Nevertheless, our *ahk1-3*-phosphoproteomic study revealed several phosphorylated proteins, predicted to be involved in phytohormone signaling (Dautel, 2016). Thus, it could be assumed that AHK1 might modify hormone signaling. However, AHK1´s significant role in many phytohormone pathways, such as: partially ABA, GA, MeJa, auxin, CK and ethylene, was already neglected (Dautel, 2016; Hauser et al., 2011; Pornsiriwong et al., 2017; Sussmilch et al., 2017). However, published data indicated that salicylic acid (SA) accumulation was significantly altered in *ahk1-3* mutant plants compared to wild type (Engelsdorf, 2018). Therefore, we tested the response of the *ahk1* mutants to exogenously applied SA at various concentrations (**Figure 3-1** B). The root and hypocotyl (Appendix) lengths of all seedlings were strongly reduced by exogenous SA independent of the genotype. There was no significant difference in the SA response between *ahk1* single mutants and wt plants. However, the seedlings of the *bak1 ahk1* double mutant and the *bak1* single mutant seemed to be less responsive to SA compared to the seedlings of the other genotypes with *bak1-1 ahk1-3* showing a dependence on *bak1-1* but not *ahk1-3*, therefore indicating, that this reaction is dependent on *bak1-1* and not *ahk1-3*. Overall, we could observe again the differences between mutants as we could see in the temperature data set. Therefore, we decided to test the mutants whether they are indeed LOF mutants.

Indeed, *ahk1-3* in Ws-2 background shows a truncated transcript derived from gene section before the T-DNA insertion (**Figure 3-1** C) and D)), which is in between the sixth and seventh exon. This was not tested, when first published ((Wohlbach et al., 2008), supplementals Fig. 1). In *ahk1-6*,

published as a knock-out mutant in Col-0 background (Kumar et al., 2013), reduced levels of full length *AHK1* transcript could be traced by reverse transcriptase (RT)-PCR. A functional protein could not be detected with AHK1^{ED} specific polyclonal antibody. Except for *ahk1-4*, all genotypes showed transcripts. *ahk1-3* shows transcript level until the insertion of T-DNA in the 6th exon. (**Figure 3-1** C)) The primers chosen for this RT-PCR are shown at a genomic DNA scheme of AHK1 in (**Figure 3-1** D)).

Consequently, we had to find a new starting point for the finding of AHK1's main physiological pathways via phenotypic analyses and, therefore, re-analyzed the phosphoproteomic data. Aggravatingly, many proteins with unknown function were found in this dataset (**Figure 1-4**). Consequently, we focused our further analysis on key players of known pathways that appeared to be post-translationally influenced by AHK1.

3.1.1 AHK1 and the light signaling pathway

After re-analyzing the phosphoproteomic data published in (Dautel, 2016), we considered, that AHK1 might be part of the light signaling pathway. The modifications of many key players of the far-red (FR) light (700-780 nm) signaling pathway seem to be regulated by AHK1, like CONSTITUTIVE PHOTOMORPHOGENIC 1 (COP1), ELONGATED HYPOCOTYL 5 (HY5), FAR-RED ELONGATED HYPOCOTYL 3 (FHY3) and SUPPRESSOR OF PHYA-105 1-2 (SPA1-2) (Delker et al., 2014), as well as photoreceptors of the phototropic blue-light (BL) pathway (450–485 nm) PHOTOTROPIN1 and 2 (PHOT1/2), NON-PHOTOTROPIC HYPOCOTYL3 (NPH3) (Briggs et al., 2001; Zhao et al., 2018) and circadian clock mediating TIME FOR COFFEE (TIC) (Shin et al., 2012). Due to the diverse background of these proteins for different light signaling pathways, we tested the response to different light regimes by dose response analyses of hypocotyl length and qPCRs on light signaling-specific reporter genes.

We set up seeds for dose response curves. All seeds were sawed first at the same time point a day and thereafter, 2 d kept at 8 °C and exposed to 8 h white light irradiation at 20 °C for the induction of seed germination. Afterwards seedlings were grown under different light conditions, such as blue light (BL), red light (R, 625-700 nm) and far-red light (FR) (**Figure 3-2**). For each light-specific dose-response analysis, the mean hypocotyl lengths were set relative to the mean of the hypocotyl length of dark grown seedlings (100 %) of each genotype. The results under LED lights were inconsistent in different seed batches. The experiments were repeated at the University of Freiburg, with lightbulbs instead of LEDs and the same intensities as before, starting with the first plate at 12 µmol/m^2*s FR

light, 20 µmol/m²*s BL light and 40 µmol/m²*s R light. The hypocotyls of the seedlings were measured until the hypocotyl lengths of a plate were similar to the dark control, which is indicated by the hypocotyl length, by reaching the size of the etiolated seedling. Therefore, each data point represents a plate, from the one with the highest light intensities at the right side, to the one with the smallest hypocotyl length.

FR light alters plant growth in general (Küpers et al., 2018; Possart et al., 2014). In *Arabidopsis* wt plants higher FR light led to shortened hypocotyl length compared to etiolated seedlings. *ahk1* and *bak1* single and double mutants were compared to wt and show no significant differences in their relative hypocotyl length. For statistics a two-sided t-test was used. The biggest differences were observed at

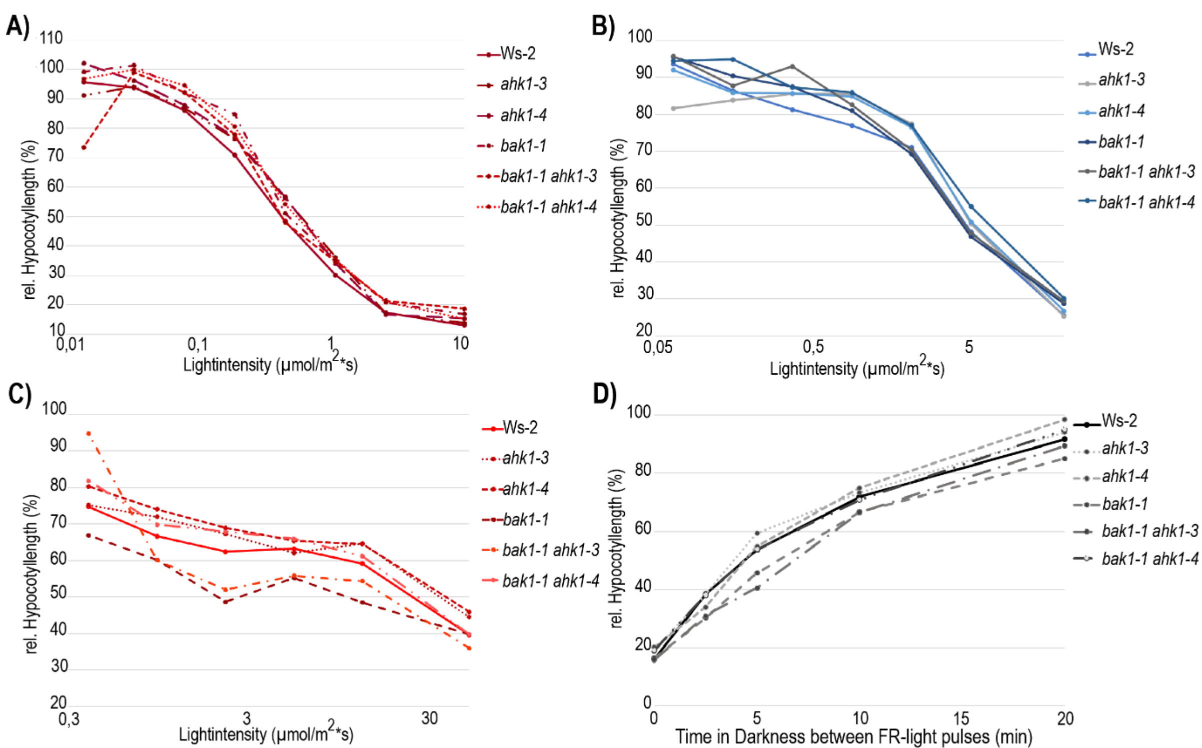

Figure 3-7: Hypocotyl length of *A. thaliana ahk1* mutant seedlings show a wt-like dose response to different light treatments.
A-D) Relative hypocotyl length of wt, *ahk1* and *bak1* single and double mutants at A) far-red (FR)-light from 12 µmol/m²*s to 0,01 µmol/m²*s, B) blue-light (BL), starting from 20 µmol/m²*s to 0,05 µmol/m²*s, C) Red-light (R) with the largest intensity at 50 µmol/m²*s to 0,05 µmol/m²*s and
D) seedlings were irradiated with multiple 2,5 min 5 µmol/m²*s FR light far-red light pulses, varying the duration of the dark phases between the light pulses, according to (Buche et al., 2000).

A -D) Hypocotyl length relative to dark grown seedlings of according to genotype; n=~ 20 plants. A&C) Performed in three replicates, C & D) were performed once. A-D) Two-sided t-test was performed for testing significance, p=0,05. No significant differences were observed.

a light intensity between 0,1-0,5 µmol/m^2*s, still not significant (**Figure 3-2** A)) alike under BL light, also at R (**Figure 3-2** B) and C)). Under R light treatment no significant differences between lines was observed (**Figure 3-2** C)). Only *bak1-1* and especially *bak1-1 ahk1-3* showed a reduced reaction. To elucidate whether the seedlings were reacting to another mode of FR light irradiation, we tested FR light associated high irradiance response (HIR persistence) by application of 2,5 min long FR pulses of 5 mol/m^2*s intensity interrupted by dark intervals of 4 min, 8 min, 12 min, and 20 min, for 3 d after white light induction of germination, according to (Buche et al., 2000). The longer the absence of light, the longer the wt-hypocotyl is. There were not any significant differences in the relative hypocotyl length between genotypes (**Figure 3-1** D)).

The last FR pathway we tested was the very low fluence response (VLFR). To clarify whether there is a significant influence of the *ahk1* mutant alleles, we tested the transcript accumulation of the VLFR reporter gene *PSEUDO-RESPONSE REGULATOR 9* (*PRR9*) via qPCR (Nakamichi et al., 2007; Wenden et al., 2011)) 0 min, 40 min, 80 min, 120 min and 160 min after onset of 1 µmol/m^2*s FR light. The seedlings were grown before for 4 days in darkness. In the end there were no significant differences in the *PRR9* transcript accumulation (**Figure 3-3** A)). The differences after 80 min are not due to expression differences, instead, there was ¼ less cDNA than needed for the qPCR approach, due to pipetting error. All in all, *PRR9* expression level is the same in the *ahk1* mutants and in the wt.

3.1.2 HY5 qPCR and Anthocyanin pathway

Additional to the *PRR9* transcript levels, we tested the levels of the light signaling key player *HY5* after 1 h and 4 h exposure to FR light of 15 µmol/m^2*s in the *ahk1* and *bak1* single and double mutants compared to wt (**Figure 3-3** B)). Transcript level peaked 1 h the levels were fallen more or less to the dark values (Yang et al., 2018a; Yang et al., 2018b). This tendency is seen in every genotype except for *bak1-1*. Significant differences were calculated between *bak1-1* and *bak1-1 ahk1-3* and *bak1-1* and *bak1-1 ahk1-4* after 1 h. Anthocyanin is produced in plants upon various environmental factors. One factor is FR light (Rabino and Mancinelli, 1986; Warnasooriya and Montgomery, 2009; Xu et al., 2017). To determine anthocyanin accumulation, seedlings were sown on ½ MS with 1 % sucrose for 4 d

(Solfanelli et al., 2006; Warnasooriya et al., 2011). The plates were transferred to 8The first anthocyanin extraction was performed for 8**Figure 3-3**Anthocyanin levels showed the same tendencies under FR light. BL and D are used as negative controls. Compared to the wt all mutant plants, with the exception of *ahk1-3*, are reacting hyposensitive to FR. Probably due to differences in the extraction timespan. No significant differences were observed, when all three extractions were combined. **Figure 3-3**The amplification of *CHS* was evaluated in darkness (D) and after 1°h and 4 h in . All seedlings had an 8 4 d in darkness (D). According to earlier publications the peak of *CHS* expression is estimated at

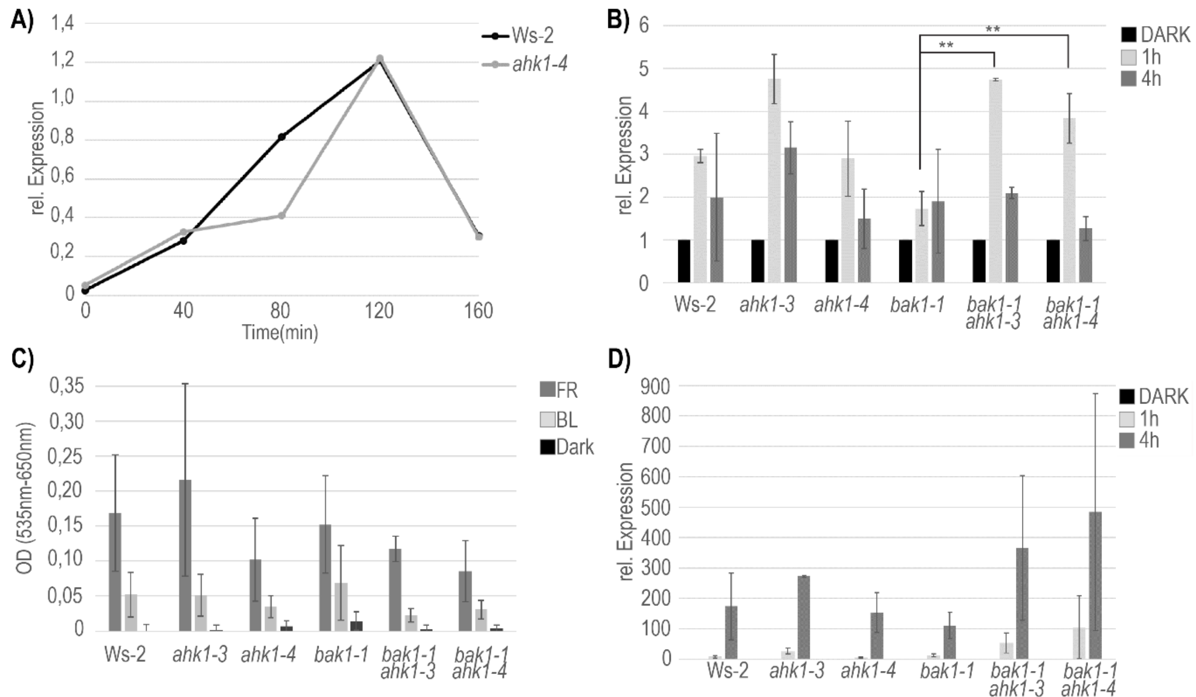

Figure 3-8: The *ahk1* mutants show a reduced sensitivity to FR light.

A) *PRR9* transcript level after different time-lengths under FR light. Treatments were performed with 1 µmol/m^2 intensity. B) *HY5* transcript levels after 1 h and 4 h irradiation with FR light (~20 µmol/m^2).C) Anthocyanin levels after 4 d under continuous FR light (~15 µmol/m^2) or continuous BL (~20 µmol/m^2) or Darkness. Optical density (OD) at 535 nm of the extract of 20 seedlings per plant genotype and treatment, were quantified. D) CHALCONE SYNTHASE (CHS)-transcript levels after 1 h and 4 h of FR light treatment. Shown are the means and standard deviations. n=~20 plants, the experiment A) was executed once B-D) three times. A, B & D) Quantification via qPCR had three technical replicas, mean of 3 biological replicas shown.
Two-sided students t-test was performed (p<0,05). p<0,05=*, p<0,01=** and p<0,001=***. For A), C), D) no significant differences were observed.

around 4 h and in D there should be no expression (Lewis et al., 2011; Zwick, 2012). Based on this, no significant differences were detected. Lighting up the phenotype on an evolutionary basis in dicotyledons

AHK1 was shown to be conserved through most dicots but is also found in non-seed plants such as mosses, streptophyta and other algae (Dautel, 2016; de Vries et al., 2020; Kabbara et al., 2019). Although *AHK1* is not well conserved in monocots, some carry an *AHK1* homolog (Hertig et al., 2020). In *Lotus japonicus* (*L. japonicus*), a dicotyledon of the Fabaceae family, the *AHK1* gene was duplicated, and the species possesses two *AHK1* homologs*: LHK4A* (LotjaGi2g1v0379900) and *LHK4B* (LotjaGi4g1v0129800) (**Figure 3-4** A)). *Medicago truncatula* , another legume, also carries two *AHK1* homologues in its genome (Tan et al., 2019).

Most Fabaceae are able to establish nitrogen fixing symbioses with rhizobia. In the presence of its symbiont *Mesorhizobium loti* (*M. loti*), *L. japonicus* is developing root nodules, which are inhabited by the rhizobia. Inside of these nodules the bacteria are able to fix nitrogen and supply the plant with ammonia (Márquez, 2006; Zahran, 1999). In exchange the symbionts are supplied with carbohydrates and other nutrients (Madigan, 2015). In the establishment and regulation of the rhizobial symbiosis many signaling components remain unknown. During the evolution of the rhizobial symbiosis many preexisting signaling pathways were adapted, like the common symbiosis pathway (Roy et al., 2020). Rhizobial symbiosis can be both beneficial but also harmful when deregulated for the plant, thus small defects in signaling can lead to strong phenotypes (Jones et al., 2007). The duplication of *AHK1* in nodulating species like *L. japonicus* and *M. truncatula* (Tan et al., 2019) could hint for an acquired function in symbiosis signaling. On Lotusbase.dk.au AHK1 was blasted against the *L. japonicus* genome sequence (Mun et al., 2016). For identification of *LHK4A* and *LHK4B* the genome version Gifu v1.2 was used, in which background the loss of function mutant *lhk4a-1*, is (Kamal et al., 2020a; Urbanski et al., 2012). To clarify, that the two found genes are truly *AHK1* homologues, I performed a Neighbor-Joining tree combined with bootstrap analysis including other *AHK's* (**Figure 3-4** A)).

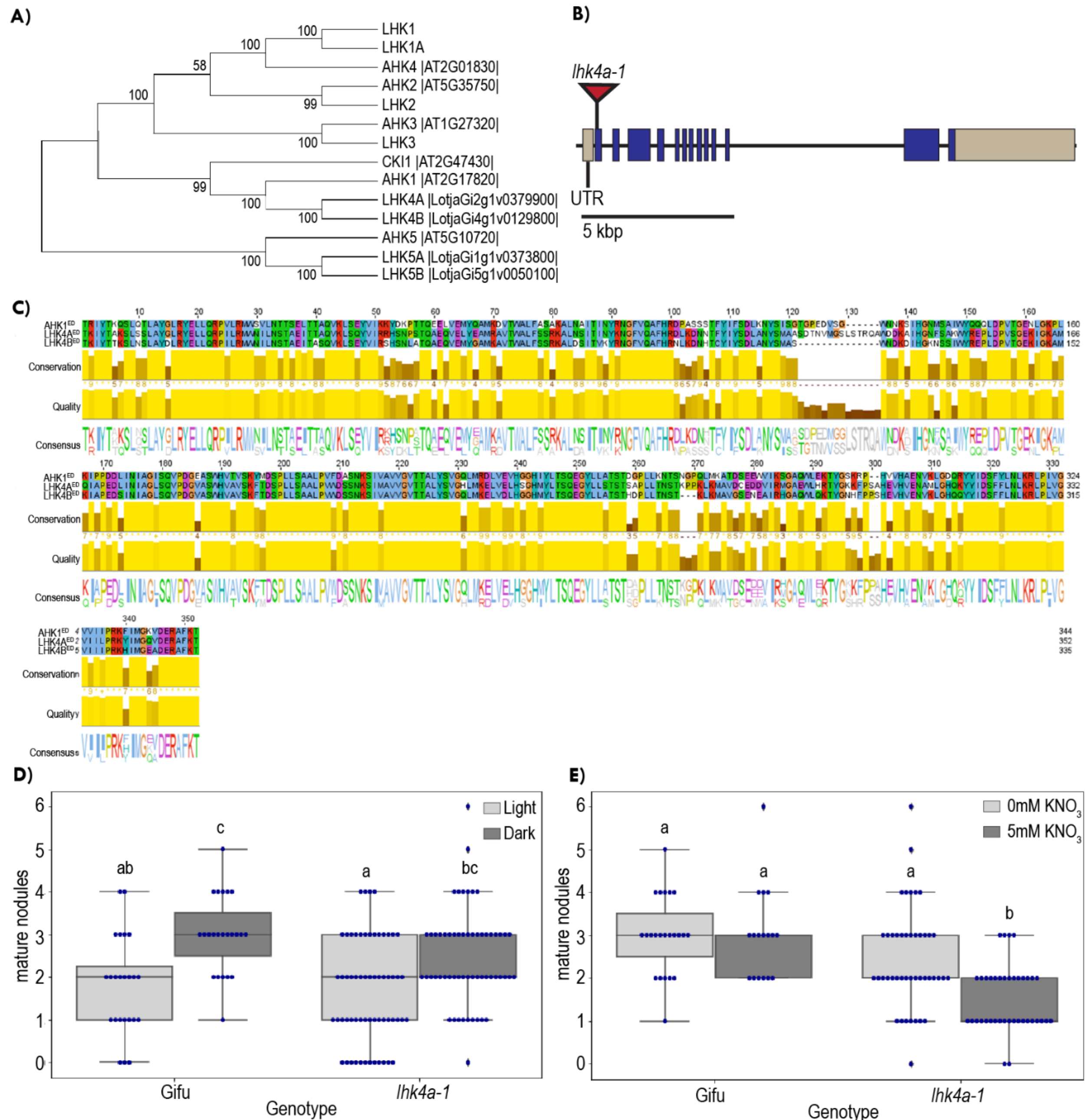

Figure 3-9: Highlighting *AHK1* gene homologues in *Lotus japonicus* and nodule formation in the *lhk4a* mutant**.**
A) Neighbor-Joining Tree with bootstrap values based on amino acid sequences of full length AHK's, the previously described LHK1-3 (Held et al., 2014) and previously undescribed, putative AHK homologues of *L. japonicus*. The analysis was executed with MEGA-X version 10,1.8 phylogenetic tool (Kumar et al., 2018; Lu et al., 2013). Accession numbers are written behind the newly identified genes. B) *Jalview* version 2.11.1.0 *ClustalW* alignment (Waterhouse et al., 2009) of AHK1^{ED} with its two *L. japonicus* homologues LHK4A and LHK4B. C) Exon/intron structure of the LHK4A genomic sequence and the position of the retrotransposon insertion indicated by red triangle in first exon (Urbanski et al., 2012). D-E) Number of mature nodules of wild type *L. japonicas* Gifu plants and the *lhk4a-1* insertion mutant three weeks post inoculation with

Figure 3-4:
Mesorhizobium loti. D) Plants were grown with their roots either exposed to light or kept in darkness at 0 mM nitrate concentration.
The data are represented as box plots: The middle lines of boxes indicate the median, the box limits embody the 25th and 75th percentiles as determined by Python Seaborn software, whiskers extend 1.5 times the interquartile range from the 25th and 75th percentiles and the single measurements are represented by points. One-way ANOVA was performed followed by Tukey HSD post-hoc test. Different characters indicate statistically significant differences (p<0,05). Lotusbase.dk.au was used for *L. japonicus* gene sequence (Mun et al., 2016) for the ecotype Gifu v1.2 (Kamal et al., 2020a; Kumar et al., 2013).

Thereby it became evident, that there was also a gene duplication of AHK5 and a deletion of CKI1. Because of AHK1's putative role in symbiosis we decided to investigate the symbiotic phenotype of the newly identified mutant *lhk4a-1*. *lhk4a-1* is caused by an insertion of the LORE retrotransposon eight basepairs after the start codon (**Figure 3-4** B)). Because there are two AHK1 homologues, we also aligned $AHK1^{ED}$, $LHK4A^{ED}$ and $LHK4B^{ED}$ and did a Pairwise distance test (**Figure 3-4** C)), to figure out, whether the ectodomain (ED) is conserved or not. Pairwise distance test, performed with MEGA-X version 10,1.8 phylogenetic tool (Kumar et al., 2018) revealed, that LHK4A is more alike AHK1 than LHK4B, but when the ED of all three genes was compared, $LHK4A^{ED}$ and $LHK4B^{ED}$ are more alike (0,183) than $AHK1^{ED}$ and $LHK4B^{ED}$ (0,353) and (0,385). A *jalview* version 2.11.1.0 *ClustalW* alignment (Waterhouse et al., 2009) showed the conserved and non-conserved amino acids (aa's) in the ED pinpointing, that there is a deletion of 17 aa and an addition of 6 aa at the same region in $LHK4B^{ED}$ compared to $AHK1^{ED}$ (aa 224 to aa 233 in AHK1, marked as aa 121 to aa 136) (**Figure 3-4** C)). After isolation of homozygous *lhk4a-1* mutants, we tested if the formation or regulation of nodules is altered compared to wild type. *Lotus* plants were grown under long day conditions either fully exposed to the light or cultivated in boxes that only allowed light to come from above to cotyledons and shoots but shadowed the roots (dark conditions). Light exposure led to a significant reduction of mature nodules in both wt and *lhk4a-1* plants (**Figure 3-4** D)). There was no significant difference between wt and *lhk4a-1* under both light conditions (**Figure 3-4** D)).

In the Autoregulation of Nodulation (AON), infection and nodulation are restricted systemically by a symbiotic state or by sufficient nitrate supply. (Nishida et al., 2018; Tsikou et al., 2018). So, we grew Gifu and *lhk4a-1* at different nitrate concentrations at shaded condition. At 0 mM nitrate there were no significant differences between the genotypes (**Figure 3-4** E)). However, nitrate supply led to a reduction in nodule numbers. This reduction is stronger in *lhk4a-1,* at 5 mM nitrate *lhk4a-1* has a

significantly reduced number of nodules compared to Gifu (**Figure 3-4** E)). A qualitative difference in nodule development could not be observed between the genotypes.

3.2 "Fishing" for an AHK1 ligand

The receptor kinase AHK1 localizes to the plasma membrane, anchored there by two transmembrane domains. It possesses a cytosolic histidine kinase domain, a H-ATPase, a receiver domain and an ectodomain (ED) that reaches into the apoplastic space (Dautel, 2016; Urao et al., 1999). As shown by Dautel (2016), AHK1 stands at the beginning of a signaling cascade. *In situ* analysis identified a Per-Arnt-Sim (PAS) domain in the ED, known for binding small molecules (Chang et al., 2010; Taylor and Zhulin, 1999). Nevertheless, the molecule (ligand), triggering AHK1 signaling is unknown. Due to the identification of the PAS-domain, which should bind a ligand, we decided to only use the ED for the "fishing" of an AHK1 ligand. To elucidate the putative ligand, we expressed AHK1^{ED} in bacteria and tried to identify the ligand in an untargeted approach *via* mass spectrometry as well as with different targeted approaches.

3.2.1 Ligand identification with the *E. coli* expressed AHK1 ectodomain (AHK1^{ED})

The AHK1 ectodomain (ED), reaching from the amino acid 103 to 446, was cloned into *E. coli* expression vectors with different tags (Dautel, 2016), to perform ligand fishing with the purified protein. The most promising results were obtained by AHK1^{ED} expression from the *pETM41-MBP-AHK1^{ED}-6xHis* vector. It was compared with the expression of AHK1^{ED} from the *pMhsSUMO-AHK1^{ED}-6xHis* plasmid (**Figure 3-5** A)). The MBP-AHK1^{ED}-6xHis showed cleaner results with our extraction method, the yield was higher than AHK1^{ED}-6xHis. The natively extracted MBP-AHK1^{ED}-6xHis and AHK1^{ED}-6xHis were purified via Ni^{2+}-NTA columns and the performance of purification was tested by western blots and Coomassie gels (**Figure 3-5** B) and C)). Thereafter, the protein amount of MBP and MBP-AHK1^{ED} was estimated *via* amidoblack staining. Additionally, the maltose binding protein (MBP) allowed us to use MBP-traps for our LC-MS analysis (see below). As the AHK1^{ED} is predicted to reach into the apoplast (Dautel, 2016), we expected the ligand to be present in the extracellular space. Therefore, I incubated MBP-AHK1^{ED} and, as control, MBP alone with apoplastic washfluid (AWF), extracted from *Phaseolus vulgaris*, French bean, supplied by Prof. Christian Zörb, University of Hohenheim. An AHK1 homolog exists also in beans according to protein sequence blast (blast.ncbi.nlm.nih.gov/). The well-established preparation of AWF from *P. vulgaris* results in a larger volume and faster harvest compared to *Arabidopsis* (O'Leary et al., 2014). Before

AWF preparation bean plants were treated either 15 min with 100 mM mannitol or mock treated. Assuming that AHK1 is an osmosensor (Urao et al., 1999), we hypothesized that the osmotically stressed beans could probably accumulate more of the putative ligand. After 1 h incubation MBP-AHK1^{ED} or MBP with AWF followed by washing steps, bound compounds were released from the trap by a heat shock treatment followed by centrifugation (2.3.7). Putative ligands should be found in the supernatant consequently they were analyzed *via* mass spectrometry.

3.2.2 Mass spectrometry

The supernatants released from MBP-AHK1^{ED} or MBP were analyzed by liquid chromatography–mass spectrometry (LC-MS). LC-MS was executed by Dr. M. Stahl. LC-MS was indicating lipids as a putative ligand due to the retention time of the putative ligand, which is the time a molecule needs from injection onto the chromatography column to detection, as well as their precise molecular mass. Although no specific ligand was identified, many different molecular weights of lipids as potential

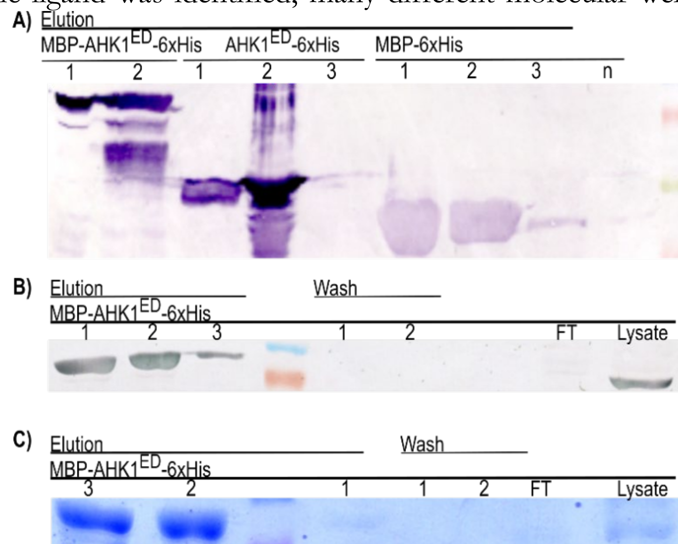

Figure 3-10: AHK1^{ED} purification.
A) Western blot of MBP-AHK1^{ED} (aa103-446 of AHK1), AHK1^{ED}-6xHis (aa100-446 of AHK1). B) Western blot of MBP-AHK1^{ED}-6xHis and MBP-6xHis. C) Coomassie gel of purified MBP-AHK1^{ED}-6xHis and MBP-6xHis.
A-C) Different steps of the purification process of native proteins with Ni-TA^{TM} columns. Elution: last purification steps of native protein, FT- flow through of protein binding step, lysate- native protein after native extraction from *E. coli* cells, not purified, Wash-washthrough.
A) and B) combined first and secondary antibody αhis-AP. Detected with 5-Bromo-4-chloro-3-indolyl phosphate (BCIP) and nitro blue tetrazolium (NBT). C) SDS gel stained with Coomassie blue.
Abbreviations: A)-C) 1,2,3- numbers for repetition of wash or elution step, aa- amino acid; FT-flow through, His- histidine; lysate- supernatant after proteins were extracted from cell culture, MBP- maltose binding protein; n- spilled over; wash- washstep.

signal have been fished. Ancillary of the LC-MS, we incubated the purified MBP and MBP-AHK1^{ED} with AWF. After we identified lipids as putative signals, we also used lipid extracts from *A. thaliana* leaves, for scaling up the amount of lipids and for identifying a lipid as putative in the LC-MS (2.4) that were solubilized in MeOH before the treatment. The treatment with AWF identified lipids as putative ligand three times, but without identifying one specific ligand; probably due to the small number of compounds in the AWF, with lipids being at nanomolar to picomolar concentrations (Bolwell et al., 2002; Misra, 2016). The LC-MS suggested that lipids might probably be binding to the ED of AHK1 hence, pointing to lipids as putative ligand. For getting a sample with higher lipid concentrations, we used lipid extracts from *Arabidops*is Ws-2 plants. Nevertheless, the results with the lipid extract were also inconclusive (Table 7-1) and did not hint for a specific lipid or class of lipids.

Furthermore, we used different functional approaches to confirm or disprove the data from the LC-MS, like ethylene production (**Figure 3-6**) and re-established an AHK1 reporter gene assay, originally developed by Dr. K. Caesar (Caesar, unpublished).

3.2.3 Approach to identifying a putative AHK1 ligand by an ethylene assay

After the LC-MS suggested a kind of lipid as a putative ligand, the phosphoproteomic dataset was re-analyzed whether there are suitable pathways that we could use for further characterization of the AHK1 ligand. Our phosphoproteomic data suggested, that AHK1 was likely to influence ethylene production (Dautel, 2016). Additionally, to the LC-MS work, we attempted different functional assays to identify and confirm a potential ligand of full length AHK1. In the ethylene assay, ethylene accumulation is measured produced by leaf discs of plants, which were treated before with an elicitor (Felix et al., 1991). For my purpose, leaf tissue samples from plants grown under short day conditions were cut into equally sized squares. As controls and elicitors, we used (2.3.11) either water (ddH_2O), flagellin22 (flg22), Pen (extract from *Penicillium chrysogenum* (*P. chrysogenum*)), AWF (diluted 1:100) from untreated plants or AWF from plants treated with mannitol (diluted 1:100). After treatment vials containing the leaf samples were sealed using gum closures. After 3 h gas from the vial was transferred into a gas chromatograph using a syringe. The amount of ethylene was calculated based on the peak area of the gas chromatograph. This ethylene assay could confirm the hypothesis and in addition could be used for further narrowing down to a putative ligand or ligand class of AHK1 through using apoplastic washfluid (AWF) and AWF treated with mannitol. Pen, an extract from *P. chrysogenum*'s mycelium, served as a positive control, due to its characteristic to induce ethylene production during resistance-related responses in many plant species (Thuerig et al., 2005). Wassiljewskja (Ws) carries a

mutation in the N-terminus of FLAGELLIN SENSITIVE2 (FLS2), the known flagellin receptor (Gomez-Gomez et al., 2001a; Zipfel et al., 2004) which is why it is not able to recognize flg22, therefore it served as another negative control (Chinchilla et al., 2006). For the assay water and flg22 served as negative controls.

In the tested plants, the relative ethylene production was similar without significant differences. Solely, AWF with mannitol treatment showed a difference in *ahk1-3* leaflets. After the treatment with AWF with mannitol treatment, a small rise in ethylene production was visible (**Figure 3-6**). The *bak1-1 ahk1-3* double mutant did not produce ethylene upon AWF treatment, alike wt and every other mutant. The peak of *bak1-1* is an outlier, probably due to a hurt leaflet.
Due to ambiguous results and needing material in inaccessible amounts, we continued another assay.

3.2.4 AHK1 dependent promotor-induced Assay

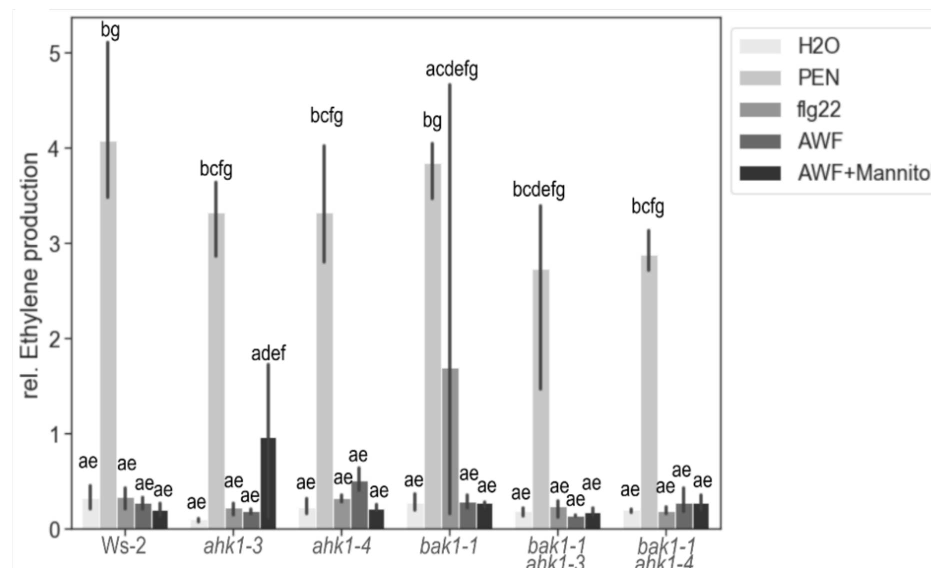

Figure 3-11: Ethylene assay with *ahk1*-plant lines.

Ethylene assay according to (Felix et al., 1991). Relative ethylene production after treatment with H_2O
as mock control, flg22 as negative control and PEN as positive control, AWF from untreated lines and AWF from lines treated with 80 mM mannitol. Error bars shown in standard deviation. p=0,05, three biological replicates 3x3mm leave squares.
One-way ANOVA was performed ($p<0,05$) followed by Tukey HSD post-hoc test. Different characters indicate statistical differences, $p<0,05$.
Abbreviations: AWF-apoplastic washfluid, flg22-flagellin22, H_2O-water, PEN- extract from *Penicillium chrysogenum*.

Results

The LC-MS data suggested that AHK1's putative ligand could be a lipid. To verify these results, we looked for a further suitable functional assay with full-length *AHK1*. I tested several assays in different organisms, like *Arabidopsis* (ethylene assay) and *E. coli* (pCOLD Assay, data not shown). It could be shown, that the pCOLD assay worked, but not with AHK1. Hence, we decided to use an *in planta* assay with full length AHK1, originally established before (Caesar, unpublished). It is a transient activator/reporter gene assay in *Nicotiana benthamiana* (*N. benthamiana)*. The use of *N. benthamiana* has the advantage, that its *AHK1*-homologues are quite different with just 56 % protein sequence identity when looked into blast from (https://solgenomics.net/). Due to this, AHK1 background is not expected. As reporter gene a plasmid is used of which the expression of nuclear NLS-mCherry is controlled by the stress inducible *RESPONSIVE TO DESICCATION 29B* (*RD29b*, AT5G52300) promotor (Liu et al., 2020; Virlouvet et al., 2014). *RD29b* expression is also induced by AHK1 in response to osmotic stress in *Arabidopsis* (Caesar, unpublished). In *N. benthamiana 35S::AHK1:GFP* serves as an activator gene construct to the *RD29b* promotor. AHK1-GFP localizes to the plasma membrane and is able to induce the accumulation of NLS-mCherry in an osmotic stress-dependent manner (Caesar, unpublished). Thereby, NLS-mCherry fluorescence is quantified by quantitative cLSM. The first aim was to reproduce the results of Dr. K. Caesar. Leaves were either infiltrated with both plasmids or only *RD29b::NLS-mCherry* and were left afterwards in the climate chamber for another 3 d. Thereafter, plants were treated with either 80 mM mannitol or ddH$_2$O for 1 h. Pictures of around 20 nuclei were taken with the same adjustments and the nuclear mCherry fluorescence intensities were measured and compared. Mannitol treatment showed an upregulation of the nuclear mCherry fluorescence compared to the water control when both plasmids were present. Hence, I could confirm that the assay succeeds and can be used for ligand or ligand class identification. However, it is crucial for this assay, that infiltrated *N. benthamiana* plants were not stressed before, as the *RD29b* promotor is also induced by other abiotic stress factors such as heat stress in the absence of AHK1-GFP (Caesar, unpublished).

Results

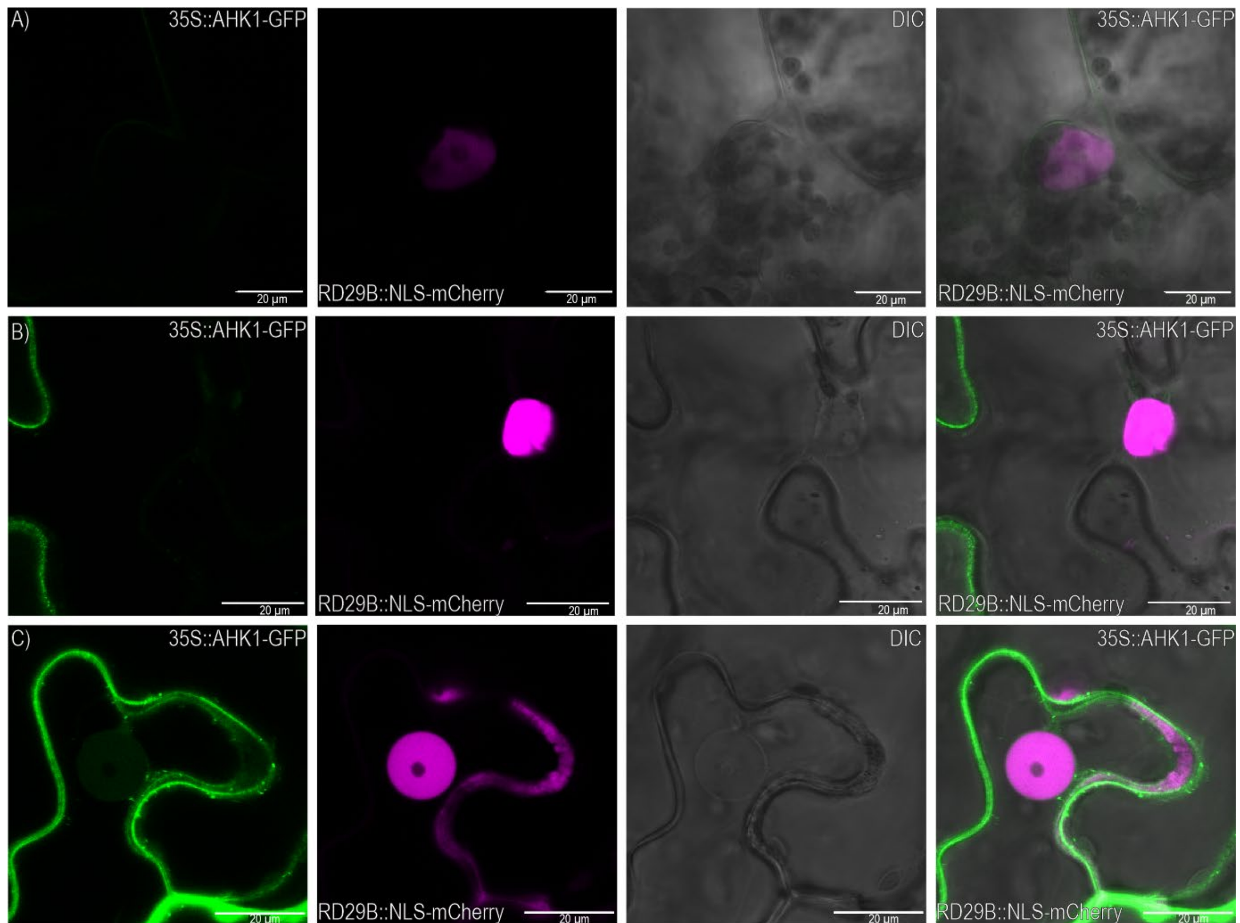

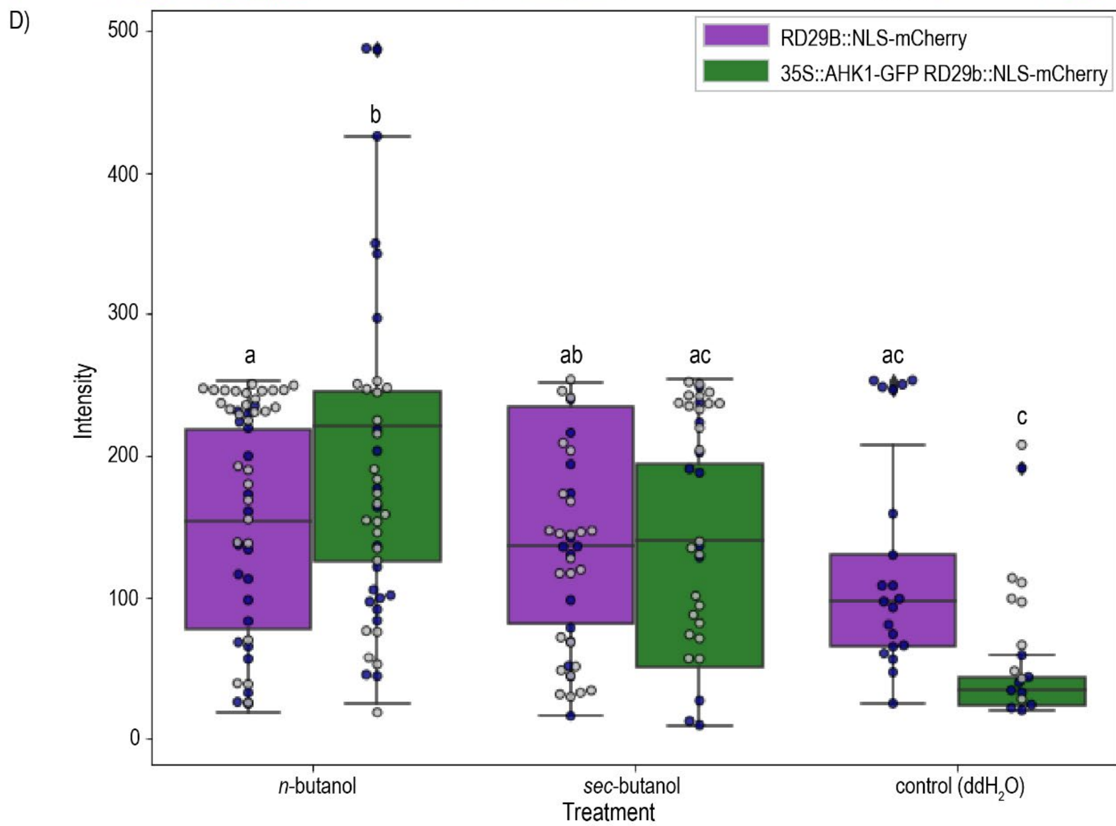

Figure 3-12: An activator/reporter gene assay suggests a lipid-dependent regulation of gene expression by AHK1 in *N. benthamiana* cells.
A) *Nicotiana benthamiana* (*N. benthamiana*) cells expressing 35S::AHK1-GFP and RD29b::NUCLEAR LOCALIZATION SIGNAL-mCherry (NLS), untreated. B) Tobacco cells expressing AHK1-GFP and RD29b::NLS-mCherry, treated with *sec*- butanol the negative control for *n*-butanol, C) *N. benthamiana* cells expressing AHK1-GFP and RD29b::NLS-mCherry, treated with *n*-butanol. D) Intensity of the NLS-mCherry fluorescence measured in *N. benthamiana* cells expressing either AHK1-GFP and RD29b::NLS-mCherry or RD29b::NLS-mCherry.
A) to C) show representative pictures of cells after the different treatments with H_2O, *n*-butanol or *sec*-butanol.
Nucleus measured: ~20 per treatment and expression. Experiment repeated three times with the same results. Boxplots show two repeats, separated by different dot colors, the third was excluded due to stressed plants, although they showed similar results.
Data is represented by box plots, middle lines of boxes indicate the median; box limits embody the 25th and 75th percentiles as determined by Python seaborn software; whiskers extend 1.5 times the interquartile range from the 25th and 75th percentiles, data points are shown as points. One-way ANOVA was performed ($p<0,05$) followed by Tukey HSD post-hoc test. Different characters indicate statistical differences, $p<0,05$.

The responses to different inhibitors of lipid synthesis, such as *n*-butanol (1-butanol) with its control *sec*-butanol, neomycin, Phenylarsine oxide (PAO), *lyso*-PA, diacylglycerol kinase inhibitor (DGKI) were tested (**Figure 1-2** Introduction). Inhibitors were chosen by lipid classes that have been confined as putative ligands in the LC-MS. Neomycin and *n*-butanol for PA synthesis, with its negative control *sec*-butanol, DGKI for inhibiting diacylglycerol kinases, another synthesis pathway of PA and PAO for phosphoinositides. For all inhibitors, the lowest published concentrations were used (**Table 2-5**) and first tested with 2 h incubation time according to Cassim *et al.* (Cassim et al., 2019). After this time, no fluorescence in the nucleus was observed. A 0,2 % dilution of *n*-butanol and *sec*-butanol and 15 min incubation time was sufficient to have an effect on leaves expressing RD29b::NLS-mCherry (**Figure 3-7**). The effect of the inhibitors on NLS-mCherry was stronger with AHK1-GFP in the same leaf.

The negative control to *n*-butanol is *sec*-butanol (**Figure 3-7** B) & D)). The toxicity of *sec*-butanol should be comparable to *n*-butanol as they are alcohols of similar molecular weight, however only *n*-butanol acts as an inhibitor of the PA-synthesis pathway. I could show, that the *RD29b::NLS:mCherry* reporter reacted least to the mock treatment with filtrated H_2O (**Figure 3-7** A) & D)), which indicates that AHK1 is needed to induce the system. Solo infiltrated *RD29b::NLS* served as an additional negative control for each treatment, due to RD29b::NLS accumulation being activated by AHK1 (**Figure 3-7** D)). Without co-infiltration of *35S-AHK1-GFP*, the nuclear NLS-mCherry fluorescence intensity rose with *n*-butanol treatment, but not significantly compared to NLS-mCherry treated with

sec-butanol. Thereby, I could observe that *n*-butanol with co-infiltrated 35S-AHK1-GFP, increased the nuclear NLS-mCherry fluorescence intensity significantly compared to *sec*-butanol treatment, although there is a huge distribution of measured fluorescence intensities with this treatment (**Figure 3-7** C) & D)).

All in all, the results show a significant reaction of AHK1 to PA lipid inhibitors, but they cannot confirm whether a lipid is the ligand of AHK1. For this, further experiments are needed.

4 Discussion

4.1 Looking for AHK1's main pathway with ahk1 alleles

AHK1 has been a suggested osmosensor, although the experiments previously executed, suggesting this function, used very different parameters. I therefore tried to identify the main pathway of AHK1 by using phenotyping. The characterization of *ahk* mutants began with looking for a function of AHK1 through analyzing *ahk1* mutants, because we were not able to reproduce published data. In the course of our experiments we saw, that exogenous salicylic acid did not result in significantly altered lengths of roots and hypocotyls of *ahk1* compared to its WT (**Figure 3-1** B)), although research showed, that SA expression levels in *ahk1-3* plants were altered significantly (Engelsdorf et al., 2018). This could be probably due to AHK1 being involved in regulating SA biosynthesis but not its signaling pathway. Similar observations were made with abscisic acid (ABA). Exogenous applied ABA on WT showed altered gene expression levels of AHK1 in transcriptome data, but exogenous applied ABA on *ahk1* mutant lines showed wildtype-like hypocotyl- and root length (Dautel, 2016; Hauser et al., 2011; Pornsiriwong et al., 2017). What we could observe after SA treatment, were significant differences between our mutants (**Figure 3-1** A) and B)). This led to testing, whether *ahk1* mutants in the ecotype backgrounds Col-0 and Ws-2 are LOF mutants as published (Kumar et al., 2013; Wohlbach et al., 2008) or whether there is transcript left before or after the T-DNA insertion in the mutants. In *ahk1-3*, we could show, that upstream of the T-DNA insertion there was *AHK1* transcript detectable in the plant (**Figure 3-1**). This includes the two TD's, the ED and the full histidine kinase domain. Still, it needs to be elucidated, whether the transcript is translated to a functional part of the protein. Based on these results and the contradictory phenotypes we compared the wt to *ahk1-3* and *ahk1-4* (**Figure 3-1,** (Dautel, 2016)), it is only certain, that *ahk1-4* is a LOF mutant. *ahk1-3* in contrast seems to be a gain of function mutant. However, we could not prove this by our results. Whether the remaining transcript in *ahk1-3* is translated into a functional protein could be shown by a test executed with an $AHK1^{ED}$ specific monoclonal antibody on *ahk1-3* plant material. We tried to detect the possible protein using a polyclonal antibody, which failed because of unspecific binding, and AHK1-levels were too low to be detected via western blot. If indeed a truncated AHK1 is translated in *ahk1-3*, it would be interesting to know, what actions it could still perform and whether it is due to being probably of a truncated protein? With the histidine kinase domain still present, it could be an autoactive form, probably being able to autophosphorylate, or bind to BAK1 and inhibit thereby their

shared pathway. This still needs to be investigated. It would also be interesting to know whether it is still able to form heterodimers with BAK1 or homodimers with itself. For *ahk1-6* there was a general detection of the full-length transcript, probably due to only a reduction of transcript level of AHK1, compared to wt (Kumar et al., 2013). This means, that it is a knock-down, rather than a knock-out mutant.

The results could explain the main differences observed in *ahk1-3* and *ahk1-4* mutants under different temperatures, light conditions, stress treatments, and phytohormone production (**Figure 3-1, Figure 3-2, Figure 3-3**). For the phytohormone salicylic acid (SA) it is necessary to point out, that it has been tested on *ahk1* plant lines before, but with concentrations being too low to trigger a sufficient response for SA according to published data (1 µM SA, (Dautel, 2016)). Moreover, levels of cellular SA have been shown to be significantly altered in *ahk1-3* mutants while JA levels were WT-like (Engelsdorf et al., 2018). Therefore, the exogenous application of SA influences *ahk1* mutants similar to the WT, but the cellular level is altered significantly (**Figure 3-1**, (Engelsdorf et al., 2018)).

Investigation of *ahk1* plants, showed altered reactions compared to wt, when treated with different light conditions. The shortened hypocotyl of the *ahk1*-alleles in comparison to wt were caused by stress during seed production due to fluctuating growing conditions of the plants. It took several reproduction cycles to get healthy seeds, noticed by a constant reduction of the FR phenotype of mutant seedlings. Seedlings grown under optimal conditions did not show a FR phenotype, seedlings grow rather wt-like (results not shown).

In cooperation with the AG Hiltbrunner at the University of Freiburg, I took the first sample of seeds of non-stressed plants to repeat the experiments under more stable conditions. Therefore, I repeated dose response curves for *A. thaliana ahk1* mutant seedlings and I could see similar results for wt plants under different light treatments (**Figure 3-2** A)-C)). The largest difference of *ahk1* hypocotyls lengths compared to wt with FR and BL seem to be around 0,01 $\mu mol/m^2*s$ (**Figure 3-2** A) and B)), which is still insignificant. This means, that AHK1 is not a directly involved in light signaling. Then we tested FR-light–associated high-irradiance responses (HIR) persistence with 5 $\mu mol/m^2*s$ 2,5 min FR light pulses. Also, with no significant outcome. For all four experiments *bak1-1* and *bak1-1 ahk1-3*, in comparison to the wt, reacted less responsive. It is not clear, whether they react that way because of the light treatment or whether it is due to germinating and growing slower in general under every condition, so these results need to be taken under careful consideration, that these plants in general show altered development, regardless to light signaling. Another issue is, that the experiments were

executed with Ws-2 plants that lack PhyD, and the consequences of this mutation still need to be better understood (Aukerman et al., 1997). Therefore, the plant lines were not optimal in general to test, whether a protein is part of light signaling.

Due to FR light showing the biggest impact on very low fluence response (VLFR) we performed qPCR with the VLFR reporter gene *PRR9* (**Figure 3-3** A)). The observed differences are due to spilled extracted RNA from *ahk1-4* plant material Additionally, we looked with qPCR at the transcript levels of *HY5* and *CHS* (**Figure 3-3** B) and D)), different genes involved in light signaling. After performing anthocyanin extraction experiments with an insignificantly reduced accumulation of anthocyanins under FR light stress in *ahk1* mutants. The double mutants *bak1-1 ahk1-3* and *bak1-1 ahk1-4* nevertheless showed significant differences to wt regarding anthocyanin accumulation, which could be due to general inhibitions of the *bak1* plants (**Figure 3-3** C) and D)). Differences in these mutants might be due to anthocyanin extraction being performed after 3 d under FR light and qPCR was performed after 1 h and after 4 h FR light treatment. Differences between the first and the other anthocyanin extraction (**Figure 3-3** C)) could be due to different extraction lengths-, one was performed over 8 h and the other two overnight. This could explain why the differences are insignificant. In another experiment we tested the expression levels of the anthocyanin reportergene *CHS* (CHALCONE SYNTHASE) to further elucidate whether AHK1 plays a role in the anthocyanin accumulation. During this experiment the only significant difference was produced by using 1/3 less cDNA as usually required for cDNA, due to lacking enough cDNA. So, it would have a matching expression level if enough cDNA of *ahk1-4* would have been there, and a direct role of AHK1 in the anthocyanin synthesis is unlikely.

HY5-levels (**Figure 3-3** D)) were increased the most after 1 h FR light treatment. No significant differences in comparison to WT levels were seen here, too. But the results of *ahk1-3* matches on a transcript level, what has been observed in our phopshoproteom (Dautel, 2016). Although HY5 is a key player in light signaling, it was shown, that it could act independently of photoreceptors (Bellegarde et al., 2019; Gaillochet et al., 2020; Zoulias et al., 2019). So we could show, that there is an influence on *HY5* transcript levels in *ahk1* alleles but the transcript levels are nor significantly altered by FR light. In addition to the phenotypic experiments under FR light, this could probably be due to *ahk1* not being part of a light signaling pathway- but on other pathways where HY5 acts as a transcription factor, like ROS homeostasis and response to nitrogen (N) (Bellegarde et al., 2019).

Discussion

As the phenotypic analysis of *ahk* mutants in *A. thaliana* was not very insightful, we decided to look at *AHK1* in another plant species. AHK1 is conserved in dicotyledons (Dautel, 2016; He et al., 2016) and among these dicots we decided to look at the Fabaceae *Lotus japonicus (L. japonicus)*. In *L. japonicus* homologues of AHK2-4 have already been described. We identified further undescribed homologues of AHK1 and AHK5, both genes seemed to underwent duplication in this species. In contrast to this, we could not identify a homologue of CKI1 (**Figure 3-4** A)). The duplication of AHK1 (LHK4a and LHK4b) and AHK5 (LHK5a and LHK5b) in *L. japonicus* could hint to an adapted function, not present in *Arabidopsis*. To elucidate differences between LHK4a and LHK4b, we did an alignment of the EDs of *Lotus* and *Arabidopsis*, following a pairwise distance analysis (**Figure 3-4** C)), which did not lead to clear results. In general, LHK4A is much more expressed in *Lotu*s than LHK4B (Kamal et al., 2020b). Furthermore, there seems to be a spatial separation of both genes: *LHK4A* is more expressed in roots and LHK4B more in leaves. This could hint to *LHK4's* role being highly specific in *Lotus* or that there is an adaptation in its role.

In contrast to *A. thaliana, L. japonicus* can establish symbiosis with both, arbuscular mycorrhiza fungi and rhizobial bacteria (Márquez, 2006; Roy et al., 2020). In this work we focused on the latter, where *L. japonicus* is establishing nodules with *Mesorhizobium loti* (*M. loti*). Nodule formation is a conserved pathway in legumes and dependent on the *AHK4* homologue *LHK1* (Held et al., 2014). A knockout of *LHK1* leads to an arrest of cortical infection thread formation, and therefore the loss of most functional nodules (Held et al., 2014; Miri et al., 2019; Murray et al., 2007). In contrast, a knock-out of *LHK1b* shows only minor effects, working partially redundant to *LHK1* and *LHK3* (Held et al., 2014; Miri et al., 2019). The duplication of AHK1 in *L. japonicus* could therefore be a hint that one of the homologues has acquired a symbiosis-specific function. Nodulation is tightly regulated and dependent on systemic and local stresses, one among others, light exposure of roots, or systemic nitrate status (Nishida et al., 2018; Roy et al., 2020; Tsikou et al., 2018). Because of these hints we decided to take a look at LHK4a in more detail. Interestingly, LHK1, the homolog of AHK4, plays a double role in rhizobial symbiosis. On the one side, *lhk1-1* appears to be linked to a lack of nodules, as the progression of cortical infection threads is arrested. On the other side, *lhk1-1* shows an increased numbers of infection threads. The observations imply a role in both nodule organogenesis as well as Autoregulation of Nodulation (AON). The autoactive *lhk1* mutant *snf2* in contrast shows spontaneous nodule formation in absence of rhizobia (Held et al., 2014; Miri et al., 2019; Plet et al., 2011; Tirichine et al., 2007). This is the opposite to what we could observe in our *lhk4a* mutants, suggesting that LHK1 and LHK4 are acting in different pathways.

However, we could not observe any light dependent differences between *lhk4a* and wildtype here (**Figure 3-4** D)). Alike there was no difference in nodule numbers between *lhk4a* and wildtype at 0 mM nitrate (**Figure 3-4** E)). Thus, *lhk4a* showed reduced nodule formation compared to wt at 5 mM KNO_3, nitrate condition (**Figure 3-4** E)). This could hint either a role of LHK4 in nodule organogenesis or autoregulation of nodulation (AON). Due to the similarity of the phenotypes of *bri1* and *cdpk1* mutants which both show a decreased number of nodules in *Medicago truncatula* , another Fabaceae which is able to form rhizobial symbiosis (Cheng et al., 2017; Ivashuta et al., 2005; Roy et al., 2020). This, and our knowledge, that AHK1 influences BRI1 in *Arabidopsis* could hint, that early nodule organogenesis is more likely the pathway in which LHK4 acts in. Interestingly, *Mtcdpk3* showed an increase in nodule number (Gargantini et al., 2006). Many CDPKs or also called CPKs have been found in the phosphoproteomic study and many have been shown to be part of stress signaling. It is suggested that they are linked to FLS2 and BAK1 (Lei et al., 2020). CDPKs are more directly linked to ion transport system (Saito and Uozumi, 2020), but both, MtBRI1 and MtCDPK1, seem to be important for early nodule formation (Cheng et al., 2017; Ivashuta et al., 2005), hence, this could be LHK4A's main pathway. As could be looking into Ca^{2+}-spiking, which is an important part of early steps in the common symbiotic pathway. The phenotype of *lhk4a-1* could suggest that it acts in this pathway. Working on *lhk4b* mutants and afterwards double mutants with *lhk4a lhk4b* to test whether it has an influence on the observed phenotype. With RT-PCR different genes could be tested to see whether their expression is altered in *lhk4* mutants, like *CDPK1*, *CCAMK*, *NSP1,* and *NIN*; important genes in symbiosis, that act downstream of Ca^{2+}. But also, DGK's, PLD's and PLC's. This could give hints whether the role here is still the same of BRI1 and AHK1/LHK4 or they adapted new roles in *Lotus*. In addition, tests like phenotyping with different phytohormones like BR, auxin, which is important for nodulation, and ethylene which is also important for nodulation, and a completed test with $CaCl_2$, and the Ca^{2+} channel blocker $LaCl_3$ could give hints, whether LHK4 is acting in early organogenesis alike BRI1 and CDPK1 and whether it is dependent on one of the phytohormones acting in early organogenesis. In addition, measuring $[Ca^{2+}]_{cyt}$ with a luminometer, could give insights (Dautel, 2016; Rentel and Knight, 2004; Zheng et al., 2020).

All in all, I could show that a role of AHK1 in light signaling is unlikely. On the contrary, the results show a subtle influence on general stress signaling in *Arabidopsis*. In *Lotus*, I could show, that there is a phenotype, which seems to point out a role in early organogenesis of LHK4, alike BRI1. BAK1's

role is still not investigated in *Lotus*. But, to be sure, further experiments with crossed lines and with qPCRs could give more insights.

4.2 Ligand fishing

The identification of the ligand of *Arabidopsis* HISTIDINE KINASE 1 (AHK1) has never been approached before. It brought some difficulties with itself. AHK1 full length cannot be expressed easily in *E. coli*. Often, there were no colonies or when colonies grew, they would stop growing at some point. AHK1 seems to be lethal for *E. coli*. Therefore, we decided to solely use its well conserved ectodomain (ED) for fishing, which covers amino acid (aa) 100-446 (Figure 1-3). The expression of the $AHK1^{ED}$ required adjustment due to the aa 100 to 103 a hydrophobic aa (aa HFT) and caused problems with the solubility of the protein (Figure 3-4). Hence, a construct starting at aa103 to 446 fused to a MALTOSE BINDING PROTEIN (MBP) tag was used. The $AHK1^{ED}$ is proposed to reach into the apoplastic space and contains a Per-Arnt-Sim- (PAS) domain (Dautel, 2016). PAS-domains were identified in Bacteria, Archaea, and Eukaryota (Henry and Crosson, 2011; Nambu et al., 1991; Rojas-Pirela et al., 2018; Vogt and Schippers, 2015). It serves as a sensor domain in a broad range of perception mechanisms (Nambu et al., 1991; Taylor and Zhulin, 1999). They are known to bind diverse small molecules. Ligand binding to PAS-domains can be dependent on different aspects (Rojas-Pirela et al., 2018). Putative ligands serve as initiators for versatile signal perception acting e.g. through photo-, redox-, chemo-, or phytohormone receptor (Chang et al., 2010; Dautel, 2016; Mougel and Zhulin, 2001; Ryo et al., 2018; Vogt and Schippers, 2015). PAS-domains seem sufficient to bind its ligand, therefore we suggested, that for ligand fishing the ED is sufficient.

Due to the ED reaching into the apoplastic space, we suggested, the putative ligand would be in the apoplast and therefore used an extract of apoplastic washfluid (AWF) of beans for its ligand analysis using mass spectrometry (O'Leary et al., 2016; O'Leary et al., 2014). It was extracted by Prof. C. Zörb. In the AWF many components were identified (Geilfus, 2017; Geilfus et al., 2015a; Geilfus et al., 2015b). Therefore, a lot of different putative ligands were found, but all in all the concentrations of them were very low. This made the identification more difficult. After three repeats with AWF, lipids were repeatedly identified as possible ligands (Table 7-1). The presence of phospholipids and fatty acids (FA) in the apoplast was previously reported (Jung et al., 2012; Misra, 2016; Xiao et al., 2004). To get a more specific result on which lipid could be AHK1's ligand, we extracted lipids from *Arabidopsis* leaves. But the results stayed inconclusive. A possibility could be, that the charge of the lipid or maybe its surrounding is more important for binding to AHK1's PAS-domain. This would be

in line with the CACHE domain pocket, a PAS-like-domain, where pH and hydrophobic binding are important for ligand binding, for example cytokinin to AHK2, AHK3, and AHK4 (Hothorn et al., 2011; Lomin et al., 2015). Identifying AHK1's ligand could be performed by using the AHK1 induced RD29b-promotor assay by treating it with an improved lipid extraction. Chromatography could be used to extract lipid classes and test those on AHK1^{ED}. However, this method would be very time consuming.

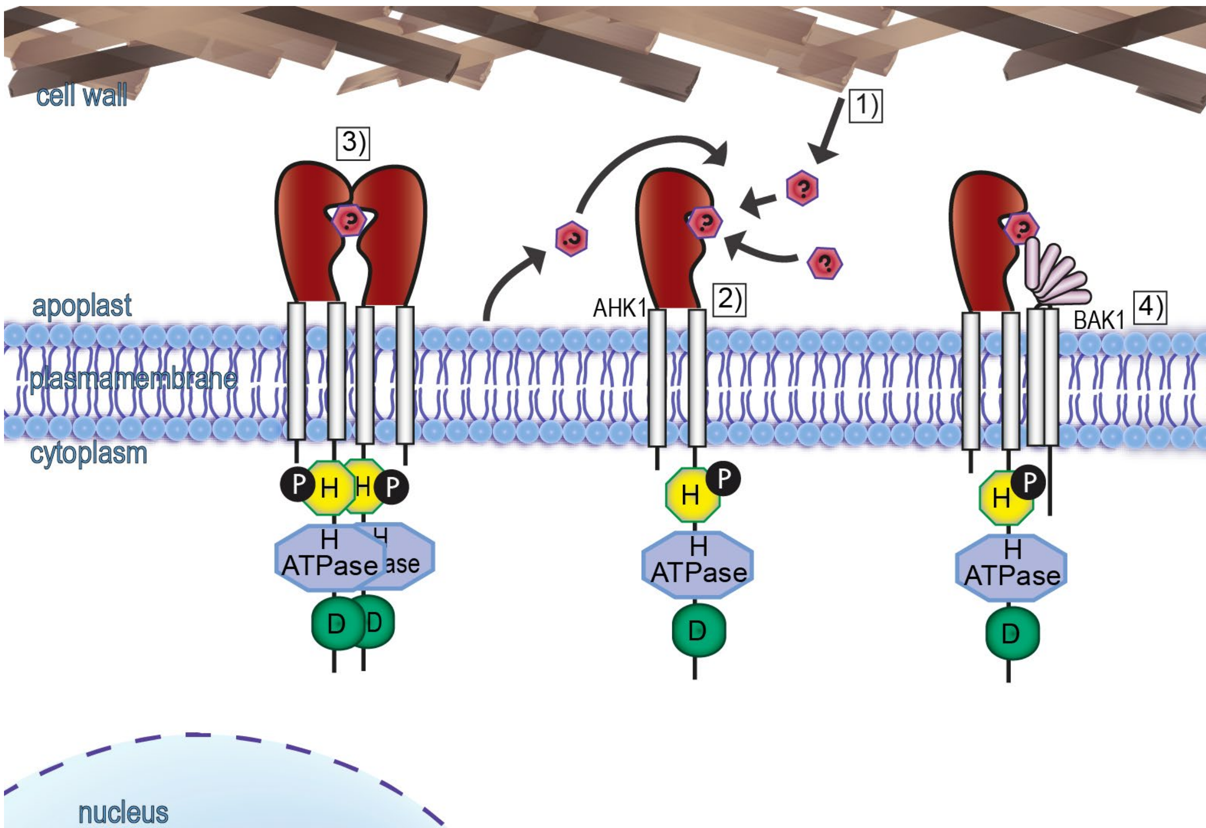

Figure 4-13: What is left to be explored for AHK1's ligand?

1) Where originates the AHK1's ligand and **2)**-**4)** How does the ligand bind to AHK? When does it bind to AHK1? Our data suggest that the putative ligand is in the AWF and that it seems, that stress could lead to a higher production or higher accessibility of the ligand. Yet the ligand could not be identified for certain. Our results suggest it to be a *lyso*-lipid, a proof is missing and some more question arise. It could be, that AHK1 needs to form homodimers to bind the ligand accurately, such is the case with other AHK'S. This could be hard to form with just the ED that we used for ligand fishing. Although just the ED could be enough for ligand binding, the structure could be stable enough to bind the signal. Another possibility could be, that BAK1 could also work as a stabilizing co-receptor of AHK1 as did it for BRI1 and FLS2 and their ligands (Chinchilla et al., 2007; Nam and Li, 2002). A crystallization of all forms would be necessary to elucidate this.

Discussion

We wanted to identify AHK1's main acting pathway, for better elucidation of its ligand. Because this was not possible, it remains to be investigated, where the signal is coming from and what is its trigger (**Figure 4-1** 1)). We seem to be able to show, that the ligand is present in the apoplast, but neither its origin is clear, nor whether it is coming from the plasma membrane, the cell wall, or whether it is mobile in the apoplast. Additional tests are needed to determine the origin of the signal regarding how the ligand binds to AHK1. It needs to be elucidated whether it is associates to its ligand like other AHK's, like AHK2 and AHK4 through homodimerization (Hothorn et al., 2011; Wulfetange et al., 2011). Another possibility would be to bind a ligand like other kinases that also interact with BAK1, supporting the recognition of the ligand as heterodimers (Chinchilla et al., 2007; Li et al., 2002; Sun et al., 2013a; Sun et al., 2013b) or completely different (**Figure 4-1** 2)). AHK1's crystal structure is not resolved yet, therefore it is not understood whether the ED is unstable alone, or it needs other domains to form an active functional protein structure. The solely ED could be deformed, which could lead to not being stable enough to bind its ligand, without AHK1's two transmembrane domains (TD). The two TDs could be necessary to maintain the structure of the ED. Furthermore, like any other AHK, AHK1 forms homodimers (Caesar et al., 2011a; Dautel, 2016; Hericourt et al., 2013), but we could not elucidate if homodimerization is essential to bind the ligand (**Figure 4-1** 3)). This seems to be essential in some HKs, but not in all AHKs (Caesar et al., 2011c; Hothorn et al., 2011; Lomin et al., 2018; West and Stock, 2001; Wulfetange et al., 2011). For the cytokinin binding histidine kinases, like AHK2, 3, and 4, but also for the leucin rich repeat receptor like kinases (LRR-RLK) FLAGELLIN INSENSETIVE 2 (FLS2) and BRASSINOSTEROID-INSENSITIVE RECEPTOR-LIKE KINASE1 (BAK1) and BRASSINOSTEROID INSENSITIVE 1 (BRI1) and BAK1, the protein structure was shown to be highly important for ligand binding (Hohmann et al., 2017; Hothorn et al., 2011; Sun et al., 2013a; Sun et al., 2013b). For AHK2 and 4 the homodimerization was also of importance for binding cyktokinin (Bhate et al., 2015; Hothorn et al., 2011). AHK4 binds different cytokinins based on charge, therefore it does not bind all cytokinins (Hothorn et al., 2011). Unlike AHK1, AHK2-4 have a PAS-like domain, the cyclase histidine kinases associated sensory extracellular (CHASE) domain, which specifically binds cytokinin by discriminating in between different isoforms of cytokinin in the structure of their CHASE-domains (Hothorn et al., 2011; Mahonen et al., 2000; Romanov et al., 2006; Spichal et al., 2004). PAS-domains are known to be able to bind diverse small molecules (Henry and Crosson, 2011; Taylor and Zhulin, 1999). They are characterized via their tertiary structure, which allows them to bind diverse kinds of ligands. Regarding AHK1, carrying a PAS-domain could mean, that its ligand is not one very specific molecule, but maybe a class of

molecules with a specific charge, alike AHK4's ligand (Hothorn et al., 2011; Romanov et al., 2006). This class of molecules could be a class of lipids (e.g. anionic lipids) for AHK1. This could explain the results of our PIP-Strip™ (**appendix**). This experiment still needs to be repeated. It was performed once with washing with PBS, TBS could be leading to cleaner results, due to its better washing abilities.

Considering, that AHK1 not only forms homodimers but also heterodimers with BAK1, and the fact that BAK1 serves as co-receptor that helps to bind the ligand of some LRR-RLKs, like its interaction partners FLS2 and BRI1, makes it necessary to investigate, if BAK1 is important for ligand binding of AHK1(**Figure 4-1** 4)) (Chinchilla et al., 2007; Li et al., 2002; Nam and Li, 2002). Homodimers of AHK1 could be an inactive or active version of AHK1 (Dautel, 2016). AHK1 homodimers could also activate a different pathway than the AHK1 BAK1 heterodimers. This should be considered when further analysis is designed, because it could have also affected our results in the LC-MS. In conclusion: our results could mean anything.

4.3 Evaluating assays for delving into putative ligands

Delving into identifying the ligand of AHK1 lead to putative ligands. But the question whether the ligand is a lipid could not be answered through LC-MS. Hence, another approach was required. We tested several assay systems, like the pCOLD assay in *E. coli*, the ethylene assay, and the AHK1-induced promotor assay in plant tissue. The pCOLD assay identified and verified putative ligands of AHK2, AHK3, AHK4, and AHK5 (Heunemann, 2016; Mizuno and Yamashino, 2010; Yamada et al., 2001). However, full length AHK1 stopped the growing process of *E. coli* completely. Hence, we continued with an other assay for ligand fishing.

Applying the ethylene assay we could solely show, that AWF treatment did neither induce an ethylene response in the wt, nor in *ahk1-4* leave discs. In contrast, *ahk1-3* showed an ethylene response upon treatment with AWF derived from mannitol treated bean leaves. In wt this is explained, by ethylene production depending on a strong elicitor, which AWF is not. Also, overexpressor lines are usually taken for this assay. Differences between the alleles could be explained by remaining transcripts in *ahk1-3*, which shows transcript until after the histidine kinase domains, *ahk1-4* in contrast is a KO mutant. Phenotypic differences between the alleles and wt could indicate *ahk1-3* being a gain of function mutant that may accumulate a somehow dominant-active AHK1 fragment (**Figure 3-5** E), **Figure 3-1** D)). The rise in ethylene production of *bak1-1* leave discs might be due to a hurt disc, which can also lead to inducing ethylene production. This could have happened after transferring the

discs from the petri dish into the glass vial. In conclusion, we did not pursue this assay for ligand identification, due to the need of a huge amount of our elicitor, the AWF, which is not easy to produce in large amounts. Furthermore, an AHK1 overexpression line would be required for clear results.

We tried to re-establish another higher through-put assay, which was used for AHK's 2-5. It is based on the KMI001 strain of *E. coli*, the pCold Assay. After testing AHK1 in this assay, it seems to not be suitable for AHK1, due to our positive control AHK5 being able to produce blue from the lacZ gene, but AHK1 was not able to. The bacteria seemed to stop reproducing at some point. It could be, that with different growing conditions this assay could work. Looking for another faster assay could still be useful due to the many questions still being left, unless the lipid inhibitors will lead fast to the ligand. Consequently, we pursued the already introduced AHK1-induced promotor assay on its functionality for our purpose.

The AHK1-GFP induced promotor assay is an assay based on transiently expressed genes in *Nicotiana benthamiana* plant leaves. AHK1-GFP, that localizes to the plasma membrane, induces the expression of the *RD29b* promotor driven NUCLEAR LOCALIZATION SIGNAL (NLS):mCherry, which localizes to the nucleus (Caesar K; unpublished). The AHK1-GFP induced promotor assay was at first reestablished with a mannitol treatment of *N. benthamiana* leaves. After 1 h of treatment, the expression of the NLS-mCherry rose. RD29b::NLS is positively regulated by AHK1 activity. In the next phase, a range of lipid inhibitors were tested on the assay. The focus has been laid on PA-pathway inhibitors: neomycin, DGK inhibitor (DGKI), *lyso*-PA and mainly *n*-butanol with its negative control *sec*-butanol due to finding similar expression patterns as after mannitol treatment (**Figure 1-2**, **Figure 3-5** A)-C)). A treatment timespan of 15 min with 0,05 % of any inhibitor was sufficient to measure significant differences between inhibitor and control treatments as well as infiltrations without degraded signals, like we could observe after 2 h (**Figure 3-6** D)). The fast reaction of AHK1-induced NLS-mCherry accumulation in response to the tested PA synthesis inhibitors could be due to a suggested involvement of PA in cellular pH dynamics (Li et al., 2019). Thereby PA signaling acts in stress tolerance and microtubule organization through its interaction partners ARABIDOPSIS SALT OVERLY SENSITIVE 1 (SOS1) (Wang et al., 2007; Yao and Xue, 2018; Yu et al., 2010), and PLASMAMEMBRANE INTRINSIC PROTEINS (PIPs, aquaporins), which could explain the similar patterns after mannitol treatment (Bellati et al., 2016; Li et al., 2019; McLoughlin et al., 2013). Another option for the fast reaction upon lipid inhibitor treatment could be the link between stress responses through the second messengers PA and Ca^{2+} upon binding directly to some RBOHs,

including RBOHD (Kadota et al., 2015; Kimura et al., 2012; Ma et al., 2012; Ogasawara et al., 2008; Yao and Xue, 2018; Zhang et al., 2009). As shown previously, exclusively RBOHD was found to be phosphorylated by AHK1 and *ahk1* mutants were shown to be less sensitive to H_2O_2 treatment (Dautel, 2016; Lu et al., 2013). In addition to SOS1, PIPs, different Ca^{2+}-channels, many proteins of the PA-pathways were also found in our phosphoproteomics assay (**Figure 4-2**) (Dautel, 2016). The results of the AHK1-induced *RD29b*-promotor assays, PIP Strip™ and LC-MS data also hint at an involvement of AHK1 in this pathway. Still, the proof of a direct binding of PA to full-length-AHK1 is missing. Also, it still needs to be investigated, whether PA is directly or indirectly influencing AHK1 or the positive regulation of AHK1 by PA biosynthesis. The inhibitor *n*-butanol indicates, that AHK1 is inhibited by PA, but not in which way (**Figure 3-6**). Our findings of a putative role of AHK1 in PA signaling are backed up by newly published data, that link BRI1 and BAK1 to PA signaling in a Ca^{2+}-dependent manner (Gully et al., 2019; Kretynin et al., 2019). According to these published data, there is a link between the BRI1/BAK1 complex PA, Ca^{2+}, BR signaling and the redox system (Kretynin et al., 2019). Our data suggests that this link may be AHK1, as it interacts at least with BAK1 (Caesar, unpublished; Dautel, 2016) (**Figure 4-2**).

In conclusion, we could re-establish the AHK1-GFP induced *RD29b*-promotor reporter assay. An assay based on the stress-inducible RD29b-promotor (Liu et al., 2020; Virlouvet et al., 2014), which was shown to be dependent on AHK1 (Caeser K, unpublished). Upon adding of elicitors, the *RD29b*-promotor drives the production of NLS-mCherry which leads to a stronger mCherry signal. This increase in signal is then measured with imageJ. With the assay we could show a significant reaction to the lipid-inhibitor *n*-butanol, that inhibits PHOSPHOLIPASE D (PLD), which forms PA from PC or PE at the PM (**Figure 1-2**). Treatments with *lyso*-PA and DGKI must be repeated, DGKI inhibits the other synthesis pathway of PA at the PM, by binding to DGK. Lesser concentrations and shorter time spans should be used. On the PIP strip™, interactions of $AHK1^{ED}$ with PA but not *lyso*-PA are detected. These results should be kept in mind, although proteins could be swapped by application and the usage of PIP strip™ is very artificial, which becomes even more so, by using just the ED of AHK1 (**appendix**). Furthermore, LC-MS data detected several lipid classes as putative ligand, but never the same one. In general, those fished ligands were phospholipids and FAs. Combining the results of the assay and the LC-MS, this might be a hint to the ligand. AHK1's putative ligand could be a lipid, but neither the lipid nor its lipid class could be determined. Although FAs were the only class of lipids shown to bind to PAS-domains, both saturated, and unsaturated (Fala et al., 2015; King-

Scott et al., 2011; Rojas-Pirela et al., 2018). All in all, it was shown, that AHK1 has a fast influence on the PA pathway. The problem is, that in the AWF only low amounts of molecules are present in general, hence, our statistics are hard to rely on. The LC-MS on AHK1^{ED}, treated with *Arabidopsis* lipid extraction showed, that lipids could be putative ligands. The LC-MS could not specify on which lipid could be the ligand due to no clear overlaps with the AWF. Both treatments lead to fishing phospholipids and FAs. This could be due to the extraction being executed on *Arabidopsis* leaves and not every lipid class is extracted with lipid extractions or with the AWF extractions, which only extracts lipids found in the apoplast.

A vital challenge for the AHK1-promotor assay was, that the signals or proteins were degraded or diffused out of the nucleus after 1 - 2 h. 1 h was the standard timespan to measure the transcriptional influence for this assay, which was used for signal intensity measurements of the nuclei, after 80 mM mannitol treatment. AHK1 reacted strongly to a minimum of lipid inhibitor treatment. 1:1000 dilution of *n*-butanol and DGK-inhibitor (results not shown). The optimal time to measure the intensity of the nuclei for *n*-butanol treatment was after 15 min incubation time (**Figure 3-7**). Both, dilution and timespan, have been previously shown to be sufficient to stimulate seedlings (Li et al., 2019). *lyso*-PA was tested with an applied dilution of 12,5 µM, an increase to 100 µM is possible, and a timespan of 1 h and DGK-inhibitor (U73122) with a dilution of 5 µM and the timespan, both should be tested after 15 min again for a better understanding (Cassim et al., 2019). After 2 h and 1 h treatment the cells looked similar to neomycin and *n*-butanol treatment of the same time span, with probably degraded signals (**Figure 3-7**). Interestingly, the leaves that have only been infiltrated with RD29b::NLS:mCherry did not show this kind of degradation after lipid inhibitor treatment. When both RD29b::NLS-mCherry and AHK1-GFP were expressed in *N. benthamiana* leaves treated with 1 h mannitol- and 2 h neomycin-, *n*- and *sec*- butanol, fluorescent dots were observed in the cytosol.

Thus, the question arises, whether it is likely, that the ligand of AHK1 is a lipid. AHK's have been shown to bind cytokinins and probably H_2O_2. HK's in general are able to bind a broad range of ligands (Cheung and Hendrickson, 2008, 2009; Sevvana et al., 2008; Zhang and Hendrickson, 2010). Ancillary, narrowing down AHK1's putative ligand through looking into specializations in the PAS-domain, which is the most likely place of a ligand to bind, is not optional. PAS-domains are known to bind many kinds of small molecules (Chang et al., 2010; Cheung and Hendrickson, 2009; Henry and Crosson, 2011; Ryo et al., 2018; Vogt and Schippers, 2015). Hence, not being a cytokinin-receptor is unusual for an AHK. Research showed several ligands of HK's in yeast and bacteria. In these

organisms, PAS-domains were shown to be able to associate with saturated and unsaturated FA, but not with any phospholipids (Fala et al., 2015; Henry and Crosson, 2011; Herrou and Crosson, 2011; King-Scott et al., 2011). Considering literature, it is possible that lipids bind to PAS-domains and therefore it is likely, thatthe AHK1 ligand is a small lipid. Upon ligand binding, AHK1 could form a complex with BAK1 and BRI1.

BRI1 is the receptor of the phytohormone brassinosteroid (BR), which biosynthesis has been linked to the Ca^{2+} signaling over e.g. the BR insensitive DWARF1 (DWF1) in the cell. It transmits a fast response from environmental stimuli to the BR pathway by regulating DWF1 (Du and Poovaiah, 2005; Noguchi et al., 1999). BAK1 and BRI1 have been both shown to react to Ca^{2+}-signaling over CNGC's, AHA1 and AHA2. BAK1 and BRI1 also interact with some of them (Dautel, 2016; Ladwig et al., 2015; Oh et al., 2012b; Yuan et al., 2018). It is suggested that they could be interacting with CPKs and the dynamic IQDs, via phosphorylation of especially IQD32, 14, and 2 (Burstenbinder et al., 2017; Dautel, 2016; Kolling et al., 2019). These proteins are found in our phosphoproteomic data (Dautel, 2016), which could hint connected crosstalk between Ca^{2+}, BR, PA, and H_2O_2 based on stress induction (Du and Poovaiah, 2005; Gao et al., 2013; Kretynin et al., 2019; Kuppe et al., 2008; Lv et al., 2018; Zhao et al., 2020; Zhao et al., 2013; Zhu et al., 2013). Moreover, our findings in the promotor assay could indicate that AHK1 can trigger these fast response pathways after stress treatment (**Figure 3-5**). PA, DGKs, PLCs, and PLDs can either be linked to the main pathway or they could be part of the main signalling pathway of AHK1 (**Figure 4-2**) (Dautel, 2016; Derevyanchuk et al., 2019; Gully et al., 2019; Han et al., 2020b; Li et al., 2019; Schlöffel et al., 2019). Noting, that there is no major phenotype in *ahk1* plants, it is not likely, that AHK1 plays a major role in its pathway, but it could serve here as a protein helping BAK1 and BRI1 to adjust to regulating a stress response pathway like the PA pathway and, by that, supporting and helping the cell to adjust to membrane stress. Ca^{2+} could link between AHK1, BRI1, and BAK1, and PA signaling on cellular stress response (**Figure 4-2**). In general, BR treated wt plants have been shown to have significantly altered transcript levels of PLD's and DGK's compared to wt. Additionally, BZR1, a transcription factor downstream of the BRI1 BR signaling pathway, has been shown to be targeted by PA over PP2A (Wu et al., 2014). It shows that BR and PA signaling could be closely entangled and a lot has yet to be investigated on this matter. PLD regulates PLA, which is able to produce FA's and PA.

Furthermore, PLA was shown to be transported into the apoplast for degradation (Jung et al., 2012). This could be a second pathway that could probably be directly targeted by AHK1, BAK1 and BRI1.

Discussion

Lipid distribution concerning plant development and plant organs needs further investigation, as it is yet quite unexplored. There are a lot of questions left in the field of lipids in plants. Their role during plant development and in which parts of the plants which lipids are present or more abundant needs to be explored. I suggest, that AHK1 has a role in lipid adjustment during plant stress, as is to be proposed by the results of our promotor assay and LC-MS data (**Figure 3-6, appendix,** Table 7-1).

Due to not being able to identify at least a specific kind of lipids, we tried to confirm the most likely by using different lipid inhibitors on AHK1 in our promotor assay (Cassim et al., 2019). The tested lipid inhibitors lead to a strong reaction in the treated *N. benthamiana* leaves with transiently overexpressed AHK1. After 2 h of the lowest established treatments, the cell degraded the fluorescence signals from AHK1 and RD29B::NLS-mCherry. This was observed after *n*-butanol, *lyso*-PA, DGKI (R59022), neomycin, and PAO treatment. The reaction was not observed when RD29B::NLS-mCherry was expressed alone in the *N. benthamiana* leaves or with an 80 mM mannitol treatment for 1 h. Therefore we reduced the time to 15 min, a timespan that has been used in recent experiments to characterize the pH-sensing ability of PA (Li et al., 2019).

wt plants treated with 100 nM BR for 6 h showed altered transcript levels of PLD and DGKI family member genes compared to mock treatment. PA was also shown to influence PP2A, which is responsible for polar auxin transport and BR signaling through dephosphorylation of BRI1 and positive regulating BAK1 (Gao et al., 2013; Li and Wang, 2019; Segonzac et al., 2014a; Wu et al., 2011; Wu et al., 2014). We therefore started to use inhibitors of those proteins. Neomycin looked the most promising due to reflecting mannitol treatment, but it is quite unspecific, so we investigated more direct inhibitors of the pathways it effects. *n*-butanol inhibits the last part of the PA production cycle (**Figure 1-1**) (Blunsom and Cockcroft, 2020; Cassim et al., 2019; Hong et al., 2016; Pokotylo et al., 2018). Upon lipid inhibitor treatment, AHK1 significantly enhanced its signaling to RD29b::NLS, eventually after 15 min with just 0,01 %, suggesting a fast activation of a signaling cascade. In consequence, upon PA treatment, AHK1's signaling cascade should be inhibited, indicating that AHK1 could be negatively regulated by the phospholipid. AHK1's putative role in PA-signaling is supported by phosphoproteomic data (Dautel, 2016). It also suggests, that it has an influence on Ca^{2+} signaling proteins as mentioned above, but also many proteins part of the PA production cycle at the PM. Interestingly, there were significant differences in root elongation observed with 1 and 10 mM $CaCl_2$ treatment on *ahk1-3* plants, in comparison to WT (Dautel, 2016). In our phosphoproteomic studies calcium channels (CNGC7, AHA1 and 2) were identified. They could be used for further

studies by being crossed into *ahk1*, *bak1,* and *bri1* plant lines. Also the CaM/CML-binding IQDs could be of interest, due to their changing association with the PM and the nucleus (Burstenbinder et al., 2017; Dautel, 2016; Kolling et al., 2019). IQD2 and 32 seem to also be very promising candidates to be analyzed with *ahk1* and *bak1* based on phosphoproteomic and published data (Burstenbinder et al., 2017; Dautel, 2016). New plant lines, from genes mentioned above, found in phosphoproteomics and that are linked to lipid signalling, could clarify the link between Ca^{2+}, PA, and BR signaling in addition to simple physiological treatment tests and qPCR analysis with marker genes similar to the published ones (Wu et al., 2014). PA also links to other second messengers over e.g. enhancing the activation of RBOHD. ROS is activated upon abiotic and biotic stress factors such as anthocyanins and ethylene, in addition RBOHD can be also activated by PAO (Jakubowicz et al., 2010; Jasso-Robles et al., 2020; Tan et al., 2018; Xu et al., 2017). Furthermore, H_2O_2 and Ca^{2+}fluctuation were also shown to be disturbed in guard cells of *ahk1-4* mutants, which could be a further hint, that AHK1 acts upon many stress signals, rather than one (Lu et al., 2013). Hence, literature, phosphoproteomic data, and our results (**Figure 3-5**, **Figure 3-6**) seem to link this further, although additional experiments are needed to manifest this, yet unsteady, hypothesis. Looking at lipids being the putative ligands, we tried to exclude some lipids, based on the formation of AHK's PAS-domain with the help of online tools, which try to predict the structure of the protein, like phyre2. This was not successful, due to inconclusive results. Identifying the putative ligand could be approached by identifying the lipids which can be found in the AWF. Solely identifying them could reduce the search immensely. Unfortunately, this experiment needs a lot of leaf material for the LC-MS. Additionally, lipids are quickly degraded or oxidized, and some lipid extraction methods are better for some lipid classes than others, which could distort the results. Therefore, the results could still be inconclusive (Shiva et al., 2018). Although the lipid distribution in the cell and at the inner and outer leaflet of the PM and the molecules in the apoplast were tried to be identified several times, further experiments are needed to exclude putative ligands. Mapping molecules in the apoplast upon different treatments could be used as an approach, thereby we need to careful not to miss a molecule group, which could be interesting, due to using an unfitting extraction method (Cassim et al., 2019; Misra, 2016; Schenk et al., 2019). Although we used different negative controls, such as RD29B::NLS:mCherry alone and with the same treatments, and as negative controls treatments *sec*-butanol and water; we did not apply a lipid inhibitor from the other side of the PA-cycle, like wortmannin (**Figure 1-1**). Those need to be further elucidated, whether *n*-butanol causes a specific reaction to the pathway or if it just reacts to the caused stress indirectly.

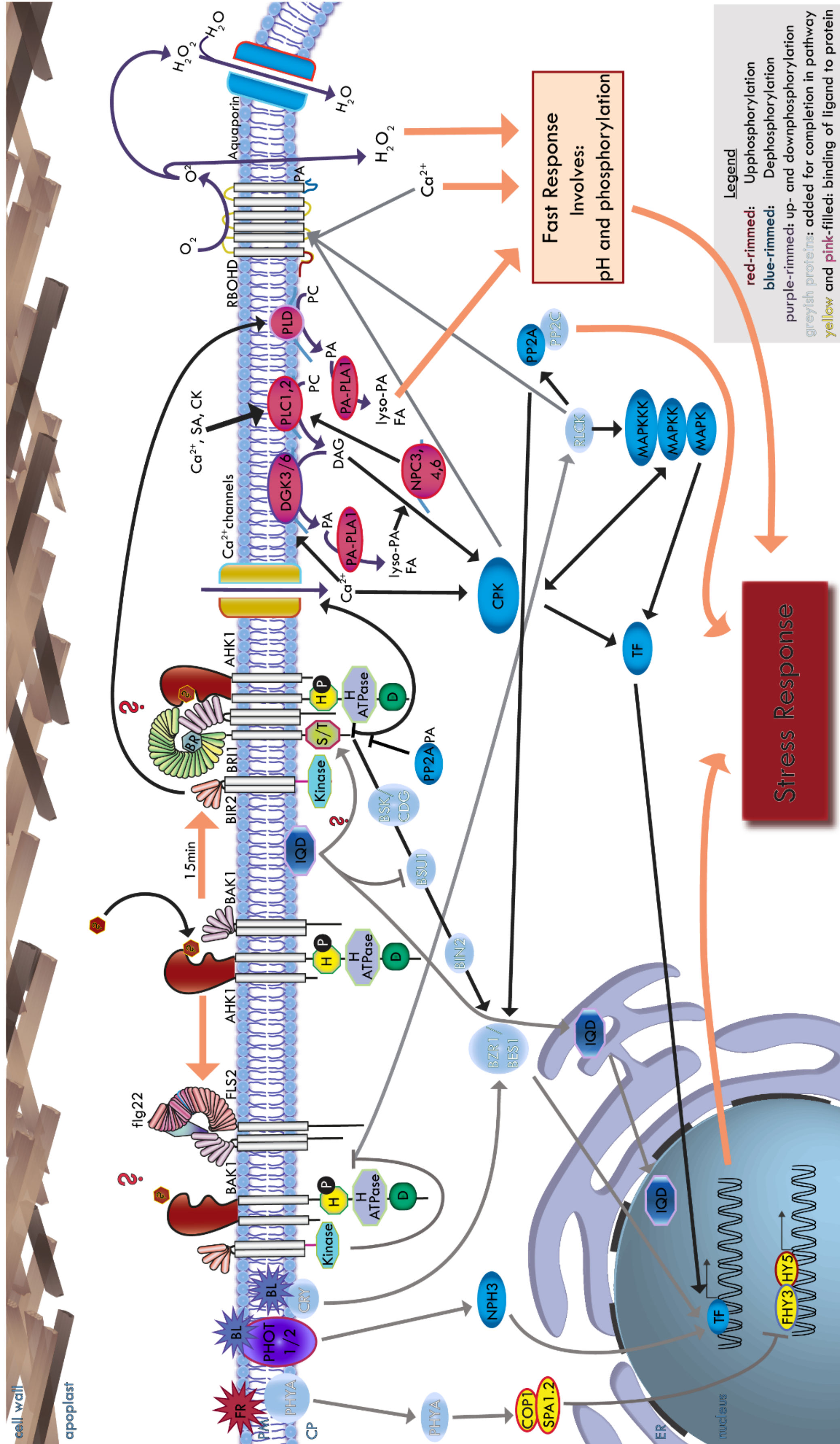

Legend
red-rimmed: Upphosphorylation
blue-rimmed: Dephosphorylation
purple-rimmed: up- and downphosphorylation
greyish proteins: added for completion in pathway
yellow and pink-filled: binding of ligand to protein
Fast Response
Involves:
pH and phosphorylation
Stress Response
cell wall
apoplast
PM
CP
ER
nucleus
Aquaporin
RBOHD
Ca²⁺channels
AHK1
BRI1
BIR2
BAK1
FLS2
flg22
15min
PLD
PLC1,2
DGK3/6
PA-PLA1
NPC3, 4,6
CPK
PP2A
PP2C
MAPKKK
MAPKK
MAPK
TF
IQD
BZR1 / BES1
BIN2
BSU1
BSK/CDG
Kinase
H ATPase
PHOT 1/2
CRY
PHYA
NPH3
COP1
SPA1,2
FHY3
HY5
FR
BL
Ca²⁺, SA, CK
lyso-PA
FA
DAG
PC
PA

Figure 4-14: A proposed signaling cascade for ligand binding activation of AHK1.

After a stress initiation, the putative ligand, most likely a phospholipid or a fatty acid (FA), of AHK1 binds to its PAS-domain. As a result of this association, AHK1 could bind to BAK1, a confirmed interaction (Dautel, 2016) and form a complex with BRI1. BAK1 and BRI1 mediate brassinosteroid signaling (Nam and Li, 2002; Wang et al., 2008b). Subsequently, a signaling cascade via serine/threonine/tyrosin phosphorylation is activated (Dautel, 2016). In addition, the second messengers PA (Cowan, 2006; Liu et al., 2019b; Michaud and Jouhet, 2019), Ca^{2+} (Burstenbinder et al., 2017; Han et al., 2020b; Kolling et al., 2019; Lu et al., 2013; Shi et al., 2018) and pH at the apoplastic PM leaflet, that seem to be affected by Ca^{2+} under certain conditions (Angelova et al., 2018; Caesar et al., 2011b; Geilfus, 2017; Ladwig et al., 2015; Martiniere et al., 2018), are stimulated shortly afterwards, this in return affects membrane lipids (Angelova et al., 2018). The two most important pathways for AHK1 seem to address AHA2, a Ca^{2+}-proton pump, direct interaction partner of BRI1 and a direct (Wanke, unpublished) and indirect of BAK1 (Ladwig et al., 2015; Yuan et al., 2018). CPKs act downstream of and regulating to AHAs (Han et al., 2020b; Shi et al., 2018), they were shown to be part of stress responses through Ca^{2+}- (Saito and Uozumi, 2020; Shi et al., 2018), as also to connect Ca^{2+} with H_2O_2 signaling via RBOHD (Pan et al., 2019). The ROS burst of AHK1 and Ser/Thr/Tyr phosphoproteomics connect it to RBOHD (Dautel, 2016). The apoplastic H_2O_2 transfers from RBOHD to aquaporins, which channel the molecule through membranes into the cell (Bienert et al., 2006; Boursiac et al., 2008). RBOHD is regulated by PA on the inner leaflet of the PM and PA is synthesized at the PM by e.g. DGKs (Arisz et al., 2009; Hothorn et al., 2011; Testerink and Munnik, 2011) and PLDs (Liscovitch et al., 2000). PLA synthesizes PA and fatty acids and is regulated by PLD (Jung et al., 2012). The PA synthesis pathway seems to be the second important pathway that AHK1 affects (Dautel, 2016; Han et al., 2020b; Wielandt et al., 2015). Additional suggested interaction partner of BRI1 and BAK1 are IQDs (Koller and Bent, 2014), proteins that link Ca^{2+} to the reorganization of microtubuli pathway (Burstenbinder et al., 2017; Kolling et al., 2019). Plants can adjust to stress via all mentioned pathways (Hong et al., 2016; Michaud and Jouhet, 2019; Saijo and Loo, 2019; Shi et al., 2018). AHK1 could act in a complex with BAK1 and BRI1 as a finetuning signaling protein, due to its fast response to lipid inhibitor application after 15 min (Gully et al., 2019; Li et al., 2019), which proposes to the connection between phospholipids and phospholipases and Ca^{2+} (Dixit and Jayabaskaran, 2012; Kuppe et al., 2008; Liu et al., 2019b; Meneghelli et al., 2008; Pappan et al., 2004; Qin and Wang, 2002). This is manifested by research linking BRI1, BAK1 to DAG (Derevyanchuk et al., 2019; Gully et al., 2019) and its inhibitors BIR2 and 3 to PLC (Schlöffel et al., 2019). A lot of the proteins in these pathways are co-regulated through PA (D'Ambrosio et al., 2017; Hong et al., 2016; Zhao, 2015). Through BRI1 to BZR1 (He et al., 2019; Ibanez et al., 2018; Li et al., 2017b; Li and He, 2016; Li et al., 2017c), and from the phototropins to NPH3 there are multiple links to blue light and temperature signalling (Briggs et al., 2001; Fiorucci and Fankhauser, 2017; Keuskamp et al., 2011; Wenden et al., 2011; Zhao et al., 2018). With COP1, SPA1.2, FHY3 and HY5 (Delker et al., 2014; Fiorucci and Fankhauser, 2017) there seem to be a probably indirect but conserved link to FR light and heat stress pathways (de Vries et al., 2020; Kim et al., 2014; Legris et al., 2016; Wang et al., 2011). Apart of the proposed complex from AHK1 with BRI1 and BAK1, BAK1 interacts also with FLS2 (Chinchilla et al., 2007; Sun et al., 2013b), to activate plant defence mechanisms, negatively regulated by BIR2 (Halter et al., 2014; Koller and Bent, 2014). With the exception of grey toned proteins, all visible proteins were found in *ahk1-3*/wt phosphoproteomics performed by (Dautel, 2016). Red-rimmed proteins are upregulated, blue-rimmed down, and purple are both.

The promotor assay had also the disadvantage, that it is not a high-throughput method. Trying different points of time and concentration and evaluating the results, is very time-consuming. All in all, our experiments could not give a clear answer to which ligand binds to AHK1, although it seems likely, that it is a lipid. They also seem to indicate, that AHK1 might act as a general stress response protein in dependence of BAK1. In general, proof is needed for these hypotheses.

4.4 Outlook

This project ends with many open questions and putative starting points for new projects. But the basis of all projects have to be proper mutant lines. Therefore, I suggest generating new overexpressor and knock-out lines. Knock-out lines could be generated using CRISPR/Cas9. Previously generated overexpressor plantlines of AHK1 were silenced, which could have multiple reasons. Silencing of transgenes is induced by smallRNAs (sRNA), and, based on new literature, depending on multiple things. It was shown that not only the promotor, but also the presence of introns is influencing the silencing of transgenes, and even the often overlooked terminator seems to play a big role in transgene silencing. (Baeg et al., 2017; Bologna and Voinnet, 2014; Dadami et al., 2013; de Felippes et al., 2020; Matzke and Matzke, 1998). The new lines should be based on the ecotype Col-0, as the mutation in the flg22 recognition-site in FLS2 makes Wassileskija (Ws-2) unsuitable to evaluate AHK1's role between BRI1 and FLS2. Additionally Ws-2 lacks a functional PhyD (Aukerman et al., 1997; Chinchilla et al., 2007), hence the reaction of *ahk1* null-mutants could be different in Col-0, although data suggests, that non-phosphorylatable PhyD leads to less responsiveness in R light (Viczian et al., 2020). Although the reactions of *lhk4a-1* suggest, that AHK1 does not play a role in light signaling. BRI1 and FLS2 phosphomimicking mutants in Col-0 background could be generated thereafter, revealing or dismissing whether there is a significant influence from AHK1 or not. This could also help to clarify whether AHK1 is significantly influenced by H_2O_2-signaling (Lu et al., 2013). In addition to this, *Lotus* double mutants could help to clarify this, too.

Furthermore, the relation between AHK1, BAK1, and BRI1 needs to be analyzed more detailed. It has been shown, that AHK1 interacts directly with BAK1, but not with BRI1 (Dautel, 2016). It still needs to be tested, whether these three proteins form a complex. There are several possibilities to address this, for example Turbo-ID, mating-based split ubiquitin bridge assay (mbSUSB) or three-fluorophore Förster Resonance Energy Transfer – Fluorescence Lifetime Imaging Microscopy (FRET-FLIM) (Arora et al., 2019; Glöckner et al., 2019; Grefen et al., 2009). Biotin based Turbo-ID and three-fluorophore FRET-FLIM would have the advantage of showing the interaction *in planta*,

which is not the case for mbSUSB. mbSUSB is an assay carried out in yeast, an organism which seemingly has no issues in expressing AHK1, BAK1, and BRI1 (Dautel, 2016).

For *ahk1-3* in Ws-2 background, AHK1^{ED} should be analyzed, whether it might be also interacting with BAK1^{ED}-assay to clarify whether *ahk1-3* is partly active. This could clarify further why *ahk1-3* and *ahk1-4* are acting so different at times. An *ahk1-3 ahk1-4* heterozygous double mutants could confirm whether it is a dominant negative form.

In future work in *L. japonicus lhk4b* mutants are needed, to identify its role and differences to *lhk4a* is needed. Therefore, generating *lhk4a lhk4b* mutants is extremely valuable. The detected phenotype of *lhk4a* is similar to MtBRI1 and MtCDPK1 mutants (Cheng et al., 2017; Ivashuta et al., 2005; Roy et al., 2020). Thus, first generated, then crossed *Ljbri1* and *Ljcdpk1* plants with *lhk4a* are necessary to clarify whether it is actually the same pathway for both proteins. Those mutants could be an interesting start to look into early organogenesis of nodule formation. Especially regarding the need of calcium in early organogenesis, as well as looking at calcium spiking upon inoculation (Roy et al., 2020). In addition, probably reformatting lipids during early organogenesis could be interesting. To save time it could be started with testing DGK and PLD transcription levels with RT-PCR of important genes in common symbiosis like NSP2 and NIN in *L. japonicus* under standard and sufficient nitrate conditions, where we detected *lhk4a*'s phenotype. Also, we know, that AHK1 does not interact directly with AtBRI1, but with BAK1, that has three potential homologs in *Lotus* (LotjaGi6g1v0354800,6, 83 % aa identity; LotjaGi2g1v0096200,1, 76 % aa identity; LotjaGi5g1v0283100,1, 78 % aa identity). Hence, it needs to be tested, if one or more interact with LHK4a and LHK4b. It also still has to be elucidated how LHK4a is linked to BRI1.

Also, the performed experiments need to be repeated with new seedling batches due to knowing, that there can be huge differences between seed batches of AHK1 even under the same growing conditions.

New analysis of the phosphoproteom revealed, that many proteins being part of lipid-signaling, -synthesis, -metabolism, and -degradation are influenced by AHK1. Lipid signaling in general is not well investigated in plants, so there are many open questions. This makes it currently even more challenging to understand how *ahk1* works. Our LC-MS data seem to suggest a lipid as AHK1's ligand, but we do not have confirmation yet for this hypothesis. For this a yeast three hybrid system could be used in future (Licitra and Liu, 1996). The data from our promotor assay, using the lipid inhibitor *n*-butanol, seem to suggest the same. Yet, different lipid-inhibitors have to be used to rule out the main

pathway being affected (**Figure 1-2**). These inhibitors would be U73122, inhibiting PLC, acting before DGK, and U59022, which inhibits DGK, one step closer to the production of PA at the PM. Both inhibitors are necessary, due to being unclear on which proteins AHK1 has more influence. The application of *lyso*-PA, a putative ligand, could be useful, too. The application of just PA is difficult due to solubility and degradation. The fluorescent dye FM1-43, which is binding to amphiphilic lipids, possibly the kind of lipids binding to AHK1, and non-fluorescent in water but strongly fluorescent under cyan light (Jelinkova et al., 2010; Schenk et al., 2018) could also be tested. It is excited when bound to lipids and could probably highlight differences when in the promotor assay the inhibitors are applied. One need to keep in mind, that the seen reaction could also be an indirect one over BAK1 and BRI1, due to AHK1's interaction with BAK1 and its phosphorylation from BRI1 (Dautel, 2016). One possibility to rule it out could be to use KO-*N. benthamiana* plants of BAK1 and BRI1 and redo the experiments of the promotor assay. Particularly BRI1 could be interesting, due to its diverse role in many different lipid pathways. A repetition of the PIP strip™ with a proper amount of protein and using TBS-T instead of PBS-T could help additionally.

All in all, the main pathway of AHK1 seems to be related to BRI1. We could identify several pathways, where BAK1 and BRI1 play an important role. As it was shown that BRI1's influence on DGK gives a direct link to lipids and back to AHK1. BRI1 was shown to phosphorylate DGK3 and (Michaud and Jouhet, 2019), several DGK'S were shown to be transcriptionally regulated after BR treatment (Wu et al., 2014). *ahk1*-mutants should be investigated in the same direction, meaning the expression levels of DGKs, PLDs and PLCs should be evaluated via RT-PCR. In addition, the link between PA, Ca^{2+}, BR and AHK1 signaling could be tested first with qPCRs, then physiologically according to the results.

Transiently expressed AHK1 showed a decrease in expression of fluorescent proteintag to DGK inhibitor after 1 h, although this reaction was quite strong, due to showing signs of degradation. Therefore, it was not possible to quantify the expression intensity. The inhibitor should be used with only 15 min of treatment. This quick reaction to the application of lipid inhibitors in general suggests that this is a calcium and/or pH related response. Yet, this has to be confirmed, probably using reporterlines, although proper fluorescent tags could be with mCherry on RD29b::NLS and 35S::AHK1 probably just GFP. At the same time, it should be looked for a putative inhibitor for apoplastic fatty acids (FAs), the second group of lipids popping up in our LC-MS results, besides

phospholipids (Table 7-1). Both, FAs and phospholipids were shown to play a role in the apoplast (Jung et al., 2012; Misra, 2016; Xiao et al., 2004).

In conclusion, this could indicate, that when the ligand, most likely a lipid, binds to the $AHK1^{ED}$, with or without BAK1 is unclear, a signaling cascade is activated, helping the plant to adjust to a range of stressors. This cascade is clearly influenced by BAK1 and possibly BRI1. In this cascade PA, BR, and Ca^{2+} seem to play a major role and SA and ABA are activated after AHK1's ligand binding, hinted by the fast response of AHK1 to applied *n*-butanol, altered SA levels in mutants, but no reaction to exogenous applied SA and ABA. Therefore, the previously observed putative role of AHK1 in osmosensing (Chefdor et al., 2006; Hao et al., 2004; Kumar et al., 2013; Tran et al., 2007; Urao et al., 1999; Wohlbach et al., 2008) could be an indirect result of these closely interacting pathways.

5 References

Afzal, A.J., Wood, A.J., and Lightfoot, D.A. (2008). Plant receptor-like serine threonine kinases: roles in signaling and plant defense. Mol Plant Microbe Interact *21*, 507-517.

Ahmad, M., Jarillo, J.A., and Cashmore, A.R. (1998). Chimeric Proteins between cry1 and cry2 Arabidopsis Blue Light Photoreceptors Indicate Overlapping Functions and Varying Protein Stability. The Plant Cell *10*, 197-207.

Ahmed, N.U., Park, J.I., Jung, H.J., Yang, T.J., Hur, Y., and Nou, I.S. (2014). Characterization of dihydroflavonol 4-reductase (DFR) genes and their association with cold and freezing stress in Brassica rapa. Gene *550*, 46-55.

Alberts B, J.A., Lewis J, et al. (2002). Molecular Biology of the Cell., 4th edition edn (New York: Garland Science).

Albrecht, C., Boutrot, F., Segonzac, C., Schwessinger, B., Gimenez-Ibanez, S., Chinchilla, D., Rathjen, J.P., de Vries, S.C., and Zipfel, C. (2012). Brassinosteroids inhibit pathogen-associated molecular pattern-triggered immune signaling independent of the receptor kinase BAK1. P Natl Acad Sci USA *109*, 303-308.

Alonso, J.M., Hirayama, T., Roman, G., Nourizadeh, S., and Ecker, J.R. (1999). EIN2, a bifunctional transducer of ethylene and stress responses in Arabidopsis. Science *284*, 2148-2152.

An, C., and Mou, Z. (2011a). Salicylic acid and its function in plant immunity. J Integr Plant Biol *53*, 412-428.

An, C., and Mou, Z. (2011b). Salicylic Acid and its Function in Plant ImmunityF. Journal of Integrative Plant Biology *53*, 412-428.

An, F.Y., Zhao, Q.O., Ji, Y.S., Li, W.Y., Jiang, Z.Q., Yu, X.C., Zhang, C., Han, Y., He, W.R., Liu, Y.D., *et al.* (2010). Ethylene-Induced Stabilization of ETHYLENE INSENSITIVE3 and EIN3-LIKE1 Is Mediated by Proteasomal Degradation of EIN3 Binding F-Box 1 and 2 That Requires EIN2 in Arabidopsis. Plant Cell *22*, 2384-2401.

Angelova, M.I., Bitbol, A.F., Seigneuret, M., Staneva, G., Kodama, A., Sakuma, Y., Kawakatsu, T., Imai, M., and Puff, N. (2018). pH sensing by lipids in membranes: The fundamentals of pH-driven migration, polarization and deformations of lipid bilayer assemblies. Bba-Biomembranes *1860*, 2042-2063.

Antolín-Llovera, M., Ried, M.K., and Parniske, M. (2014). Cleavage of the SYMBIOSIS RECEPTOR-LIKE KINASE ectodomain promotes complex formation with Nod factor receptor 5. Curr Biol *24*, 422-427.

Arisz, S.A., Testerink, C., and Munnik, T. (2009). Plant PA signaling via diacylglycerol kinase. Biochim Biophys Acta *1791*, 869-875.

Arora, D., Abel, N.B., Liu, C., Van Damme, P., Vu, L.D., Tornkvist, A., Impens, F., Eeckhout, D., Goossens, A., De Jaeger, G., *et al.* (2019). Establishment of Proximity-dependent Biotinylation Approaches in Different Plant Model Systems. bioRxiv, 701425.

References

Arsovski, A.A., Galstyan, A., Guseman, J.M., and Nemhauser, J.L. (2012). Photomorphogenesis. Arabidopsis Book *10*, e0147.

Aukerman, M.J., Hirschfeld, M., Wester, L., Weaver, M., Clack, T., Amasino, R.M., and Sharrock, R.A. (1997). A deletion in the PHYD gene of the Arabidopsis Wassilewskija ecotype defines a role for phytochrome D in red/far-red light sensing. Plant Cell *9*, 1317-1326.

Backer, R., Mahomed, W., Reeksting, B.J., Engelbrecht, J., Ibarra-Laciette, E., and van den Berg, N. (2015). Phylogenetic and expression analysis of the NPR1-like gene family from Persea americana (Mill.). Front Plant Sci *6*.

Baeg, K., Iwakawa, H., and Tomari, Y. (2017). The poly(A) tail blocks RDR6 from converting self mRNAs into substrates for gene silencing. Nat Plants *3*.

Bali, S., Kaur, P., Sharma, A., Ohri, P., Bhardwaj, R., Alyemeni, M.N., Wijaya, L., and Ahmad, P. (2018). Jasmonic acid-induced tolerance to root-knot nematodes in tomato plants through altered photosynthetic and antioxidative defense mechanisms. Protoplasma *255*, 471-484.

Barneda, D., Cosulich, S., Stephens, L., and Hawkins, P. (2019). How is the acyl chain composition of phosphoinositides created and does it matter? Biochem Soc T *47*, 1291-1305.

Beck, M., Wyrsch, I., Strutt, J., Wimalasekera, R., Webb, A., Boller, T., and Robatzek, S. (2014). Expression patterns of FLAGELLIN SENSING 2 map to bacterial entry sites in plant shoots and roots. Journal of Experimental Botany *65*, 6487-6498.

Belkhadir, Y., and Chory, J. (2006). Brassinosteroid signaling: a paradigm for steroid hormone signaling from the cell surface. Science *314*, 1410-1411.

Bellati, J., Champeyroux, C., Hem, S., Rofidal, V., Krouk, G., Maurel, C., and Santoni, V. (2016). Novel Aquaporin Regulatory Mechanisms Revealed by Interactomics. Mol Cell Proteomics *15*, 3473-3487.

Bellegarde, F., Maghiaoui, A., Boucherez, J., Krouk, G., Lejay, L., Bach, L., Gojon, A., and Martin, A. (2019). The Chromatin Factor HNI9 and ELONGATED HYPOCOTYL5 Maintain ROS Homeostasis under High Nitrogen Provision. Plant Physiology *180*, 582-592.

Bender, K.W., Blackburn, R.K., Monaghan, J., Derbyshire, P., Menke, F.L., Zipfel, C., Goshe, M.B., Zielinski, R.E., and Huber, S.C. (2017). Autophosphorylation-based Calcium (Ca(2+)) Sensitivity Priming and Ca(2+)/Calmodulin Inhibition of Arabidopsis thaliana Ca(2+)-dependent Protein Kinase 28 (CPK28). J Biol Chem *292*, 3988-4002.

Best, J.T., Xu, P., and Graham, T.R. (2019). Phospholipid flippases in membrane remodeling and transport carrier biogenesis. Current Opinion in Cell Biology *59*, 8-15.

Bhate, M.P., Molnar, K.S., Goulian, M., and DeGrado, W.F. (2015). Signal Transduction in Histidine Kinases: Insights from New Structures. Structure *23*, 981-994.

Bienert, G.P., Schjoerring, J.K., and Jahn, T.P. (2006). Membrane transport of hydrogen peroxide. Biochim Biophys Acta *1758*, 994-1003.

References

Bieza, K., and Lois, R. (2001). An Arabidopsis mutant tolerant to lethal ultraviolet-B levels shows constitutively elevated accumulation of flavonoids and other phenolics. Plant Physiol *126*, 1105-1115.

Bisson, M.M., and Groth, G. (2010). New insight in ethylene signaling: autokinase activity of ETR1 modulates the interaction of receptors and EIN2. Mol Plant *3*, 882-889.

Blazquez, M.A., Nelson, D.C., and Weijers, D. (2020). Evolution of Plant Hormone Response Pathways. Annu Rev Plant Biol *71*, 327-353.

Bleecker, A.B., Estelle, M.A., Somerville, C., and Kende, H. (1988). Insensitivity to Ethylene Conferred by a Dominant Mutation in Arabidopsis thaliana. Science *241*, 1086-1089.

Bleecker, A.B., and Kende, H. (2000). Ethylene: a gaseous signal molecule in plants. Annu Rev Cell Dev Biol *16*, 1-18.

Blum, J.J., Lehman, J.A., Horn, J.M., and Gomez-Cambronero, J. (2001). Phospholipase D (PLD) is present in Leishmania donovani and its activity increases in response to acute osmotic stress. J Eukaryot Microbiol *48*, 102-110,

Blunsom, N.J., and Cockcroft, S. (2020). Phosphatidylinositol synthesis at the endoplasmic reticulum. Bba-Mol Cell Biol L *1865*.

Bohn, M., Heinz, E., and Luthje, S. (2001). Lipid composition and fluidity of plasma membranes isolated from corn (Zea mays L.) roots. Arch Biochem Biophys *387*, 35-40,

Bologna, N.G., and Voinnet, O. (2014). The diversity, biogenesis, and activities of endogenous silencing small RNAs in Arabidopsis. Annu Rev Plant Biol *65*, 473-503.

Bolwell, G.P., Bindschedler, L.V., Blee, K.A., Butt, V.S., Davies, D.R., Gardner, S.L., Gerrish, C., and Minibayeva, F. (2002). The apoplastic oxidative burst in response to biotic stress in plants: a three-component system. J Exp Bot *53*, 1367-1376.

Bonaventure, G., Gfeller, A., Proebsting, W.M., Hortensteiner, S., Chetelat, A., Martinoia, E., and Farmer, E.E. (2007). A gain-of-function allele of TPC1 activates oxylipin biogenesis after leaf wounding in Arabidopsis. Plant J *49*, 889-898.

Borsani, O., Valpuesta, V., and Botella, M.A. (2001). Evidence for a role of salicylic acid in the oxidative damage generated by NaCl and osmotic stress in Arabidopsis seedlings. Plant Physiol *126*, 1024-1030,

Boursiac, Y., Boudet, J., Postaire, O., Luu, D.T., Tournaire-Roux, C., and Maurel, C. (2008). Stimulus-induced downregulation of root water transport involves reactive oxygen species-activated cell signaling and plasma membrane intrinsic protein internalization. Plant J *56*, 207-218.

Brazaityte, A., Virsile, A., Jankauskiene, J., Sakalauskiene, S., Samuoliene, G., Sirtautas, R., Novickovas, A., Dabasinskas, L., Miliauskiene, J., Vastakaite, V., *et al.* (2015). Effect of supplemental UV-A irradiation in solid-state lighting on the growth and phytochemical content of microgreens. Int Agrophys *29*, 13-22.

References

Briggs, W.R., Beck, C.F., Cashmore, A.R., Christie, J.M., Hughes, J., Jarillo, J.A., Kagawa, T., Kanegae, H., Liscum, E., Nagatani, A., *et al.* (2001). The phototropin family of photoreceptors. Plant Cell *13*, 993-997.

Briggs, W.R., and Christie, J.M. (2002). Phototropins 1 and 2: versatile plant blue-light receptors. Trends Plant Sci *7*, 204-210,

Broghammer, A., Krusell, L., Blaise, M., Sauer, J., Sullivan, J.T., Maolanon, N., Vinther, M., Lorentzen, A., Madsen, E.B., Jensen, K.J., *et al.* (2012a). Legume receptors perceive the rhizobial lipochitin oligosaccharide signal molecules by direct binding. Proceedings of the National Academy of Sciences *109*, 13859-13864.

Broghammer, A., Krusell, L., Blaise, M., Sauer, J., Sullivan, J.T., Maolanon, N., Vinther, M., Lorentzen, A., Madsen, E.B., Jensen, K.J., *et al.* (2012b). Legume receptors perceive the rhizobial lipochitin oligosaccharide signal molecules by direct binding. Proc Natl Acad Sci U S A *109*, 13859-13864.

Broughton, W.J., and Dilworth, M.J. (1971). Control of leghaemoglobin synthesis in snake beans. Biochem J *125*, 1075-1080,

Bruessow, F., Gouhier-Darimont, C., Buchala, A., Metraux, J.P., and Reymond, P. (2010). Insect eggs suppress plant defence against chewing herbivores. Plant J *62*, 876-885.

Buche, C., Poppe, C., Schafer, E., and Kretsch, T. (2000). eid1: a new Arabidopsis mutant hypersensitive in phytochrome A-dependent high-irradiance responses. Plant Cell *12*, 547-558.

Burstenbinder, K., Moller, B., Plotner, R., Stamm, G., Hause, G., Mitra, D., and Abel, S. (2017). The IQD Family of Calmodulin-Binding Proteins Links Calcium Signaling to Microtubules, Membrane Subdomains, and the Nucleus. Plant Physiology *173*, 1692-1708.

Cacas, J.-L., Gerbeau-Pissot, P., Fromentin, J., Cantrel, C., Thomas, D., Jeannette, E., Kalachova, T., Mongrand, S., Simon-Plas, F., and Ruelland, E. (2017). Diacylglycerol kinases activate *N. benthamiana* NADPH oxidase-dependent oxidative burst in response to cryptogein. Plant, Cell & Environment *40*, 585-598.

Cacas, J.L., Bure, C., Grosjean, K., Gerbeau-Pissot, P., Lherminier, J., Rombouts, Y., Maes, E., Bossard, C., Gronnier, J., Furt, F., *et al.* (2016). Revisiting Plant Plasma Membrane Lipids in Tobacco: A Focus on Sphingolipids. Plant Physiol *170*, 367-384.

Caesar, K. (unpublished).

Caesar, K., Elgass, K., Chen, Z., Huppenberger, P., Witthoft, J., Schleifenbaum, F., Blatt, M.R., Oecking, C., and Harter, K. (2011a). A fast brassinolide-regulated response pathway in the plasma membrane of Arabidopsis thaliana. Plant J *66*, 528-540,

Caesar, K., Elgass, K., Chen, Z.H., Huppenberger, P., Witthoft, J., Schleifenbaum, F., Blatt, M.R., Oecking, C., and Harter, K. (2011b). A fast brassinolide-regulated response pathway in the plasma membrane of Arabidopsis thaliana. Plant Journal *66*, 528-540,

References

Caesar, K., Thamm, A.M., Witthoft, J., Elgass, K., Huppenberger, P., Grefen, C., Horak, J., and Harter, K. (2011c). Evidence for the localization of the Arabidopsis cytokinin receptors AHK3 and AHK4 in the endoplasmic reticulum. J Exp Bot *62*, 5571-5580,

Canfield, D.E., Glazer, A.N., and Falkowski, P.G. (2010). The evolution and future of Earth's nitrogen cycle. Science *330*, 192-196.

Cao, H., Bowling, S.A., Gordon, A.S., and Dong, X.N. (1994). Characterization of an Arabidopsis Mutant That Is Nonresponsive to Inducers of Systemic Acquired-Resistance. Plant Cell *6*, 1583-1592.

Capra, E.J., and Laub, M.T. (2012). Evolution of Two-Component Signal Transduction Systems. Annual Review of Microbiology, Vol 66 *66*, 325-347.

Cassim, A.M., Gouguet, P., Gronnier, J., Laurent, N., Germain, V., Grison, M., Boutte, Y., Gerbeau-Pissot, P., Simon-Plas, F., and Mongrand, S. (2019). Plant lipids: Key players of plasma membrane organization and function. Prog Lipid Res *73*, 1-27.

Castello, M.J., Medina-Puche, L., Lamilla, J., and Tornero, P. (2018). NPR1 paralogs of Arabidopsis and their role in salicylic acid perception. Plos One *13*.

Chalker-Scott, L. (1999). Environmental significance of anthocyanins in plant stress responses. Photochem Photobiol *70*, 1-9.

Chang, C., Kwok, S.F., Bleecker, A.B., and Meyerowitz, E.M. (1993a). ARABIDOPSIS ETHYLENE-RESPONSE GENE ETR1 - SIMILARITY OF PRODUCT TO 2-COMPONENT REGULATORS. Science *262*, 539-544.

Chang, C., Kwok, S.F., Bleecker, A.B., and Meyerowitz, E.M. (1993b). Arabidopsis ethylene-response gene ETR1: similarity of product to two-component regulators. Science *262*, 539-544.

Chang, C., Tesar, C., Gu, M.Y., Babnigg, G., Joachimiak, A., Pokkuluri, P.R., Szurmant, H., and Schiffer, M. (2010). Extracytoplasmic PAS-Like Domains Are Common in Signal Transduction Proteins. Journal of Bacteriology *192*, 1156-1159.

Charpentier, M., Sun, J., Martins, T.V., Radhakrishnan, G.V., Findlay, K., Soumpourou, E., Thouin, J., Véry, A.-A., Sanders, D., Morris, R.J., *et al.* (2016). Nuclear-localized cyclic nucleotide–gated channels mediate symbiotic calcium oscillations. Science *352*, 1102-1105.

Chefdor, F., Benedetti, H., Depierreux, C., Delmotte, F., Morabito, D., and Carpin, S. (2006). Osmotic stress sensing in Populus: components identification of a phosphorelay system. FEBS Lett *580*, 77-81.

Chen, D., Xu, G., Tang, W., Jing, Y., Ji, Q., Fei, Z., and Lin, R. (2013). Antagonistic basic helix-loop-helix/bZIP transcription factors form transcriptional modules that integrate light and reactive oxygen species signaling in Arabidopsis. Plant Cell *25*, 1657-1673.

Chen, F., Shi, X., Chen, L., Dai, M., Zhou, Z., Shen, Y., Li, J., Li, G., Wei, N., and Deng, X.W. (2012). Phosphorylation of FAR-RED ELONGATED HYPOCOTYL1 is a key mechanism defining signaling dynamics of phytochrome A under red and far-red light in Arabidopsis. Plant Cell *24*, 1907-1920,

References

Chen, Y., Chen, W., Li, X., Jiang, H., Wu, P., Xia, K., Yang, Y., and Wu, G. (2014). Knockdown of LjIPT3 influences nodule development in Lotus japonicus. Plant Cell Physiol *55*, 183-193.

Cheng, X., Gou, X., Yin, H., Mysore, K.S., Li, J., and Wen, J. (2017). Functional characterisation of brassinosteroid receptor MtBRI1 in Medicago truncatula. Sci Rep *7*, 9327.

Cheung, J., and Hendrickson, W.A. (2008). Crystal Structures of C-4-Dicarboxylate Ligand Complexes with Sensor Domains of Histidine Kinases DcuS and DctB. Journal of Biological Chemistry *283*, 30256-30265.

Cheung, J., and Hendrickson, W.A. (2009). Structural Analysis of Ligand Stimulation of the Histidine Kinase NarX. Structure *17*, 190-201.

Chinchilla, D., Bauer, Z., Regenass, M., Boller, T., and Felix, G. (2006). The Arabidopsis receptor kinase FLS2 binds flg22 and determines the specificity of flagellin perception. Plant Cell *18*, 465-476.

Chinchilla, D., Zipfel, C., Robatzek, S., Kemmerling, B., Nurnberger, T., Jones, J.D.G., Felix, G., and Boller, T. (2007). A flagellin-induced complex of the receptor FLS2 and BAK1 initiates plant defence. Nature *448*, 497-U412.

Chory, J., Peto, C., Feinbaum, R., Pratt, L., and Ausubel, F. (1989). Arabidopsis thaliana mutant that develops as a light-grown plant in the absence of light. Cell *58*, 991-999.

Clark, S.E. (2001). Cell signaling at the shoot meristem. Nat Rev Mol Cell Bio *2*, 276-284.

Consentino, L., Lambert, S., Martino, C., Jourdan, N., Bouchet, P.E., Witczak, J., Castello, P., El-Esawi, M., Corbineau, F., d'Harlingue, A., *et al.* (2015). Blue-light dependent reactive oxygen species formation by Arabidopsis cryptochrome may define a novel evolutionarily conserved signaling mechanism. New Phytol *206*, 1450-1462.

Cortleven, A., Leuendorf, J.E., Frank, M., Pezzetta, D., Bolt, S., and Schmülling, T. (2019). Cytokinin action in response to abiotic and biotic stresses in plants. Plant, Cell & Environment *42*, 998-1018.

Cowan, A.K. (2006). Phospholipids as plant growth regulators. Plant Growth Regul *48*, 97-109.

D'Agostino, I.B., Deruere, J., and Kieber, J.J. (2000). Characterization of the response of the Arabidopsis response regulator gene family to cytokinin. Plant Physiol *124*, 1706-1717.

D'Ambrosio, J.M., Couto, D., Fabro, G., Scuffi, D., Lamattina, L., Munnik, T., Andersson, M.X., Alvarez, M.E., Zipfel, C., and Laxalt, A.M. (2017). Phospholipase C2 Affects MAMP-Triggered Immunity by Modulating ROS Production. Plant Physiol *175*, 970-981.

Dadami, E., Moser, M., Zwiebel, M., Krczal, G., Wassenegger, M., and Dalakouras, A. (2013). An endogene-resembling transgene delays the onset of silencing and limits siRNA accumulation. Febs Letters *587*, 706-710,

Dautel, R. (2016). Molecular characterization of the *Arabidopsis thaliana* histidine kinase 1 and transitions from the multistep phosphorelay system to Ser/Thr/Tyr phosphorylation (Eberhard Karls Universität Tübingen), pp. 239.

References

Dautel, R., Wu, X.N., Heunemann, M., Schulze, W.X., and Harter, K. (2016). The Sensor Histidine Kinases AHK2 and AHK3 Proceed into Multiple Serine/Threonine/Tyrosine Phosphorylation Pathways in Arabidopsis thaliana. Mol Plant *9*, 182-186.

de Felippes, F.F., Mchale, M., Doran, R.L., Roden, S., Eamens, A.L., Finnegan, E.J., and Waterhouse, P.M. (2020). The key role of terminators on the expression and post-transcriptional gene silencing of transgenes. The Plant Journal *n/a*.

de Vries, J., de Vries, S., Curtis, B.A., Zhou, H., Penny, S., Feussner, K., Pinto, D.M., Steinert, M., Cohen, A., von Schwartzenberg, K., *et al.* (2020). Heat stress response in the closest algal relatives of land plants reveals conserved stress signaling circuits. Plant J.

Deikman, J., and Hammer, P.E. (1995). Induction of Anthocyanin Accumulation by Cytokinins in Arabidopsis thaliana. Plant Physiology *108*, 47-57.

Delker, C., Sonntag, L., James, G.V., Janitza, P., Ibanez, C., Ziermann, H., Peterson, T., Denk, K., Mull, S., Ziegler, J., *et al.* (2014). The DET1-COP1-HY5 Pathway Constitutes a Multipurpose Signaling Module Regulating Plant Photomorphogenesis and Thermomorphogenesis. Cell Reports *9*, 1983-1989.

Denarie, J., and Cullimore, J. (1993). Lipo-oligosaccharide nodulation factors: a minireview new class of signaling molecules mediating recognition and morphogenesis. Cell *74*, 951-954.

Derevyanchuk, M., Kretynin, S., Kolesnikov, Y., Litvinovskaya, R., Martinec, J., Khripach, V., and Kravets, V. (2019). Seed germination, respiratory processes and phosphatidic acid accumulation in Arabidopsis diacylglycerol kinase knockouts - The effect of brassinosteroid, brassinazole and salinity. Steroids *147*, 28-36.

Desikan, R., Last, K., Harrett-Williams, R., Tagliavia, C., Harter, K., Hooley, R., Hancock, J.T., and Neill, S.J. (2006a). Ethylene-induced stomatal closure in Arabidopsis occurs via AtrbohF-mediated hydrogen peroxide synthesis. Plant J *47*, 907-916.

Desikan, R., Last, K., Harrett-Williams, R., Tagliavia, C., Harter, K., Hooley, R., Hancock, J.T., and Neill, S.J. (2006b). Ethylene-induced stomatal closure in Arabidopsis occurs via AtrbohF-mediated hydrogen peroxide synthesis. The Plant Journal *47*, 907-916.

Despres, C., DeLong, C., Glaze, S., Liu, E., and Fobert, P.R. (2000). The arabidopsis NPR1/NIM1 protein enhances the DNA binding activity of a subgroup of the TGA family of bZIP transcription factors. Plant Cell *12*, 279-290,

Dieterle, M., Buche, C., Schafer, E., and Kretsch, T. (2003). Characterization of a novel non-constitutive photomorphogenic cop1 allele. Plant Physiol *133*, 1557-1564.

Ding, P., and Ding, Y. (2020). Stories of Salicylic Acid: A Plant Defense Hormone. Trends Plant Sci *25*, 549-565.

Ding, Y., Sun, T., Ao, K., Peng, Y., Zhang, Y., Li, X., and Zhang, Y. (2018). Opposite Roles of Salicylic Acid Receptors NPR1 and NPR3/NPR4 in Transcriptional Regulation of Plant Immunity. Cell *173*, 1454-1467 e1415.

References

Divi, U.K., Rahman, T., and Krishna, P. (2010). Brassinosteroid-mediated stress tolerance in Arabidopsis shows interactions with abscisic acid, ethylene and salicylic acid pathways. BMC Plant Biol *10*, 151.

Dixit, A.K., and Jayabaskaran, C. (2012). Phospholipid mediated activation of calcium dependent protein kinase 1 (CaCDPK1) from chickpea: a new paradigm of regulation. PLoS One *7*, e51591.

Doyle, J.J., and Luckow, M.A. (2003). The rest of the iceberg. Legume diversity and evolution in a phylogenetic context. Plant Physiology *131*, 900-910,

Du, L., Ali, G.S., Simons, K.A., Hou, J., Yang, T., Reddy, A.S., and Poovaiah, B.W. (2009). Ca(2+)/calmodulin regulates salicylic-acid-mediated plant immunity. Nature *457*, 1154-1158.

Du, L.Q., and Poovaiah, B.W. (2005). Ca2+/calmodulin is critical for brassinosteroid biosynthesis and plant growth. Nature *437*, 741-745.

Duclos, B., Marcandier, S., and Cozzone, A.J. (1991). Chemical properties and separation of phosphoamino acids by thin-layer chromatography and/or electrophoresis. Methods Enzymol *201*, 10-21.

Eichenberg, K., Bäurle, I., Paulo, N., Sharrock, R.A., Rüdiger, W., and Schäfer, E. (2000). Arabidopsis phytochromes C and E have different spectral characteristics from those of phytochromes A and B. FEBS Letters *470*, 107-112.

El-Esawi, M., Arthaut, L.-D., Jourdan, N., d'Harlingue, A., Link, J., Martino, C.F., and Ahmad, M. (2017). Blue-light induced biosynthesis of ROS contributes to the signaling mechanism of Arabidopsis cryptochrome. Scientific Reports *7*, 13875.

Engelsdorf, T., Gigli-Bisceglia, N., Veerabagu, M., McKenna, J.F., Vaahtera, L., Augstein, F., Van der Does, D., Zipfel, C., and Hamann, T. (2018). The plant cell wall integrity maintenance and immune signaling systems cooperate to control stress responses in Arabidopsis thaliana. Science Signaling *11*.

Engstrom, E.M., Ehrhardt, D.W., Mitra, R.M., and Long, S.R. (2002). Pharmacological Analysis of Nod Factor-Induced Calcium Spiking inMedicago truncatula. Evidence for the Requirement of Type IIA Calcium Pumps and Phosphoinositide Signaling. Plant Physiology *128*, 1390-1401.

Fala, A.M., Oliveira, J.F., Adamoski, D., Aricetti, J.A., Dias, M.M., Dias, M.V.B., Sforça, M.L., Lopes-de-Oliveira, P.S., Rocco, S.A., Caldana, C., *et al.* (2015). Unsaturated fatty acids as high-affinity ligands of the C-terminal Per-ARNT-Sim domain from the Hypoxia-inducible factor 3α. Scientific Reports *5*, 12698.

Favory, J.J., Stec, A., Gruber, H., Rizzini, L., Oravecz, A., Funk, M., Albert, A., Cloix, C., Jenkins, G.I., Oakeley, E.J., *et al.* (2009). Interaction of COP1 and UVR8 regulates UV-B-induced photomorphogenesis and stress acclimation in Arabidopsis. EMBO J *28*, 591-601.

Felix, G., Grosskopf, D.G., Regenass, M., Basse, C.W., and Boller, T. (1991). Elicitor-induced ethylene biosynthesis in tomato cells: characterization and use as a bioassay for elicitor action. Plant Physiol *97*, 19-25.

References

Finkelstein, R.R., Gampala, S.S.L., and Rock, C.D. (2002). Abscisic Acid Signaling in Seeds and Seedlings. The Plant Cell *14*, S15-S45.

Fiorucci, A.S., and Fankhauser, C. (2017). Plant Strategies for Enhancing Access to Sunlight. Current Biology *27*, R931-R940,

Fujii, H., and Zhu, J.-K. (2012). Osmotic stress signaling via protein kinases. Cellular and Molecular Life Sciences *69*, 3165-3173.

Fujita, Y., Fujita, M., Satoh, R., Maruyama, K., Parvez, M.M., Seki, M., Hiratsu, K., Ohme-Takagi, M., Shinozaki, K., and Yamaguchi-Shinozaki, K. (2005). AREB1 is a transcription activator of novel ABRE-dependent ABA signaling that enhances drought stress tolerance in Arabidopsis. Plant Cell *17*, 3470-3488.

Fukai, E., Soyano, T., Umehara, Y., Nakayama, S., Hirakawa, H., Tabata, S., Sato, S., and Hayashi, M. (2012). Establishment of a Lotus japonicus gene tagging population using the exon-targeting endogenous retrotransposon LORE1. Plant J *69*, 720-730,

Gaillochet, C., Burko, Y., Platre, M.P., Zhang, L., Simura, J., Kumar, V., Ljung, K., Chory, J., and Busch, W. (2020). Shoot and root thermomorphogenesis are linked by a developmental trade-off. bioRxiv, 2020,2005.2007.083246.

Galen, C., Huddle, J., and Liscum, E. (2004). An experimental test of the adaptive evolution of phototropins: blue-light photoreceptors controlling phototropism in Arabidopsis thaliana. Evolution *58*, 515-523.

Gao, D., Knight, M.R., Trewavas, A.J., Sattelmacher, B., and Plieth, C. (2004). Self-Reporting Arabidopsis Expressing pH and Ca^{2+} Indicators Unveil Ion Dynamics in the Cytoplasm and in the Apoplast under Abiotic Stress. Plant Physiology *134*, 898-908.

Gao, H.B., Chu, Y.J., and Xue, H.W. (2013). Phosphatidic acid (PA) binds PP2AA1 to regulate PP2A activity and PIN1 polar localization. Mol Plant *6*, 1692-1702.

Gargantini, P.R., Gonzalez-Rizzo, S., Chinchilla, D., Raices, M., Giammaria, V., Ulloa, R.M., Frugier, F., and Crespi, M.D. (2006). A CDPK isoform participates in the regulation of nodule number in Medicago truncatula. The Plant Journal *48*, 843-856.

Geilfus, C.M. (2017). The pH of the Apoplast: Dynamic Factor with Functional Impact Under Stress. Mol Plant *10*, 1371-1386.

Geilfus, C.M., Mithofer, A., Ludwig-Muller, J., Zorb, C., and Muehling, K.H. (2015a). Chloride-inducible transient apoplastic alkalinizations induce stomata closure by controlling abscisic acid distribution between leaf apoplast and guard cells in salt-stressed Vicia faba. New Phytologist *208*, 803-816.

Geilfus, C.M., Niehaus, K., Godde, V., Hasler, M., Zorb, C., Gorzolka, K., Jezek, M., Senbayram, M., Ludwig-Muller, J., and Muhling, K.H. (2015b). Fast responses of metabolites in Vicia faba L. to moderate NaCl stress. Plant Physiology and Biochemistry *92*, 19-29.

Ghelis, T. (2011). Signal processing by protein tyrosine phosphorylation in plants. Plant Signal Behav *6*, 942-951.

References

Ghelis, T., Bolbach, G., Clodic, G., Habricot, Y., Miginiac, E., Sotta, B., and Jeannette, E. (2008). Protein tyrosine kinases and protein tyrosine phosphatases are involved in abscisic acid-dependent processes in Arabidopsis seeds and suspension cells. Plant Physiol *148*, 1668-1680,

Giliberto, L., Perrotta, G., Pallara, P., Weller, J.L., Fraser, P.D., BramLey, P.M., Fiore, A., Tavazza, M., and Giuliano, G. (2005). Manipulation of the Blue Light Photoreceptor Cryptochrome 2 in Tomato Affects Vegetative Development, Flowering Time, and Fruit Antioxidant Content. Plant Physiology *137*, 199-208.

Giovannoni, J.J. (2004). Genetic regulation of fruit development and ripening. Plant Cell *16*, S170-S180,

Glöckner, N., zur Oven-Krockhaus, S., Wackenhut, F., Burmeister, M., Wanke, F., Holzwart, E., Meixner, A.J., Wolf, S., and Harter, K. (2019). Three-fluorophore FRET-FLIM enables the study of trimeric protein interactions and complex formation with nanoscale resolution in living plant cells. bioRxiv, 722124.

Gomez-Gomez, L., Bauer, Z., and Boller, T. (2001a). Both the extracellular leucine-rich repeat domain and the kinase activity of FLS2 are required for flagellin binding and signaling in arabidopsis. Plant Cell *13*, 1155-1163.

Gomez-Gomez, L., Bauer, Z., and Boller, T. (2001b). Both the extracellular leucine-rich repeat domain and the kinase activity of FSL2 are required for flagellin binding and signaling in Arabidopsis. Plant Cell *13*, 1155-1163.

Gomez-Merino, F.C., Brearley, C.A., Ornatowska, M., Abdel-Haliem, M.E., Zanor, M.I., and Mueller-Roeber, B. (2004). AtDGK2, a novel diacylglycerol kinase from Arabidopsis thaliana, phosphorylates 1-stearoyl-2-arachidonoyl-sn-glycerol and 1,2-dioleoyl-sn-glycerol and exhibits cold-inducible gene expression. J Biol Chem *279*, 8230-8241.

Gonzalez-Villagra, J., Kurepin, L.V., and Reyes-Diaz, M.M. (2017). Evaluating the involvement and interaction of abscisic acid and miRNA156 in the induction of anthocyanin biosynthesis in drought-stressed plants. Planta *246*, 299-312.

Goring, D.R., and Walker, J.C. (2004). Self-rejection - A new kinase connection. Science *303*, 1474-1475.

Goto, E., Hayashi, K., Furuyama, S., Hikosaka, S., and Ishigami, Y. (2016). Effect of UV light on phytochemical accumulation and expression of anthocyanin biosynthesis genes in red leaf lettuce. Acta Hortic *1134*, 179-185.

Grefen, C., Obrdlik, P., and Harter, K. (2009). The determination of protein-protein interactions by the mating-based split-ubiquitin system (mbSUS). Methods Mol Biol *479*, 217-233.

Grefen, C., Stadele, K., Ruzicka, K., Obrdlik, P., Harter, K., and Horak, J. (2008). Subcellular localization and in vivo interactions of the Arabidopsis thaliana ethylene receptor family members. Mol Plant *1*, 308-320,

References

Grison, M.S., Brocard, L., Fouillen, L., Nicolas, W., Wewer, V., Dormann, P., Nacir, H., Benitez-Alfonso, Y., Claverol, S., Germain, V., *et al.* (2015). Specific Membrane Lipid Composition Is Important for Plasmodesmata Function in Arabidopsis. Plant Cell *27*, 1228-1250,

Grunewald, W., van Noorden, G., Van Isterdael, G., Beeckman, T., Gheysen, G., and Mathesius, U. (2009). Manipulation of auxin transport in plant roots during Rhizobium symbiosis and nematode parasitism. Plant Cell *21*, 2553-2562.

Gujjar, R.S., and Supaibulwatana, K. (2019). The Mode of Cytokinin Functions Assisting Plant Adaptations to Osmotic Stresses. Plants (Basel) *8*.

Gully, K., Pelletier, S., Guillou, M.C., Ferrand, M., Aligon, S., Pokotylo, I., Perrin, A., Vergne, E., Fagard, M., Ruelland, E., *et al.* (2019). The SCOOP12 peptide regulates defense response and root elongation in Arabidopsis thaliana. J Exp Bot *70*, 1349-1365.

Guo, H., Li, L., Aluru, M., Aluru, S., and Yin, Y. (2013). Mechanisms and networks for brassinosteroid regulated gene expression. Current Opinion in Plant Biology *16*, 545-553.

Hall, A.E., and Bleecker, A.B. (2003). Analysis of combinatorial loss-of-function mutants in the Arabidopsis ethylene receptors reveals that the ers1 etr1 double mutant has severe developmental defects that are EIN2 dependent. Plant Cell *15*, 2032-2041.

Hall, B.P., Shakeel, S.N., Amir, M., Haq, N.U., Qu, X., and Schaller, G.E. (2012). Histidine Kinase Activity of the Ethylene Receptor ETR1 Facilitates the Ethylene Response in Arabidopsis Plant Physiology *159*, 682-695.

Halter, T., Imkampe, J., Mazzotta, S., Wierzba, M., Postel, S., Bucherl, C., Kiefer, C., Stahl, M., Chinchilla, D., Wang, X.F., *et al.* (2014). The Leucine-Rich Repeat Receptor Kinase BIR2 Is a Negative Regulator of BAK1 in Plant Immunity. Current Biology *24*, 134-143.

Han, X., Huang, X., and Deng, X.W. (2020a). The Photomorphogenic Central Repressor COP1: Conservation and Functional Diversification during Evolution. Plant Communications *1*, 100044.

Han, X., Yang, Y., Zhao, F., Zhang, T., and Yu, X. (2020b). An improved protein lipid overlay assay for studying lipid-protein interactions. Plant Methods *16*, 33.

Haney, C.H., Riely, B.K., Tricoli, D.M., Cook, D.R., Ehrhardt, D.W., and Long, S.R. (2011). Symbiotic rhizobia bacteria trigger a change in localization and dynamics of the Medicago truncatula receptor kinase LYK3. Plant Cell *23*, 2774-2787.

Hanks, S.K., Quinn, A.M., and Hunter, T. (1988). The protein kinase family: conserved features and deduced phylogeny of the catalytic domains. Science *241*, 42-52.

Hao, G.P., Wu, Z.Y., Chen, M.S., Cao, M.Q., Pelletier, G., Huang, C.L., and Yang, Q. (2004). ATHK1 gene regulates signal transduction of osmotic stress in Arabidopsis thaliana. Zhi Wu Sheng Li Yu Fen Zi Sheng Wu Xue Xue Bao *30*, 553-560,

Hass, C., Lohrmann, J., Albrecht, V., Sweere, U., Hummel, F., Yoo, S.D., Hwang, I., Zhu, T., Schafer, E., Kudla, J., *et al.* (2004). The response regulator 2 mediates ethylene signaling and hormone signal integration in Arabidopsis. EMBO J *23*, 3290-3302.

References

Hauser, F., Waadt, R., and Schroeder, J.I. (2011). Evolution of abscisic acid synthesis and signaling mechanisms. Curr Biol *21*, R346-355.

Hayashi, T., Banba, M., Shimoda, Y., Kouchi, H., Hayashi, M., and Imaizumi-Anraku, H. (2010). A dominant function of CCaMK in intracellular accommodation of bacterial and fungal endosymbionts. Plant J *63*, 141-154.

He, G., Liu, J., Dong, H., and Sun, J. (2019). The Blue-Light Receptor CRY1 Interacts with BZR1 and BIN2 to Modulate the Phosphorylation and Nuclear Function of BZR1 in Repressing BR Signaling in Arabidopsis. Mol Plant *12*, 689-703.

He, J.X., Gendron, J.M., Yang, Y., Li, J., and Wang, Z.Y. (2002). The GSK3-like kinase BIN2 phosphorylates and destabilizes BZR1, a positive regulator of the brassinosteroid signaling pathway in Arabidopsis. Proc Natl Acad Sci U S A *99*, 10185-10190,

He, Y., Liu, X., Ye, L., Pan, C., Chen, L., Zou, T., and Lu, G. (2016). Genome-Wide Identification and Expression Analysis of Two-Component System Genes in Tomato. Int J Mol Sci *17*, 1204.

Heese, A., Hann, D.R., Gimenez-Ibanez, S., Jones, A.M.E., He, K., Li, J., Schroeder, J.I., Peck, S.C., and Rathjen, J.P. (2007). The receptor-like kinase SERK3/BAK1 is a central regulator of innate immunity in plants. P Natl Acad Sci USA *104*, 12217-12222.

Held, M., Hou, H., Miri, M., Huynh, C., Ross, L., Hossain, M.S., Sato, S., Tabata, S., Perry, J., Wang, T.L., *et al.* (2014). *Lotus japonicus* Cytokinin Receptors Work Partially Redundantly to Mediate Nodule Formation. The Plant Cell *26*, 678-694.

Henry, J.T., and Crosson, S. (2011). Ligand-binding PAS-domains in a genomic, cellular, and structural context. Annu Rev Microbiol *65*, 261-286.

Hentrich, M., Böttcher, C., Düchting, P., Cheng, Y., Zhao, Y., Berkowitz, O., Masle, J., Medina, J., and Pollmann, S. (2013). The jasmonic acid signaling pathway is linked to auxin homeostasis through the modulation of YUCCA8 and YUCCA9 gene expression. The Plant journal : for cell and molecular biology *74*, 626-637.

Hericourt, F., Chefdor, F., Bertheau, L., Tanigawa, M., Maeda, T., Guirimand, G., Courdavault, V., Larcher, M., Depierreux, C., Benedetti, H., *et al.* (2013). Characterization of histidine-aspartate kinase HK1 and identification of histidine phosphotransfer proteins as potential partners in a Populus multistep phosphorelay. Physiol Plant *149*, 188-199.

Herrou, J., and Crosson, S. (2011). Function, structure and mechanism of bacterial photosensory LOV proteins. Nat Rev Microbiol *9*, 713-723.

Hertig, C., Melzer, M., Rutten, T., Erbe, S., Hensel, G., KumLehn, J., Weschke, W., Weber, H., and Thiel, J. (2020). Barley HISTIDINE KINASE 1 (HvHK1) coordinates transfer cell specification in the young endosperm. Plant J.

Heunemann, M. (2016). H_2O_2-Perception and Signaltransduction: Functional and structural Characterization of the *Arabidopsis* Histidine Kinase 5 (AHK5) (University of Tuebingen), pp. 119.

Hilfiker, O., Groux, R., Bruessow, F., Kiefer, K., Zeier, J., and Reymond, P. (2014). Insect eggs induce a systemic acquired resistance in Arabidopsis. Plant J *80*, 1085-1094.

References

Hiltbrunner, A. (2019). Shedding light on the evolution of light signaling. New Phytol *224*, 1412-1414.

Hisada, A., Hanzawa, H., Weller, J.L., Nagatani, A., Reid, J.B., and Furuya, M. (2000). Light-induced nuclear translocation of endogenous pea phytochrome A visualized by immunocytochemical procedures. Plant Cell *12*, 1063-1078.

Hoballah, M.E., Gubitz, T., Stuurman, J., Broger, L., Barone, M., Mandel, T., Dell'Olivo, A., Arnold, M., and Kuhlemeier, C. (2007). Single gene-mediated shift in pollinator attraction in Petunia. Plant Cell *19*, 779-790,

Hoecker, U. (2017). The activities of the E3 ubiquitin ligase COP1/SPA, a key repressor in light signaling. Curr Opin Plant Biol *37*, 63-69.

Hoffman, P.D., Batschauer, A., and Hays, J.B. (1996). PHH1, a novel gene from Arabidopsis thaliana that encodes a protein similar to plant blue-light photoreceptors and microbial photolyases. Mol Gen Genet *253*, 259-265.

Hofmann, A., Muller, S., Drechsler, T., Berleth, M., Caesar, K., Rohr, L., Harter, K., and Groth, G. (2020). High-Level Expression, Purification and Initial Characterization of Recombinant Arabidopsis Histidine Kinase AHK1. Plants (Basel) *9*.

Hohmann, U., Lau, K., and Hothorn, M. (2017). The Structural Basis of Ligand Perception and Signal Activation by Receptor Kinases. In Annual Review of Plant Biology, Vol 68, S.S. Merchant, ed., pp. 109-137.

Holtkotte, X., Ponnu, J., Ahmad, M., and Hoecker, U. (2017). The blue light-induced interaction of cryptochrome 1 with COP1 requires SPA proteins during Arabidopsis light signaling. PLoS Genet *13*, e1007044.

Hong, Y., Pan, X., Welti, R., and Wang, X. (2008). Phospholipase Dalpha3 is involved in the hyperosmotic response in Arabidopsis. Plant Cell *20*, 803-816.

Hong, Y.Y., Zhao, J., Guo, L., Kim, S.C., Deng, X.J., Wang, G.L., Zhang, G.Y., Li, M.Y., and Wang, X.M. (2016). Plant phospholipases D and C and their diverse functions in stress responses. Prog Lipid Res *62*, 55-74.

Hothorn, M., Dabi, T., and Chory, J. (2011). Structural basis for cytokinin recognition by Arabidopsis thaliana histidine kinase 4. Nature Chemical Biology *7*, 766-768.

Hua, J., and Meyerowitz, E.M. (1998). Ethylene responses are negatively regulated by a receptor gene family in Arabidopsis thaliana. Cell *94*, 261-271.

Hua, J., Sakai, H., Nourizadeh, S., Chen, Q.G., Bleecker, A.B., Ecker, J.R., and Meyerowitz, E.M. (1998). EIN4 and ERS2 are members of the putative ethylene receptor gene family in Arabidopsis. Plant Cell *10*, 1321-1332.

Huang, H., Ullah, F., Zhou, D.X., Yi, M., and Zhao, Y. (2019a). Mechanisms of ROS Regulation of Plant Development and Stress Responses. Front Plant Sci *10*, 800,

References

Huang, L., Yu, L.J., Zhang, X., Fan, B., Wang, F.Z., Dai, Y.S., Qi, H., Zhou, Y., Xie, L.J., and Xiao, S. (2019b). Autophagy regulates glucose-mediated root meristem activity by modulating ROS production in Arabidopsis. Autophagy *15*, 407-422.

Huang, X., Hou, L., Meng, J., You, H., Li, Z., Gong, Z., Yang, S., and Shi, Y. (2018). The Antagonistic Action of Abscisic Acid and Cytokinin Signaling Mediates Drought Stress Response in Arabidopsis. Mol Plant *11*, 970-982.

Huber, S.C. (2007). Exploring the role of protein phosphorylation in plants: from signaling to metabolism. Biochem Soc Trans *35*, 28-32.

Huo, X., Schnabel, E., Hughes, K., and Frugoli, J. (2006). RNAi Phenotypes and the Localization of a Protein::GUS Fusion Imply a Role for Medicago truncatula PIN Genes in Nodulation. J Plant Growth Regul *25*, 156-165.

Hutchison, C.E., and Kieber, J.J. (2007). Signaling via Histidine-Containing Phosphotransfer Proteins in Arabidopsis. Plant Signal Behav *2*, 287-289.

Hwang, I., and Sheen, J. (2001). Two-component circuitry in Arabidopsis cytokinin signal transduction. Nature *413*, 383-389.

Ibanez, C., Delker, C., Martinez, C., Burstenbinder, K., Janitza, P., Lippmann, R., Ludwig, W., Sun, H., James, G.V., Klecker, M., *et al.* (2018). Brassinosteroids Dominate Hormonal Regulation of Plant Thermomorphogenesis via BZR1. Curr Biol *28*, 303-310 e303.

Inada, S., Ohgishi, M., Mayama, T., Okada, K., and Sakai, T. (2004). RPT2 is a signal transducer involved in phototropic response and stomatal opening by association with phototropin 1 in Arabidopsis thaliana. Plant Cell *16*, 887-896.

Iqbal, N., Khan, N.A., Ferrante, A., Trivellini, A., Francini, A., and Khan, M.I.R. (2017). Ethylene Role in Plant Growth, Development and Senescence: Interaction with Other Phytohormones. Front Plant Sci *8*.

Ivashuta, S., Liu, J., Liu, J., Lohar, D.P., Haridas, S., Bucciarelli, B., VandenBosch, K.A., Vance, C.P., Harrison, M.J., and Gantt, J.S. (2005). RNA Interference Identifies a Calcium-Dependent Protein Kinase Involved in *Medicago truncatula* Root Development. The Plant Cell *17*, 2911-2921.

Jakubowicz, M., Galganska, H., Nowak, W., and Sadowski, J. (2010). Exogenously induced expression of ethylene biosynthesis, ethylene perception, phospholipase D, and Rboh-oxidase genes in broccoli seedlings. J Exp Bot *61*, 3475-3491.

Janiak-Spens, F., Sparling, J.M., Gurfinkel, M., and West, A.H. (1999). Differential stabilities of phosphorylated response regulator domains reflect functional roles of the yeast osmoregulatory SLN1 and SSK1 proteins. J Bacteriol *181*, 411-417.

Jasso-Robles, F.I., Gonzalez, M.E., Pieckenstain, F.L., Ramirez-Garcia, J.M., Guerrero-Gonzalez, M.D., Jimenez-Bremont, J.F., and Rodriguez-Kessler, M. (2020). Decrease of Arabidopsis PAO activity entails increased RBOH activity, ROS content and altered responses to Pseudomonas. Plant Science *292*.

References

Jelinkova, A., Malinska, K., Simon, S., Kleine-Vehn, J., Parezova, M., Pejchar, P., Kubes, M., Martinec, J., FrimL, J., Zazimalova, E., *et al.* (2010). Probing plant membranes with FM dyes: tracking, dragging or blocking? Plant J *61*, 883-892.

Jiang, M., Ren, L., Lian, H., Liu, Y., and Chen, H. (2016). Novel insight into the mechanism underlying light-controlled anthocyanin accumulation in eggplant (Solanum melongena L.). Plant Sci *249*, 46-58.

Jones, K.M., Kobayashi, H., Davies, B.W., Taga, M.E., and Walker, G.C. (2007). How rhizobial symbionts invade plants: the Sinorhizobium-Medicago model. Nat Rev Microbiol *5*, 619-633.

Joshi, R., Wani, S.H., Singh, B., Bohra, A., Dar, Z.A., Lone, A.A., Pareek, A., and Singla-Pareek, S.L. (2016). Transcription Factors and Plants Response to Drought Stress: Current Understanding and Future Directions. Front Plant Sci *7*, 1029.

Jourdan, N., Martino, C.F., El-Esawi, M., Witczak, J., Bouchet, P.-E., d'Harlingue, A., and Ahmad, M. (2015). Blue-light dependent ROS formation by Arabidopsis cryptochrome-2 may contribute toward its signaling role. Plant signaling & behavior *10*, e1042647-e1042647.

Ju, C.L., Yoon, G.M., Shemansky, J.M., Lin, D.Y., Ying, Z.I., Chang, J.H., Garrett, W.M., Kessenbrock, M., Groth, G., Tucker, M.L., *et al.* (2012). CTR1 phosphorylates the central regulator EIN2 to control ethylene hormone signaling from the ER membrane to the nucleus in Arabidopsis. P Natl Acad Sci USA *109*, 19486-19491.

Jung, C., Lyou, S.H., Yeu, S., Kim, M.A., Rhee, S., Kim, M., Lee, J.S., Choi, Y.D., and Cheong, J.J. (2007). Microarray-based screening of jasmonate-responsive genes in Arabidopsis thaliana. Plant Cell Rep *26*, 1053-1063.

Jung, C., Seo, J.S., Han, S.W., Koo, Y.J., Kim, C.H., Song, S.I., Nahm, B.H., Choi, Y.D., and Cheong, J.J. (2008). Overexpression of AtMYB44 enhances stomatal closure to confer abiotic stress tolerance in transgenic Arabidopsis. Plant Physiol *146*, 623-635.

Jung, J., Kumar, K., Lee, H.Y., Park, Y.I., Cho, H.T., and Ryu, S.B. (2012). Translocation of phospholipase A2alpha to apoplasts is modulated by developmental stages and bacterial infection in Arabidopsis. Front Plant Sci *3*, 126.

Kabbara, S., Herivaux, A., Duge de Bernonville, T., Courdavault, V., Clastre, M., Gastebois, A., Osman, M., Hamze, M., Cock, J.M., Schaap, P., *et al.* (2019). Diversity and Evolution of Sensor Histidine Kinases in Eukaryotes. Genome Biol Evol *11*, 86-108.

Kadota, Y., Shirasu, K., and Zipfel, C. (2015). Regulation of the NADPH Oxidase RBOHD During Plant Immunity. Plant and Cell Physiology *56*, 1472-1480,

Kadota, Y., Sklenar, J., Derbyshire, P., Stransfeld, L., Asai, S., Ntoukakis, V., Jones, J.D., Shirasu, K., Menke, F., Jones, A., *et al.* (2014a). Direct regulation of the NADPH oxidase RBOHD by the PRR-associated kinase BIK1 during plant immunity. Mol Cell *54*, 43-55.

Kadota, Y., Sklenar, J., Derbyshire, P., Stransfeld, L., Asai, S., Ntoukakis, V., Jones, Jonathan D., Shirasu, K., Menke, F., Jones, A., *et al.* (2014b). Direct Regulation of the NADPH Oxidase RBOHD by the PRR-Associated Kinase BIK1 during Plant Immunity. Molecular Cell *54*, 43-55.

References

Kalantari, A., Derouiche, A., Shi, L., and Mijakovic, I. (2015). Serine/threonine/tyrosine phosphorylation regulates DNA binding of bacterial transcriptional regulators. Microbiology *161*, 1720-1729.

Kamal, N., Mun, T., Reid, D., Lin, J.-s., Akyol, T.Y., Sandal, N., Asp, T., Hirakawa, H., Stougaard, J., Mayer, K.F.X., *et al.* (2020a). A chromosome-scale *Lotus japonicus* Gifu genome assembly indicates that symbiotic islands are not general features of legume genomes. bioRxiv, 2020,2004.2017.042473.

Kamal, N., Mun, T., Reid, D., Lin, J.-s., Akyol, T.Y., Sandal, N., Asp, T., Hirakawa, H., Stougaard, J., Mayer, K.F.X., *et al.* (2020b). Insights into the evolution of symbiosis gene copy number and distribution from a chromosome-scale Lotus japonicus Gifu genome sequence. DNA Research.

Kawasaki, T., Yamada, K., Yoshimura, S., and Yamaguchi, K. (2017). Chitin receptor-mediated activation of MAP kinases and ROS production in rice and Arabidopsis. Plant Signal Behav *12*, e1361076.

Keuskamp, D.H., Sasidharan, R., Vos, I., Peeters, A.J.M., Voesenek, L., and Pierik, R. (2011). Blue-light-mediated shade avoidance requires combined auxin and brassinosteroid action in Arabidopsis seedlings. Plant Journal *67*, 208-217.

Kevei, Z., Lougnon, G., Mergaert, P., Horváth, G.V., Kereszt, A., Jayaraman, D., Zaman, N., Marcel, F., Regulski, K., Kiss, G.B., *et al.* (2007). 3-hydroxy-3-methylglutaryl coenzyme a reductase 1 interacts with NORK and is crucial for nodulation in Medicago truncatula. Plant Cell *19*, 3974-3989.

Khalid, M., Saeed ur, R., Bilal, M., and Huang, D.-f. (2019). Role of flavonoids in plant interactions with the environment and against human pathogens — A review. Journal of Integrative Agriculture *18*, 211-230,

Khare, S., Singh, N.B., Singh, A., Hussain, I., Niharika, K., Yadav, V., Bano, C., Yadav, R.K., and Amist, N. (2020). Plant secondary metabolites synthesis and their regulations under biotic and abiotic constraints. Journal of Plant Biology *63*, 203-216.

Khoo, H.E., Azlan, A., Tang, S.T., and Lim, S.M. (2017). Anthocyanidins and anthocyanins: colored pigments as food, pharmaceutical ingredients, and the potential health benefits. Food Nutr Res *61*, 1361779-1361779.

Kieber, J.J., Rothenberg, M., Roman, G., Feldmann, K.A., and Ecker, J.R. (1993). CTR1, a negative regulator of the ethylene response pathway in Arabidopsis, encodes a member of the raf family of protein kinases. Cell *72*, 427-441.

Kim, B., Kwon, M., Jeon, J., Schulz, B., Corvalan, C., Jeong, Y.J., and Choe, S. (2014). The arabidopsis gulliver2/phyB mutant exhibits reduced sensitivity to brassinazole. J Plant Biol *57*, 20-27.

Kim, L., Kircher, S., Toth, R., Adam, E., Schäfer, E., and Nagy, F. (2000). Light-induced nuclear import of phytochrome-A:GFP fusion proteins is differentially regulated in transgenic *N. benthamiana* and Arabidopsis. Plant J *22*, 125-133.

References

Kim, T.W., Guan, S., Burlingame, A.L., and Wang, Z.Y. (2011). The CDG1 kinase mediates brassinosteroid signal transduction from BRI1 receptor kinase to BSU1 phosphatase and GSK3-like kinase BIN2. Mol Cell *43*, 561-571.

Kim, T.W., Guan, S., Sun, Y., Deng, Z., Tang, W., Shang, J.X., Sun, Y., Burlingame, A.L., and Wang, Z.Y. (2009). Brassinosteroid signal transduction from cell-surface receptor kinases to nuclear transcription factors. Nat Cell Biol *11*, 1254-1260,

Kim, Y.K., Kim, S., Um, J.H., Kim, K., Choi, S.K., Um, B.H., Kang, S.W., Kim, J.W., Takaichi, S., Song, S.B., *et al.* (2013). Functional implication of beta-carotene hydroxylases in soybean nodulation. Plant Physiol *162*, 1420-1433.

Kimura, S., Kaya, H., Kawarazaki, T., Hiraoka, G., Senzaki, E., Michikawa, M., and Kuchitsu, K. (2012). Protein phosphorylation is a prerequisite for the Ca2+-dependent activation of Arabidopsis NADPH oxidases and may function as a trigger for the positive feedback regulation of Ca2+ and reactive oxygen species. Biochimica et Biophysica Acta (BBA) - Molecular Cell Research *1823*, 398-405.

King-Scott, J., Konarev, P.V., Panjikar, S., Jordanova, R., Svergun, D.I., and Tucker, P.A. (2011). Structural Characterization of the Multidomain Regulatory Protein Rv1364c from Mycobacterium tuberculosis. Structure *19*, 56-69.

Kinkema, M., Scott, P.T., and Gresshoff, P.M. (2006). Legume nodulation: successful symbiosis through short- and long-distance signaling %J Functional Plant Biology. *33*, 707-721.

Kircher, S., Kozma-Bognar, L., Kim, L., Adam, E., Harter, K., Schafer, E., and Nagy, F. (1999). Light quality-dependent nuclear import of the plant photoreceptors phytochrome A and B. Plant Cell *11*, 1445-1456.

Klein, R.R., Bourdon, D.M., Costales, C.L., Wagner, C.D., White, W.L., Williams, J.D., Hicks, S.N., Sondek, J., and Thakker, D.R. (2011). Direct activation of human phospholipase C by its well known inhibitor u73122. J Biol Chem *286*, 12407-12416.

Kliebenstein, D.J., Lim, J.E., Landry, L.G., and Last, R.L. (2002). Arabidopsis UVR8 regulates ultraviolet-B signal transduction and tolerance and contains sequence similarity to human regulator of chromatin condensation 1. Plant Physiol *130*, 234-243.

Klimecka, M., Bucholc, M., Maszkowska, J., Krzywinska, E., Goch, G., Lichocka, M., Szczegielniak, J., and Dobrowolska, G. (2020). Regulation of ABA-Non-Activated SNF1-Related Protein Kinase 2 Signaling Pathways by Phosphatidic Acid. Int J Mol Sci *21*.

Klumpp, S., and Krieglstein, J. (2002). Phosphorylation and dephosphorylation of histidine residues in proteins. European Journal of Biochemistry *269*, 1067-1071.

Koller, T., and Bent, A.F. (2014). FLS2-BAK1 Extracellular Domain Interaction Sites Required for Defense Signaling Activation. Plos One *9*.

Kolling, M., Kumari, P., and Burstenbinder, K. (2019). Calcium- and calmodulin-regulated microtubule-associated proteins as signal-integration hubs at the plasma membrane-cytoskeleton nexus. J Exp Bot *70*, 387-396.

References

Kollist, H., Zandalinas, S.I., Sengupta, S., Nuhkat, M., Kangasjarvi, J., and Mittler, R. (2019). Rapid Responses to Abiotic Stress: Priming the Landscape for the Signal Transduction Network. Trends in Plant Science *24*, 25-37.

Kranz, H.D., Denekamp, M., Greco, R., Jin, H., Leyva, A., Meissner, R.C., Petroni, K., Urzainqui, A., Bevan, M., Martin, C., *et al.* (1998). Towards functional characterisation of the members of the R2R3-MYB gene family from Arabidopsis thaliana. Plant J *16*, 263-276.

Krasensky-Wrzaczek, J., and Kangasjärvi, J. (2018). The role of reactive oxygen species in the integration of temperature and light signals. Journal of Experimental Botany *69*, 3347-3358.

Kretynin, S.V., Kolesnikov, Y.S., Derevyanchuk, M.V., Kalachova, T.A., Blume, Y.B., Khripach, V.A., and Kravets, V.S. (2019). Brassinosteroids application induces phosphatidic acid production and modify antioxidant enzymes activity in *N. benthamiana* in calcium-dependent manner. Steroids, 108444.

Kumar, M.N., Jane, W.N., and Verslues, P.E. (2013). Role of the Putative Osmosensor Arabidopsis Histidine Kinase1 in Dehydration Avoidance and Low-Water-Potential Response. Plant Physiology *161*, 942-953.

Kumar, S., Stecher, G., Li, M., Knyaz, C., and Tamura, K. (2018). MEGA X: Molecular Evolutionary Genetics Analysis across Computing Platforms. Mol Biol Evol *35*, 1547-1549.

Küpers, J.J., van Gelderen, K., and Pierik, R. (2018). Location Matters: Canopy Light Responses over Spatial Scales. Trends in Plant Science *23*, 865-873.

Kuppe, K., Kerth, A., Blume, A., and Ulbrich-Hofmann, R. (2008). Calcium-induced membrane microdomains trigger plant phospholipase D activity. Chembiochem *9*, 2853-2859.

Ladwig, F., Dahlke, R.I., Stuhrwohldt, N., Hartmann, J., Harter, K., and Sauter, M. (2015). Phytosulfokine Regulates Growth in Arabidopsis through a Response Module at the Plasma Membrane That Includes CYCLIC NUCLEOTIDE-GATED CHANNEL17, H+-ATPase, and BAK1. Plant Cell *27*, 1718-1729.

Laub, M.T., and Goulian, M. (2007). Specificity in two-component signal transduction pathways. Annu Rev Genet *41*, 121-145.

Laubinger, S., Fittinghoff, K., and Hoecker, U. (2004). The SPA quartet: a family of WD-repeat proteins with a central role in suppression of photomorphogenesis in arabidopsis. Plant Cell *16*, 2293-2306.

Lee, J.S., and Ellis, B.E. (2007). Arabidopsis MAPK phosphatase 2 (MKP2) positively regulates oxidative stress tolerance and inactivates the MPK3 and MPK6 MAPKs. J Biol Chem *282*, 25020-25029.

Legris, M., Klose, C., Burgie, E.S., Rojas, C.C., Neme, M., Hiltbrunner, A., Wigge, P.A., Schafer, E., Vierstra, R.D., and Casal, J.J. (2016). Phytochrome B integrates light and temperature signals in Arabidopsis. Science *354*, 897-900,

Lei, L., Stevens, D.M., and Coaker, G. (2020). Phosphorylation of the Pseudomonas Effector AvrPtoB by Arabidopsis SnRK2.8 Is Required for Bacterial Virulence. Mol Plant *13*, 1513-1522.

References

Leivar, P., Monte, E., Oka, Y., Liu, T., Carle, C., Castillon, A., Huq, E., and Quail, P.H. (2008). Multiple phytochrome-interacting bHLH transcription factors repress premature seedling photomorphogenesis in darkness. Curr Biol *18*, 1815-1823.

Lewis, D.R., Ramirez, M.V., Miller, N.D., Vallabhaneni, P., Ray, W.K., Helm, R.F., Winkel, B.S.J., and Muday, G.K. (2011). Auxin and Ethylene Induce Flavonol Accumulation through Distinct Transcriptional Networks. Plant Physiology *156*, 144-164.

Li, B., Kamiya, T., Kalmbach, L., Yamagami, M., Yamaguchi, K., Shigenobu, S., Sawa, S., Danku, J.M., Salt, D.E., Geldner, N., *et al.* (2017a). Role of LOTR1 in Nutrient Transport through Organization of Spatial Distribution of Root Endodermal Barriers. Curr Biol *27*, 758-765.

Li, C.J., Shi, L., Wang, Y.N., Li, W., Chen, B.Q., Zhu, L., and Fu, Y. (2020). Arabidopsis ECAP Is a New Adaptor Protein that Connects JAZ Repressors with the TPR2 Co-repressor to Suppress Jasmonate-Responsive Anthocyanin Accumulation. Mol Plant *13*, 246-265.

Li, H., Ye, K., Shi, Y., Cheng, J., Zhang, X., and Yang, S. (2017b). BZR1 Positively Regulates Freezing Tolerance via CBF-Dependent and CBF-Independent Pathways in Arabidopsis. Mol Plant *10*, 545-559.

Li, J., Li, G., Wang, H., and Wang Deng, X. (2011). Phytochrome signaling mechanisms. Arabidopsis Book *9*, e0148.

Li, J., and Wang, X. (2019). Phospholipase D and phosphatidic acid in plant immunity. Plant Sci *279*, 45-50,

Li, J., Wen, J.Q., Lease, K.A., Doke, J.T., Tax, F.E., and Walker, J.C. (2002). BAK1, an Arabidopsis LRR receptor-like protein kinase, interacts with BRI1 and modulates brassinosteroid signaling. Cell *110*, 213-222.

Li, L., Li, M., Yu, L., Zhou, Z., Liang, X., Liu, Z., Cai, G., Gao, L., Zhang, X., Wang, Y., *et al.* (2014a). The FLS2-Associated Kinase BIK1 Directly Phosphorylates the NADPH Oxidase RbohD to Control Plant Immunity. Cell Host & Microbe *15*, 329-338.

Li, M., Hong, Y., and Wang, X. (2009). Phospholipase D- and phosphatidic acid-mediated signaling in plants. Biochim Biophys Acta *1791*, 927-935.

Li, M., Welti, R., and Wang, X. (2006). Quantitative profiling of Arabidopsis polar glycerolipids in response to phosphorus starvation. Roles of phospholipases D zeta1 and D zeta2 in phosphatidylcholine hydrolysis and digalactosyldiacylglycerol accumulation in phosphorus-starved plants. Plant Physiol *142*, 750-761.

Li, Q.F., and He, J.X. (2016). BZR1 Interacts with HY5 to Mediate Brassinosteroid- and Light-Regulated Cotyledon Opening in Arabidopsis in Darkness. Mol Plant *9*, 113-125.

Li, Q.F., Huang, L.C., Wei, K., Yu, J.W., Zhang, C.Q., and Liu, Q.Q. (2017c). Light involved regulation of BZR1 stability and phosphorylation status to coordinate plant growth in Arabidopsis. Biosci Rep *37*.

References

Li, T., Jia, K.P., Lian, H.L., Yang, X., Li, L., and Yang, H.Q. (2014b). Jasmonic acid enhancement of anthocyanin accumulation is dependent on phytochrome A signaling pathway under far-red light in Arabidopsis. Biochemical and Biophysical Research Communications *454*, 78-83.

Li, W., Song, T., Wallrad, L., Kudla, J., Wang, X., and Zhang, W. (2019). Tissue-specific accumulation of pH-sensing phosphatidic acid determines plant stress tolerance. Nat Plants *5*, 1012-1021.

Licitra, E.J., and Liu, J.O. (1996). A three-hybrid system for detecting small ligand-protein receptor interactions. Proc Natl Acad Sci U S A *93*, 12817-12821.

Lin, C., Robertson, D.E., Ahmad, M., Raibekas, A.A., Jorns, M.S., Dutton, P.L., and Cashmore, A.R. (1995). Association of flavin adenine dinucleotide with the Arabidopsis blue light receptor CRY1. Science *269*, 968-970,

Lin, C., Yang, H., Guo, H., Mockler, T., Chen, J., and Cashmore, A.R. (1998). Enhancement of blue-light sensitivity of Arabidopsis seedlings by a blue light receptor cryptochrome 2. Proceedings of the National Academy of Sciences *95*, 2686-2690,

Lin, J., Frank, M., and Reid, D. (2020). No Home without Hormones: How Plant Hormones Control Legume Nodule Organogenesis. Plant Communications *1*, 100104.

Liscovitch, M., Czarny, M., Fiucci, G., and Tang, X. (2000). Phospholipase D: molecular and cell biology of a novel gene family. Biochem J *345 Pt 3*, 401-415.

Liu, C.W., Breakspear, A., Guan, D., Cerri, M.R., Jackson, K., Jiang, S.Y., Robson, F., Radhakrishnan, G.V., Roy, S., Bone, C., *et al.* (2019a). NIN Acts as a Network Hub Controlling a Growth Module Required for Rhizobial Infection. Plant Physiology *179*, 1704-1722.

Liu, W., Sikora, E., and Park, S.-W. (2020). Plant growth-promoting rhizobacterium, Paenibacillus polymyxa CR1, upregulates dehydration-responsive genes, RD29A and RD29B, during priming drought tolerance in arabidopsis. Plant Physiology and Biochemistry *156*, 146-154.

Liu, X.X., Ma, D.K., Zhang, Z.Y., Wang, S.W., Du, S., Deng, X.P., and Yin, L.N. (2019b). Plant lipid remodeling in response to abiotic stresses. Environ Exp Bot *165*, 174-184.

Liu, Y., Tikunov, Y., Schouten, R.E., Marcelis, L.F.M., Visser, R.G.F., and Bovy, A. (2018). Anthocyanin Biosynthesis and Degradation Mechanisms in Solanaceous Vegetables: A Review. Frontiers in Chemistry *6*.

Lohrmann, J., and Harter, K. (2002). Plant two-component signaling systems and the role of response regulators. Plant Physiol *128*, 363-369.

Lomin, S.N., Krivosheev, D.M., Steklov, M.Y., Arkhipov, D.V., Osolodkin, D.I., Schmulling, T., and Romanov, G.A. (2015). Plant membrane assays with cytokinin receptors underpin the unique role of free cytokinin bases as biologically active ligands. J Exp Bot *66*, 1851-1863.

Lomin, S.N., Myakushina, Y.A., Arkhipov, D.V., Leonova, O.G., Popenko, V.I., Schmülling, T., and Romanov, G.A. (2018). Studies of cytokinin receptor–phosphotransmitter interaction provide evidences for the initiation of cytokinin signaling in the endoplasmic reticulum. Functional Plant Biology *45*, 192-202.

References

Lorenc-Kukula, K., Jafra, S., Oszmianski, J., and Szopa, J. (2005). Ectopic expression of anthocyanin 5-o-glucosyltransferase in potato tuber causes increased resistance to bacteria. J Agric Food Chem *53*, 272-281.

Lu, D., Wang, W., and Miao, C. (2013). ATHK1 acts downstream of hydrogen peroxide to mediate ABA signaling through regulation of calcium channel activity in Arabidopsis guard cells. Chinese Science Bulletin *58*, 336-343.

Lutts, S., Kinet, J.M., and Bouharmont, J. (1996). NaCl-induced Senescence in Leaves of Rice (Oryza sativa L.) Cultivars Differing in Salinity Resistance. Annals of Botany *78*, 389-398.

Lv, B., Tian, H., Zhang, F., Liu, J., Lu, S., Bai, M., Li, C., and Ding, Z. (2018). Brassinosteroids regulate root growth by controlling reactive oxygen species homeostasis and dual effect on ethylene synthesis in Arabidopsis. PLoS Genet *14*, e1007144.

Ma, D., Li, X., Guo, Y., Chu, J., Fang, S., Yan, C., Noel, J.P., and Liu, H. (2016). Cryptochrome 1 interacts with PIF4 to regulate high temperature-mediated hypocotyl elongation in response to blue light. Proc Natl Acad Sci U S A *113*, 224-229.

Ma, L., Gao, Y., Qu, L., Chen, Z., Li, J., Zhao, H., and Deng, X.W. (2002). Genomic evidence for COP1 as a repressor of light-regulated gene expression and development in Arabidopsis. Plant Cell *14*, 2383-2398.

Ma, L.Y., Zhang, H., Sun, L.R., Jiao, Y.H., Zhang, G.Z., Miao, C., and Hao, F.S. (2012). NADPH oxidase AtrbohD and AtrbohF function in ROS-dependent regulation of Na+/K+ homeostasis in Arabidopsis under salt stress. J Exp Bot *63*, 305-317.

Ma, Y., Szostkiewicz, I., Korte, A., Moes, D., Yang, Y., Christmann, A., and Grill, E. (2009). Regulators of PP2C Phosphatase Activity Function as Abscisic Acid Sensors. Science *324*, 1064-1068.

Macho, A.P., Lozano-Duran, R., and Zipfel, C. (2015). Importance of tyrosine phosphorylation in receptor kinase complexes. Trends Plant Sci *20*, 269-272.

Macho, A.P., and Zipfel, C. (2014). Plant PRRs and the activation of innate immune signaling. Mol Cell *54*, 263-272.

Madigan, M.T.M., John M.; Bender, Kelly S.; Buckley, Daniel H.; Stahl, David A. (2015). Brock biology of microorganisms (Pearson).

Madsen, E.B., Antolín-Llovera, M., Grossmann, C., Ye, J., Vieweg, S., Broghammer, A., Krusell, L., Radutoiu, S., Jensen, O.N., Stougaard, J., *et al.* (2011). Autophosphorylation is essential for the in vivo function of the Lotus japonicus Nod factor receptor 1 and receptor-mediated signaling in cooperation with Nod factor receptor 5. The Plant Journal *65*, 404-417.

Mahonen, A.P., Bonke, M., Kauppinen, L., Riikonen, M., Benfey, P.N., and Helariutta, Y. (2000). A novel two-component hybrid molecule regulates vascular morphogenesis of the Arabidopsis root. Genes Dev *14*, 2938-2943.

References

Mahonen, A.P., Higuchi, M., Tormakangas, K., Miyawaki, K., Pischke, M.S., Sussman, M.R., Helariutta, Y., and Kakimoto, T. (2006). Cytokinins regulate a bidirectional phosphorelay network in Arabidopsis. Curr Biol *16*, 1116-1122.

Maier, A., Schrader, A., Kokkelink, L., Falke, C., Welter, B., Iniesto, E., Rubio, V., Uhrig, J.F., Hülskamp, M., and Hoecker, U. (2013). Light and the E3 ubiquitin ligase COP1/SPA control the protein stability of the MYB transcription factors PAP1 and PAP2 involved in anthocyanin accumulation in Arabidopsis. The Plant Journal *74*, 638-651.

Malolepszy, A., Mun, T., Sandal, N., Gupta, V., Dubin, M., Urbanski, D., Shah, N., Bachmann, A., Fukai, E., Hirakawa, H., *et al.* (2016). The LORE1 insertion mutant resource. Plant J *88*, 306-317.

Mancinelli, A. (1994). The physiology of phytochrome action., Vol 2 (Kluwer Academic Publishers, Dordrecht.).

Manohar, M., Tian, M., Moreau, M., Park, S.W., Choi, H.W., Fei, Z., Friso, G., Asif, M., Manosalva, P., von Dahl, C.C., *et al.* (2015). Identification of multiple salicylic acid-binding proteins using two high throughput screens. Front Plant Sci *5*.

Marhavy, P., Kurenda, A., Siddique, S., Denervaud Tendon, V., Zhou, F., Holbein, J., Hasan, M.S., Grundler, F.M., Farmer, E.E., and Geldner, N. (2019). Single-cell damage elicits regional, nematode-restricting ethylene responses in roots. EMBO J *38*.

Markham, J.E., Li, J., Cahoon, E.B., and Jaworski, J.G. (2006). Separation and identification of major plant sphingolipid classes from leaves. Journal of Biological Chemistry *281*, 22684-22694.

Márquez, A.J., Stougaard J., Udvardi M., Parniske M., Spaink H., Saalbach G., Webb J., and Chiurazzi M. (2006). *Lotus japonicus* Handbook (Springer).

Martiniere, A., Gibrat, R., Sentenac, H., Dumont, X., Gaillard, I., and Paris, N. (2018). Uncovering pH at both sides of the root plasma membrane interface using noninvasive imaging. P Natl Acad Sci USA *115*, 6488-6493.

Maruyama, K., Urano, K., Yoshiwara, K., Morishita, Y., Sakurai, N., Suzuki, H., Kojima, M., Sakakibara, H., Shibata, D., Saito, K., *et al.* (2014). Integrated analysis of the effects of cold and dehydration on rice metabolites, phytohormones, and gene transcripts. Plant Physiol *164*, 1759-1771.

Masclaux-Daubresse, C., Daniel-Vedele, F., Dechorgnat, J., Chardon, F., Gaufichon, L., and Suzuki, A. (2010). Nitrogen uptake, assimilation and remobilization in plants: challenges for sustainable and productive agriculture. Ann Bot *105*, 1141-1157.

Mason, M.G., Mathews, D.E., Argyros, D.A., Maxwell, B.B., Kieber, J.J., Alonso, J.M., Ecker, J.R., and Schaller, G.E. (2005). Multiple Type-B Response Regulators Mediate Cytokinin Signal Transduction in Arabidopsis. The Plant Cell *17*, 3007-3018.

Masood, A., Iqbal, N., and Khan, N.A. (2012). Role of ethylene in alleviation of cadmium-induced photosynthetic capacity inhibition by sulphur in mustard. Plant, Cell & Environment *35*, 524-533.

Maszkowska, J., Dębski, J., Kulik, A., Kistowski, M., Bucholc, M., Lichocka, M., Klimecka, M., Sztatelman, O., Szymańska, K.P., Dadlez, M., *et al.* (2019). Phosphoproteomic analysis reveals that

dehydrins ERD10 and ERD14 are phosphorylated by SNF1-related protein kinase 2.10 in response to osmotic stress. Plant, Cell & Environment *42*, 931-946.

Matthews, H.R. (1995). Protein kinases and phosphatases that act on histidine, lysine, or arginine residues in eukaryotic proteins: a possible regulator of the mitogen-activated protein kinase cascade. Pharmacol Ther *67*, 323-350,

Matzke, M.A., and Matzke, A.J.M. (1998). Epigenetic silencing of plant transgenes as a consequence of diverse cellular defence responses. Cellular and Molecular Life Sciences CMLS *54*, 94-103.

McLean, T.C., Lo, R., Tschowri, N., Hoskisson, P.A., Al Bassam, M.M., Hutchings, M.I., and Som, N.F. (2019). Sensing and responding to diverse extracellular signals: an updated analysis of the sensor kinases and response regulators of Streptomyces species. Microbiology-Sgm *165*, 929-952.

McLoughlin, F., Arisz, S.A., Dekker, H.L., Kramer, G., de Koster, C.G., Haring, M.A., Munnik, T., and Testerink, C. (2013). Identification of novel candidate phosphatidic acid-binding proteins involved in the salt-stress response of Arabidopsis thaliana roots. Biochem J *450*, 573-581.

Meneghelli, S., Fusca, T., Luoni, L., and De Michelis, M.I. (2008). Dual mechanism of activation of plant plasma membrane Ca2+-ATPase by acidic phospholipids: Evidence for a phospholipid binding site which overlaps the calmodulin-binding site. Molecular Membrane Biology *25*, 539-546.

Merchante, C., Alonso, J.M., and Stepanova, A.N. (2013). Ethylene signaling: simple ligand, complex regulation. Curr Opin Plant Biol *16*, 554-560,

Meringer, M.V., Villasuso, A.L., Margutti, M.P., Usorach, J., Pasquare, S.J., Giusto, N.M., Machado, E.E., and Racagni, G.E. (2016). Saline and osmotic stresses stimulate PLD/diacylglycerol kinase activities and increase the level of phosphatidic acid and proline in barley roots. Environ Exp Bot *128*, 69-78.

Michaud, M., and Jouhet, J. (2019). Lipid Trafficking at Membrane Contact Sites During Plant Development and Stress Response. Front Plant Sci *10,*

Mikolajczyk, M., Awotunde, O.S., Muszynska, G., Klessig, D.F., and Dobrowolska, G. (2000). Osmotic stress induces rapid activation of a salicylic acid-induced protein kinase and a homolog of protein kinase ASK1 in *N. benthamiana* cells. Plant Cell *12*, 165-178.

Miri, M., Janakirama, P., Huebert, T., Ross, L., McDowell, T., Orosz, K., Markmann, K., and Szczyglowski, K. (2019). Inside out: root cortex-localized LHK1 cytokinin receptor limits epidermal infection of Lotus japonicus roots by Mesorhizobium loti. New Phytologist *222*, 1523-1537.

Misra, B.B. (2016). The Black-Box of Plant Apoplast Lipidomes. Front Plant Sci *7*, 323.

Mizuno, T., and Yamashino, T. (2010). Biochemical Characterization of Plant Hormone Cytokinin-Receptor Histidine Kinases Using Microorganisms. Method Enzymol *471*, 335-356.

References

Moling, S., Pietraszewska-Bogiel, A., Postma, M., Fedorova, E., Hink, M.A., Limpens, E., Gadella, T.W., and Bisseling, T. (2014). Nod factor receptors form heteromeric complexes and are essential for intracellular infection in medicago nodules. Plant Cell *26*, 4188-4199.

Monroe-Augustus, M., Zolman, B.K., and Bartel, B. (2003). IBR5, a dual-specificity phosphatase-like protein modulating auxin and abscisic acid responsiveness in Arabidopsis. Plant Cell *15*, 2979-2991.

Mora-Garcia, S., Vert, G., Yin, Y., Cano-Delgado, A., Cheong, H., and Chory, J. (2004). Nuclear protein phosphatases with Kelch-repeat domains modulate the response to brassinosteroids in Arabidopsis. Genes Dev *18*, 448-460,

Mortier, V., Wasson, A., Jaworek, P., De Keyser, A., Decroos, M., Holsters, M., Tarkowski, P., Mathesius, U., and Goormachtig, S. (2014). Role of LONELY GUY genes in indeterminate nodulation on Medicago truncatula. New Phytol *202*, 582-593.

Mougel, C., and Zhulin, I.B. (2001). CHASE: an extracellular sensing domain common to transmembrane receptors from prokaryotes, lower eukaryotes and plants. Trends in Biochemical Sciences *26*, 582-584.

Mun, T., Bachmann, A., Gupta, V., Stougaard, J., and Andersen, S.U. (2016). Lotus Base: An integrated information portal for the model legume Lotus japonicus. Sci Rep *6*, 39447.

Munnik, T. (2001). Phosphatidic acid: an emerging plant lipid second messenger. Trends Plant Sci *6*, 227-233.

Munnik, T., Arisz, S.A., De Vrije, T., and Musgrave, A. (1995). G Protein Activation Stimulates Phospholipase D Signaling in Plants. Plant Cell *7*, 2197-2210,

Munnik, T., Meijer, H.J., Ter Riet, B., Hirt, H., Frank, W., Bartels, D., and Musgrave, A. (2000). Hyperosmotic stress stimulates phospholipase D activity and elevates the levels of phosphatidic acid and diacylglycerol pyrophosphate. Plant J *22*, 147-154.

Munnik, T., and Vermeer, J.E.M. (2010). Osmotic stress-induced phosphoinositide and inositol phosphate signaling in plants. Plant, Cell & Environment *33*, 655-669.

Murray, J.D., Karas, B.J., Sato, S., Tabata, S., Amyot, L., and Szczyglowski, K. (2007). A Cytokinin Perception Mutant Colonized by *Rhizobium* in the Absence of Nodule Organogenesis. Science *315*, 101-104.

Nakagawa, T., and Kawaguchi, M. (2006). Shoot-applied MeJA Suppresses Root Nodulation in Lotus japonicus. Plant and Cell Physiology *47*, 176-180,

Nakamichi, N., Kita, M., Niinuma, K., Ito, S., Yamashino, T., Mizoguchi, T., and Mizuno, T. (2007). Arabidopsis clock-associated pseudo-response regulators PRR9, PRR7 and PRR5 coordinately and positively regulate flowering time through the canonical CONSTANS-dependent photoperiodic pathway. Plant and Cell Physiology *48*, 822-832.

Nam, K.H., and Li, J.M. (2002). BRI1/BAK1, a receptor kinase pair mediating brassinosteroid signaling. Cell *110*, 203-212.

References

Nambu, J.R., Lewis, J.O., Wharton, K.A., Jr., and Crews, S.T. (1991). The Drosophila single-minded gene encodes a helix-loop-helix protein that acts as a master regulator of CNS midline development. Cell *67*, 1157-1167.

Naoi, K., and Hashimoto, T. (2004). A semidominant mutation in an Arabidopsis mitogen-activated protein kinase phosphatase-like gene compromises cortical microtubule organization. Plant Cell *16*, 1841-1853.

Nazar, R., Khan, M.I., Iqbal, N., Masood, A., and Khan, N.A. (2014). Involvement of ethylene in reversal of salt-inhibited photosynthesis by sulfur in mustard. Physiol Plant *152*, 331-344.

Nelson, D.L.C., Michael M. (2008). Lehninger- Principles of Biochemistry, 5th Edition edn (New York: W. H. Freemann and Company).

Nishida, H., Tanaka, S., Handa, Y., Ito, M., Sakamoto, Y., Matsunaga, S., Betsuyaku, S., Miura, K., Soyano, T., Kawaguchi, M., *et al.* (2018). A NIN-LIKE PROTEIN mediates nitrate-induced control of root nodule symbiosis in Lotus japonicus. Nat Commun *9*, 499.

Nishiyama, R., Watanabe, Y., Fujita, Y., Le, D.T., Kojima, M., Werner, T., Vankova, R., Yamaguchi-Shinozaki, K., Shinozaki, K., Kakimoto, T., *et al.* (2011). Analysis of cytokinin mutants and regulation of cytokinin metabolic genes reveals important regulatory roles of cytokinins in drought, salt and abscisic acid responses, and abscisic acid biosynthesis. Plant Cell *23*, 2169-2183.

Nizampatnam, N.R., Schreier, S.J., Damodaran, S., Adhikari, S., and Subramanian, S. (2015). microRNA160 dictates stage-specific auxin and cytokinin sensitivities and directs soybean nodule development. Plant Journal *84*, 140-153.

Noguchi, T., Fujioka, S., Choe, S., Takatsuto, S., Yoshida, S., Yuan, H., Feldmann, K.A., and Tax, F.E. (1999). Brassinosteroid-insensitive dwarf mutants of Arabidopsis accumulate brassinosteroids. Plant Physiol *121*, 743-752.

O'Leary, B.M., Neale, H.C., Geilfus, C.M., Jackson, R.W., Arnold, D.L., and Preston, G.M. (2016). Early changes in apoplast composition associated with defence and disease in interactions between Phaseolus vulgaris and the halo blight pathogen Pseudomonas syringae Pv. phaseolicola. Plant Cell and Environment *39*, 2172-2184.

O'Leary, B.M., Rico, A., McCraw, S., Fones, H.N., and Preston, G.M. (2014). The Infiltration-centrifugation Technique for Extraction of Apoplastic Fluid from Plant Leaves Using Phaseolus vulgaris as an Example. Jove-Journal of Visualized Experiments.

Ogasawara, Y., Kaya, H., Hiraoka, G., Yumoto, F., Kimura, S., Kadota, Y., Hishinuma, H., Senzaki, E., Yamagoe, S., Nagata, K., *et al.* (2008). Synergistic activation of the Arabidopsis NADPH oxidase AtrbohD by Ca2+ and phosphorylation. J Biol Chem *283*, 8885-8892.

Oh, M.-H., Wang, X., Kota, U., Goshe, M.B., Clouse, S.D., and Huber, S.C. (2009a). Tyrosine phosphorylation of the BRI1 receptor kinase emerges as a component of brassinosteroid signaling in Arabidopsis. Proceedings of the National Academy of Sciences *106*, 658-663.

References

Oh, M.H., Clouse, S.D., and Huber, S.C. (2012a). Tyrosine Phosphorylation of the BRI1 Receptor Kinase Occurs via a Post-Translational Modification and is Activated by the Juxtamembrane Domain. Front Plant Sci *3*, 175.

Oh, M.H., Kim, H.S., Wu, X., Clouse, S.D., Zielinski, R.E., and Huber, S.C. (2012b). Calcium/calmodulin inhibition of the Arabidopsis BRASSINOSTEROID-INSENSITIVE 1 receptor kinase provides a possible link between calcium and brassinosteroid signaling. Biochemical Journal *443*, 515-523.

Oh, M.H., Wang, X., Kota, U., Goshe, M.B., Clouse, S.D., and Huber, S.C. (2009b). Tyrosine phosphorylation of the BRI1 receptor kinase emerges as a component of brassinosteroid signaling in Arabidopsis. Proc Natl Acad Sci U S A *106*, 658-663.

Oh, M.H., Wu, X., Clouse, S.D., and Huber, S.C. (2011). Functional importance of BAK1 tyrosine phosphorylation in vivo. Plant Signal Behav *6*, 400-405.

Ohgishi, M., Saji, K., Okada, K., and Sakai, T. (2004). Functional analysis of each blue light receptor, cry1, cry2, phot1, and phot2, by using combinatorial multiple mutants in Arabidopsis. Proc Natl Acad Sci U S A *101*, 2223-2228.

Oldroyd, G.E. (2013). Speak, friend, and enter: signaling systems that promote beneficial symbiotic associations in plants. Nat Rev Microbiol *11*, 252-263.

Ordonez-Herrera, N., Fackendahl, P., Yu, X., Schaefer, S., Koncz, C., and Hoecker, U. (2015). A cop1 spa mutant deficient in COP1 and SPA proteins reveals partial co-action of COP1 and SPA during Arabidopsis post-embryonic development and photomorphogenesis. Mol Plant *8*, 479-481.

Osakabe, Y., Yamaguchi-Shinozaki, K., Shinozaki, K., and Tran, L.S.P. (2013). Sensing the environment: key roles of membrane-localized kinases in plant perception and response to abiotic stress. Journal of Experimental Botany *64*, 445-458.

Osterlund, M.T., Hardtke, C.S., Wei, N., and Deng, X.W. (2000). Targeted destabilization of HY5 during light-regulated development of Arabidopsis. Nature *405*, 462-466.

Ouzounis, T., Rosenqvist, E., and Ottosen, C.-O. (2015). Spectral Effects of Artificial Light on Plant Physiology and Secondary Metabolism: A Review. HortScience: a publication of the American Society for Horticultural Science *50*, 1128-1135.

Pan, G.Y., Zhang, H.F., Chen, B.Y., Gao, S.D., Yang, B., and Jiang, Y.Q. (2019). Rapeseed calcium-dependent protein kinase CPK6L modulates reactive oxygen species and cell death through interacting and phosphorylating RBOHD. Biochemical and Biophysical Research Communications *518*, 719-725.

Pappan, K., Austin-Brown, S., Chapman, K.D., and Wang, X. (1998). Substrate selectivities and lipid modulation of plant phospholipase D alpha, -beta, and -gamma. Arch Biochem Biophys *353*, 131-140,

References

Pappan, K., Zheng, L., Krishnamoorthi, R., and Wang, X.M. (2004). Evidence for and characterization of Ca2+ binding to the catalytic region of Arabidopsis thaliana phospholipase D beta. Journal of Biological Chemistry *279*, 47833-47839.

Parniske, M. (2008). Arbuscular mycorrhiza: the mother of plant root endosymbioses. Nat Rev Microbiol *6*, 763-775.

Parre, E., Ghars, M.A., Leprince, A.S., Thiery, L., Lefebvre, D., Bordenave, M., Richard, L., Mazars, C., Abdelly, C., and Savouré, A. (2007). Calcium signaling via phospholipase C is essential for proline accumulation upon ionic but not nonionic hyperosmotic stresses in Arabidopsis. Plant Physiol *144*, 503-512.

Pattison, P.M., Tsao, J.Y., Brainard, G.C., and Bugbee, B. (2018). LEDs for photons, physiology and food. Nature *563*, 493-500,

Pedmale, Ullas V., Huang, S.-shan C., Zander, M., Cole, Benjamin J., Hetzel, J., Ljung, K., Reis, Pedro A.B., Sridevi, P., Nito, K., Nery, Joseph R., *et al.* (2016). Cryptochromes Interact Directly with PIFs to Control Plant Growth in Limiting Blue Light. Cell *164*, 233-245.

Pekarova, B., Szmitkowska, A., Dopitova, R., Degtjarik, O., Zidek, L., and Hejatko, J. (2016). Structural Aspects of Multistep Phosphorelay-Mediated Signaling in Plants. Mol Plant *9*, 71-85.

Peters, N.K., Frost, J.W., and Long, S.R. (1986). A plant flavone, luteolin, induces expression of Rhizobium meliloti nodulation genes. Science *233*, 977-980,

Phuong, L.T., Fitrianti, A.N., Luan, M.T., Matsui, H., Noutoshi, Y., Yamamoto, M., Ichinose, Y., Shiraishi, T., and Toyoda, K. (2020). Antagonism between SA- and JA-signaling conditioned by saccharin in Arabidopsis thaliana renders resistance to a specific pathogen. Journal of General Plant Pathology *86*, 86-99.

Pierik, R., Tholen, D., Poorter, H., Visser, E.J.W., and Voesenek, L.A.C.J. (2006). The Janus face of ethylene: growth inhibition and stimulation. Trends in Plant Science *11*, 176-183.

Planas-Riverola, A., Gupta, A., Betegon-Putze, I., Bosch, N., Ibanes, M., and Cano-Delgado, A.I. (2019). Brassinosteroid signaling in plant development and adaptation to stress. Development *146*, 11.

Plet, J., Wasson, A., Ariel, F., Le Signor, C., Baker, D., Mathesius, U., Crespi, M., and Frugier, F. (2011). MtCRE1-dependent cytokinin signaling integrates bacterial and plant cues to coordinate symbiotic nodule organogenesis in Medicago truncatula. The Plant Journal *65*, 622-633.

Podolec, R., and Ulm, R. (2018). Photoreceptor-mediated regulation of the COP1/SPA E3 ubiquitin ligase. Curr Opin Plant Biol *45*, 18-25.

Pokotylo, I., Kravets, V., Martinec, J., and Ruelland, E. (2018). The phosphatidic acid paradox: Too many actions for one molecule class? Lessons from plants. Prog Lipid Res *71*, 43-53.

Ponnu, J., Riedel, T., Penner, E., Schrader, A., and Hoecker, U. (2019). Cryptochrome 2 competes with COP1 substrates to repress COP1 ubiquitin ligase activity during Arabidopsis photomorphogenesis. Proc Natl Acad Sci U S A.

References

Poovaiah, B.W., Du, L., Wang, H., and Yang, T. (2013). Recent advances in calcium/calmodulin-mediated signaling with an emphasis on plant-microbe interactions. Plant Physiol *163*, 531-542.

Pornsiriwong, W., Estavillo, G.M., Chan, K.X., Tee, E.E., Ganguly, D., Crisp, P.A., Phua, S.Y., Zhao, C., Qiu, J., Park, J., *et al.* (2017). A chloroplast retrograde signal, 3'-phosphoadenosine 5'-phosphate, acts as a secondary messenger in abscisic acid signaling in stomatal closure and germination. Elife *6*.

Possart, A., Fleck, C., and Hiltbrunner, A. (2014). Shedding (far-red) light on phytochrome mechanisms and responses in land plants. Plant Science *217-218*, 36-46.

Qiao, H., Shen, Z., Huang, S.S., Schmitz, R.J., Urich, M.A., Briggs, S.P., and Ecker, J.R. (2012). Processing and subcellular trafficking of ER-tethered EIN2 control response to ethylene gas. Science *338*, 390-393.

Qin, C.B., and Wang, X.M. (2002). The Arabidopsis phospholipase D family. Characterozation of a calcium-independent and phosphatidylcholine-selective PLD zeta 1 with distinct regulatory domains. Plant Physiology *128*, 1057-1068.

Quattrocchio, F., Verweij, W., Kroon, A., Spelt, C., Mol, J., and Koes, R. (2006). PH4 of Petunia Is an R2R3 MYB Protein That Activates Vacuolar Acidification through Interactions with Basic-Helix-Loop-Helix Transcription Factors of the Anthocyanin Pathway. The Plant Cell *18*, 1274-1291.

Rabino, I., and Mancinelli, A.L. (1986). Light, Temperature, and Anthocyanin Production. Plant Physiology *81*, 922-924.

Radutoiu, S., Madsen, L.H., Madsen, E.B., Jurkiewicz, A., Fukai, E., Quistgaard, E.M.H., Albrektsen, A.S., James, E.K., Thirup, S., and Stougaard, J. (2007). LysM domains mediate lipochitin-oligosaccharide recognition and Nfr genes extend the symbiotic host range. The EMBO journal *26*, 3923-3935.

Redmond, J.W., Batley, M., Djordjevic, M.A., Innes, R.W., Kuempel, P.L., and Rolfe, B.G. (1986). Flavones Induce Expression of Nodulation Genes in Rhizobium. Nature *323*, 632-635.

Reid, D.E., Heckmann, A.B., Novak, O., Kelly, S., and Stougaard, J. (2016). CYTOKININ OXIDASE/DEHYDROGENASE3 Maintains Cytokinin Homeostasis during Root and Nodule Development in Lotus japonicus. Plant Physiol *170*, 1060-1074.

Rentel, M.C., and Knight, M.R. (2004). Oxidative Stress-Induced Calcium Signaling in Arabidopsis. Plant Physiology *135*, 1471-1479.

Robert-Seilaniantz, A., Grant, M., and Jones, J.D. (2011). Hormone crosstalk in plant disease and defense: more than just jasmonate-salicylate antagonism. Annu Rev Phytopathol *49*, 317-343.

Rodriguez, C., Torre, S., and Solhaug, K.A. (2014). Low levels of ultraviolet-B radiation from fluorescent tubes induce an efficient flavonoid synthesis in Lollo Rosso lettuce without negative impact on growth. Acta Agr Scand B-S P *64*, 178-184.

References

Rojas-Pirela, M., Rigden, D.J., Michels, P.A., Cáceres, A.J., Concepción, J.L., and Quiñones, W. (2018). Structure and function of Per-ARNT-Sim domains and their possible role in the life-cycle biology of Trypanosoma cruzi. Molecular and Biochemical Parasitology *219*, 52-66.

Romanov, G.A., Lomin, S.N., and Schmulling, T. (2006). Biochemical characteristics and ligand-binding properties of Arabidopsis cytokinin receptor AHK3 compared to CRE1/AHK4 as revealed by a direct binding assay. J Exp Bot *57*, 4051-4058.

Roux, M., Schwessinger, B., Albrecht, C., Chinchilla, D., Jones, A., Holton, N., Malinovsky, F.G., Tor, M., de Vries, S., and Zipfel, C. (2011). The Arabidopsis Leucine-Rich Repeat Receptor-Like Kinases BAK1/SERK3 and BKK1/SERK4 Are Required for Innate Immunity to Hemibiotrophic and Biotrophic Pathogens. Plant Cell *23*, 2440-2455.

Roy, S., Liu, W., Nandety, R.S., Crook, A., Mysore, K.S., Pislariu, C.I., Frugoli, J., Dickstein, R., and Udvardi, M.K. (2020). Celebrating 20 Years of Genetic Discoveries in Legume Nodulation and Symbiotic Nitrogen Fixation. The Plant Cell *32*, 15-41.

Roy, S., Robson, F., Lilley, J., Liu, C.W., Cheng, X.F., Wen, J.Q., Walker, S., Sun, J., Cousins, D., Bone, C., *et al.* (2017). MtLAX2, a Functional Homologue of the Arabidopsis Auxin Influx Transporter AUX1, Is Required for Nodule Organogenesis. Plant Physiology *174*, 326-338.

Ryals, J., Uknes, S., and Ward, E. (1994). Systemic Acquired Resistance. Plant Physiology *104*, 1109-1112.

Ryo, M., Yamashino, T., Yamakawa, H., Fujita, Y., and Aoki, S. (2018). PAS-histidine kinases PHK1 and PHK2 exert oxygen-dependent dual and opposite effects on gametophore formation in the moss Physcomitrella patens. Biochemical and Biophysical Research Communications *503*, 2861-2865.

Saijo, Y., and Loo, E.P.I. (2019). Plant immunity in signal integration between biotic and abiotic stress responses. New Phytologist.

Saijo, Y., Sullivan, J.A., Wang, H., Yang, J., Shen, Y., Rubio, V., Ma, L., Hoecker, U., and Deng, X.W. (2003). The COP1-SPA1 interaction defines a critical step in phytochrome A-mediated regulation of HY5 activity. Genes Dev *17*, 2642-2647.

Saito, S., and Uozumi, N. (2020). Calcium-Regulated Phosphorylation Systems Controlling Uptake and Balance of Plant Nutrients. Front Plant Sci *11*.

Sakai, H., Hua, J., Chen, Q.G., Chang, C., Medrano, L.J., Bleecker, A.B., and Meyerowitz, E.M. (1998a). ETR2 is an ETR1-like gene involved in ethylene signaling in Arabidopsis. Proc Natl Acad Sci U S A *95*, 5812-5817.

Sakai, H., Hua, J., Chen, Q.H.G., Chang, C.R., Medrano, L.J., Bleecker, A.B., and Meyerowitz, E.M. (1998b). ETR2 is an ETR1-like gene involved in ethylene signaling in Arabidopsis. P Natl Acad Sci USA *95*, 5812-5817.

Saleem, M., Fariduddin, Q., and Janda, T. (2020). Multifaceted Role of Salicylic Acid in Combating Cold Stress in Plants: A Review. J Plant Growth Regul, 22.

References

Salvi, P., Manna, M., Kaur, H., Thakur, T., Gandass, N., Bhatt, D., and Muthamilarasan, M. Phytohormone signaling and crosstalk in regulating drought stress response in plants. Plant Cell Reports, 25.

Sanchez-Barcelo, E.J., Mediavilla, M.D., Vriend, J., and Reiter, R.J. (2016). Constitutive photomorphogenesis protein 1 (COP1) and COP9 signalosome, evolutionarily conserved photomorphogenic proteins as possible targets of melatonin. J Pineal Res *61*, 41-51.

Sato, S., Nakamura, Y., Kaneko, T., Asamizu, E., Kato, T., Nakao, M., Sasamoto, S., Watanabe, A., Ono, A., Kawashima, K., *et al.* (2008). Genome structure of the legume, Lotus japonicus. DNA Res *15*, 227-239.

Schacht, J. (1978). PURIFICATION OF POLYPHOSPHOINOSITIDES BY CHROMATOGRAPHY ON IMMOBILIZED NEOMYCIN. J Lipid Res *19*, 1063-1067.

Scharein, B., and Groth, G. (2011). Phosphorylation alters the interaction of the Arabidopsis phosphotransfer protein AHP1 with its sensor kinase ETR1. PLoS One *6*, e24173.

Schenk, H.J., Espino, S., Rich-Cavazos, S.M., and Jansen, S. (2018). From the sap's perspective: The nature of vessel surfaces in angiosperm xylem. Am J Bot *105*, 172-185.

Schenk, H.J., Michaud, J.M., Espino, S., Melendres, T., Roth, M.R., Welti, R., Kaack, L., and Jansen, S. (2019). Lipids in xylem sap of woody plants across the angiosperm phylogeny. bioRxiv, 763771.

Schlöffel, M.A., Salzer, A., Wan, W.-L., van Wijk, R., Šemanjski, M., Symeonidi, E., Slaby, P., Kilian, J., Maček, B., Munnik, T., *et al.* (2019). The BIR2/BIR3-interacting Phospholipase D gamma 1 negatively regulates immunity in Arabidopsis. bioRxiv, 815282.

Schulze, B., Mentzel, T., Jehle, A.K., Mueller, K., Beeler, S., Boller, T., Felix, G., and Chinchilla, D. (2010). Rapid Heteromerization and Phosphorylation of Ligand-activated Plant Transmembrane Receptors and Their Associated Kinase BAK1. Journal of Biological Chemistry *285*, 9444-9451.

Schwessinger, B., Roux, M., Kadota, Y., Ntoukakis, V., Sklenar, J., Jones, A., and Zipfel, C. (2011). Phosphorylation-Dependent Differential Regulation of Plant Growth, Cell Death, and Innate Immunity by the Regulatory Receptor-Like Kinase BAK1. Plos Genetics *7*.

Segonzac, C., Macho, A.P., Sanmartin, M., Ntoukakis, V., Sanchez-Serrano, J.J., and Zipfel, C. (2014a). Negative control of BAK1 by protein phosphatase 2A during plant innate immunity. EMBO J *33*, 2069-2079.

Segonzac, C., Macho, A.P., Sanmartín, M., Ntoukakis, V., Sánchez-Serrano, J.J., and Zipfel, C. (2014b). Negative control of BAK1 by protein phosphatase 2A during plant innate immunity. Embo j *33*, 2069-2079.

Seo, H.S., Yang, J.Y., Ishikawa, M., Bolle, C., Ballesteros, M.L., and Chua, N.H. (2003). LAF1 ubiquitination by COP1 controls photomorphogenesis and is stimulated by SPA1. Nature *423*, 995-999.

Sevvana, M., Vijayan, V., Zweckstetter, M., Reinelt, S., Madden, D.R., Herbst-Irmer, R., Sheldrick, G.M., Bott, M., Griesinger, C., and Becker, S. (2008). A ligand-induced switch in the periplasmic domain of sensor histidine kinase CitA. Journal of Molecular Biology *377*, 512-523.

References

Sharma, A., Kumar, V., Yuan, H., Kanwar, M.K., Bhardwaj, R., Thukral, A.K., and Zheng, B. (2018). Jasmonic Acid Seed Treatment Stimulates Insecticide Detoxification in Brassica juncea L. Front Plant Sci *9*, 1609.

Sheard, L.B., Tan, X., Mao, H., Withers, J., Ben-Nissan, G., Hinds, T.R., Kobayashi, Y., Hsu, F.-F., Sharon, M., Browse, J., *et al.* (2010). Jasmonate perception by inositol-phosphate-potentiated COI1–JAZ co-receptor. Nature *468*, 400-405.

Shi, C., Qi, C., Ren, H., Huang, A., Hei, S., and She, X. (2015). Ethylene mediates brassinosteroid-induced stomatal closure via Gα protein-activated hydrogen peroxide and nitric oxide production in Arabidopsis. The Plant Journal *82*, 280-301.

Shi, S.J., Li, S.G., Asim, M., Mao, J.J., Xu, D.Z., Ullah, Z., Liu, G.S., Wang, Q., and Liu, H.B. (2018). The Arabidopsis Calcium-Dependent Protein Kinases (CDPKs) and Their Roles in Plant Growth Regulation and Abiotic Stress Responses. Int J Mol Sci *19*.

Shimoda, Y., Han, L., Yamazaki, T., Suzuki, R., Hayashi, M., and Imaizumi-Anraku, H. (2012). Rhizobial and fungal symbioses show different requirements for calmodulin binding to calcium calmodulin-dependent protein kinase in Lotus japonicus. Plant Cell *24*, 304-321.

Shiva, S., Enninful, R., Roth, M.R., Tamura, P., Jagadish, K., and Welti, R. (2018). An efficient modified method for plant leaf lipid extraction results in improved recovery of phosphatidic acid. Plant Methods *14*.

Skirycz, A., De Bodt, S., Obata, T., De Clercq, I., Claeys, H., De Rycke, R., Andriankaja, M., Van Aken, O., Van Breusegem, F., Fernie, A.R., *et al.* (2010). Developmental stage specificity and the role of mitochondrial metabolism in the response of Arabidopsis leaves to prolonged mild osmotic stress. Plant Physiol *152*, 226-244.

Solano, R., Stepanova, A., Chao, Q.M., and Ecker, J.R. (1998). Nuclear events in ethylene signaling: a transcriptional cascade mediated by ETHYLENE-INSENSITIVE3 and ETHYLENE-RESPONSE-FACTOR1. Gene Dev *12*, 3703-3714.

Solfanelli, C., Poggi, A., Loreti, E., Alpi, A., and Perata, P. (2006). Sucrose-Specific Induction of the Anthocyanin Biosynthetic Pathway in Arabidopsis. Plant Physiology *140*, 637-646.

Soma, F., Mogami, J., Yoshida, T., Abekura, M., Takahashi, F., Kidokoro, S., Mizoi, J., Shinozaki, K., and Yamaguchi-Shinozaki, K. (2017). ABA-unresponsive SnRK2 protein kinases regulate mRNA decay under osmotic stress in plants. Nat Plants *3*, 16204.

Spichal, L., Rakova, N.Y., Riefler, M., Mizuno, T., Romanov, G.A., Strnad, M., and Schmulling, T. (2004). Two cytokinin receptors of Arabidopsis thaliana, CRE1/AHK4 and AHK3, differ in their ligand specificity in a bacterial assay. Plant Cell Physiol *45*, 1299-1305.

Staxen, I., Pical, C., Montgomery, L.T., Gray, J.E., Hetherington, A.M., and McAinsh, M.R. (1999). Abscisic acid induces oscillations in guard-cell cytosolic free calcium that involve phosphoinositide-specific phospholipase C. Proc Natl Acad Sci U S A *96*, 1779-1784.

Staxén, I., Pical, C., Montgomery, L.T., Gray, J.E., Hetherington, A.M., and McAinsh, M.R. (1999). Abscisic acid induces oscillations in guard-cell cytosolic free calcium that involve

phosphoinositide-specific phospholipase C. Proceedings of the National Academy of Sciences *96*, 1779-1784.

Stracke, S., Kistner, C., Yoshida, S., Mulder, L., Sato, S., Kaneko, T., Tabata, S., Sandal, N., Stougaard, J., Szczyglowski, K., *et al.* (2002). A plant receptor-like kinase required for both bacterial and fungal symbiosis. Nature *417*, 959-962.

Street, I.H., Aman, S., Zubo, Y., Ramzan, A., Wang, X., Shakeel, S.N., Kieber, J.J., and Schaller, G.E. (2015). Ethylene Inhibits Cell Proliferation of the Arabidopsis Root Meristem. Plant Physiol *169*, 338-350,

Sun, Y.D., Han, Z.F., Tang, J., Hu, Z.H., Chai, C.L., Zhou, B., and Chai, J.J. (2013a). Structure reveals that BAK1 as a co-receptor recognizes the BRI1-bound brassinolide. Cell Res *23*, 1326-1329.

Sun, Y.D., Li, L., Macho, A.P., Han, Z.F., Hu, Z.H., Zipfel, C., Zhou, J.M., and Chai, J.J. (2013b). Structural Basis for flg22-Induced Activation of the Arabidopsis FLS2-BAK1 Immune Complex. Science *342*, 624-628.

Sussmilch, F.C., Brodribb, T.J., and McAdam, S.A.M. (2017). Up-regulation of NCED3 and ABA biosynthesis occur within minutes of a decrease in leaf turgor but AHK1 is not required. J Exp Bot *68*, 2913-2918.

Sutton, M.A., Oenema, O., Erisman, J.W., Leip, A., van Grinsven, H., and Winiwarter, W. (2011). Too much of a good thing. Nature *472*, 159-161.

Suzuki, A., Suriyagoda, L., Shigeyama, T., Tominaga, A., Sasaki, M., Hiratsuka, Y., Yoshinaga, A., Arima, S., Agarie, S., Sakai, T., *et al.* (2011). Lotus japonicus nodulation is photomorphogenetically controlled by sensing the red/far red (R/FR) ratio through jasmonic acid (JA) signaling. P Natl Acad Sci USA *108*, 16837-16842.

Suzuki, N. (2016). Hormone signaling pathways under stress combinations. Plant Signaling & Behavior *11*.

Suzuki, T., Sakurai, K., Imamura, A., Nakamura, A., Ueguchi, C., and Mizuno, T. (2000). Compilation and characterization of histidine-containing phosphotransmitters implicated in His-to-Asp phosphorelay in plants: AHP signal transducers of Arabidopsis thaliana. Biosci Biotechnol Biochem *64*, 2486-2489.

Taiz, L.Z.E. (2006). Plant Physiology, 4th Edition edn (Springer-Verlag).

Takahashi, S., Katagiri, T., Hirayama, T., Yamaguchi-Shinozaki, K., and Shinozaki, K. (2001). Hyperosmotic stress induces a rapid and transient increase in inositol 1,4,5-trisphosphate independent of abscisic acid in Arabidopsis cell culture. Plant Cell Physiol *42*, 214-222.

Tan, S., Debellé, F., Gamas, P., Frugier, F., and Brault, M. (2019). Diversification of cytokinin phosphotransfer signaling genes in Medicago truncatula and other legume genomes. BMC Genomics *20*, 373.

Tan, W.J., Yang, Y.C., Zhou, Y., Huang, L.P., Xu, L., Chen, Q.F., Yu, L.J., and Xiao, S. (2018). DIACYLGLYCEROL ACYLTRANSFERASE and DIACYLGLYCEROL KINASE Modulate

References

Triacylglycerol and Phosphatidic Acid Production in the Plant Response to Freezing Stress. Plant Physiology *177*, 1303-1318.

Tang, W., Kim, T.W., Oses-Prieto, J.A., Sun, Y., Deng, Z., Zhu, S., Wang, R., Burlingame, A.L., and Wang, Z.Y. (2008). BSKs mediate signal transduction from the receptor kinase BRI1 in Arabidopsis. Science *321*, 557-560,

Tang, W., Yuan, M., Wang, R., Yang, Y., Wang, C., Oses-Prieto, J.A., Kim, T.W., Zhou, H.W., Deng, Z., Gampala, S.S., *et al.* (2011). PP2A activates brassinosteroid-responsive gene expression and plant growth by dephosphorylating BZR1. Nat Cell Biol *13*, 124-131.

Tanigawa, M., Kihara, A., Terashima, M., Takahara, T., and Maeda, T. (2012). Sphingolipids Regulate the Yeast High-Osmolarity Glycerol Response Pathway. Mol Cell Biol *32*, 2861-2870,

Taylor, B.L., and Zhulin, I.B. (1999). PAS-domains: internal sensors of oxygen, redox potential, and light. Microbiol Mol Biol Rev *63*, 479-506.

Testerink, C., Dekker, H.L., Lim, Z.Y., Johns, M.K., Holmes, A.B., Koster, C.G., Ktistakis, N.T., and Munnik, T. (2004). Isolation and identification of phosphatidic acid targets from plants. Plant J *39*, 527-536.

Testerink, C., and Munnik, T. (2011). Molecular, cellular, and physiological responses to phosphatidic acid formation in plants. J Exp Bot *62*, 2349-2361.

Thoma, F., Somborn-Schulz, A., Schlehuber, D., Keuter, V., and Deerberg, G. (2020). Effects of Light on Secondary Metabolites in Selected Leafy Greens: A Review. Front Plant Sci *11*, 497.

Thuerig, B., Felix, G., Binder, A., Boller, T., and Tamm, L. (2005). An extract of Penicillium chrysogenum elicits early defense-related responses and induces resistance in Arabidopsis thaliana independently of known signaling pathways. Physiol Mol Plant P *67*, 180-193.

Tian, Y., Fan, M., Qin, Z., Lv, H., Wang, M., Zhang, Z., Zhou, W., Zhao, N., Li, X., Han, C., *et al.* (2018). Hydrogen peroxide positively regulates brassinosteroid signaling through oxidation of the BRASSINAZOLE-RESISTANT1 transcription factor. Nat Commun *9*, 1063.

Tirichine, L., Sandal, N., Madsen, L.H., Radutoiu, S., Albrektsen, A.S., Sato, S., Asamizu, E., Tabata, S., and Stougaard, J. (2007). A gain-of-function mutation in a cytokinin receptor triggers spontaneous root nodule organogenesis. Science *315*, 104-107.

Tissot, N., and Ulm, R. (2020). Cryptochrome-mediated blue-light signaling modulates UVR8 photoreceptor activity and contributes to UV-B tolerance in Arabidopsis. Nat Commun *11*, 1323.

To, J.P.C., Haberer, G., Ferreira, F.J., Deruère, J., Mason, M.G., Schaller, G.E., Alonso, J.M., Ecker, J.R., and Kieber, J.J. (2004). Type-A Arabidopsis Response Regulators Are Partially Redundant Negative Regulators of Cytokinin Signaling. The Plant Cell *16*, 658-671.

Tran, L.S.P., Urao, T., Qin, F., Maruyama, K., Kakimoto, T., Shinozaki, K., and Yamaguchi-Shinozaki, K. (2007). Functional analysis of AHK1/ATHK1 and cytokinin receptor histidine kinases in response to abscisic acid, drought, and salt stress in Arabidopsis. P Natl Acad Sci USA *104*, 20623-20628.

References

Truchet, G., Roche, P., Lerouge, P., Vasse, J., Camut, S., de Billy, F., Promé, J.-C., and Dénarié, J. (1991). Sulphated lipo-oligosaccharide signals of Rhizobium meliloti elicit root nodule organogenesis in alfalfa. Nature *351*, 670-673.

Tsikou, D., Yan, Z., Holt, D.B., Abel, N.B., Reid, D.E., Madsen, L.H., Bhasin, H., Sexauer, M., Stougaard, J., and Markmann, K. (2018). Systemic control of legume susceptibility to rhizobial infection by a mobile microRNA. Science *362*, 233-236.

Tuteja, N., and Mahajan, S. (2007). Calcium signaling network in plants: an overview. Plant Signal Behav *2*, 79-85.

Uemura, M., Joseph, R.A., and Steponkus, P.L. (1995). Cold Acclimation of Arabidopsis thaliana (Effect on Plasma Membrane Lipid Composition and Freeze-Induced Lesions). Plant Physiol *109*, 15-30,

Uemura, M., and Steponkus, P.L. (1994). A Contrast of the Plasma Membrane Lipid Composition of Oat and Rye Leaves in Relation to Freezing Tolerance. Plant Physiol *104*, 479-496.

Upadhyay, A.A., Fleetwood, A.D., Adebali, O., Finn, R.D., and Zhulin, I.B. (2016). Cache Domains That are Homologous to, but Different from PAS Domains Comprise the Largest Superfamily of Extracellular Sensors in Prokaryotes. Plos Computational Biology *12*.

Urao, T., Yakubov, B., Satoh, R., Yamaguchi-Shinozaki, K., Seki, M., Hirayama, T., and Shinozaki, K. (1999). A transmembrane hybrid-type histidine kinase in arabidopsis functions as an osmosensor. Plant Cell *11*, 1743-1754.

Urbanski, D.F., Malolepszy, A., Stougaard, J., and Andersen, S.U. (2012). Genome-wide LORE1 retrotransposon mutagenesis and high-throughput insertion detection in Lotus japonicus. Plant J *69*, 731-741.

Vastakaite, V., Virsile, A., Brazaityte, A., Samuoliene, G., Jankauskiene, J., Sirtautas, R., and Duchovskis, P. (2015). The Effect of Uv-a Supplemental Lighting on Antioxidant Properties of Ocimum Basilicum L. Microgreens in Greenhouse. Rural Development.

Viczian, A., Adam, E., Staudt, A.M., Lambert, D., Klement, E., Montepaone, S.R., Hiltbrunner, A., Casal, J., Schafer, E., Nagy, F., *et al.* (2020). Differential phosphorylation of the N-terminal extension regulates phytochrome B signaling. New Phytologist *225*, 1635-1650,

Virlouvet, L., Ding, Y., Fujii, H., Avramova, Z., and Fromm, M. (2014). ABA signaling is necessary but not sufficient for RD29B transcriptional memory during successive dehydration stresses in Arabidopsis thaliana. The Plant Journal *79*, 150-161.

Vogt, J.H.M., and Schippers, J.H.M. (2015). Setting the PAS, the role of circadian PAS-domain proteins during environmental adaptation in plants. Front Plant Sci *6*, 513-513.

Walker, E.H., Pacold, M.E., Perisic, O., Stephens, L., Hawkins, P.T., Wymann, M.P., and Williams, R.L. (2000). Structural determinants of phosphoinositide 3-kinase inhibition by wortmannin, LY294002, quercetin, myricetin, and staurosporine. Mol Cell *6*, 909-919.

Wang, C., Li, J., and Yuan, M. (2007). Salt tolerance requires cortical microtubule reorganization in Arabidopsis. Plant Cell Physiol *48*, 1534-1547.

References

Wang, K.L., Li, H., and Ecker, J.R. (2002). Ethylene biosynthesis and signaling networks. Plant Cell *14 Suppl*, S131-151.

Wang, R., Liu, M., Yuan, M., Oses-Prieto, J.A., Cai, X., Sun, Y., Burlingame, A.L., Wang, Z.Y., and Tang, W. (2016a). The Brassinosteroid-Activated BRI1 Receptor Kinase Is Switched off by Dephosphorylation Mediated by Cytoplasm-Localized PP2A B' Subunits. Mol Plant *9*, 148-157.

Wang, W.Y., Hall, A.E., O'Malley, R., and Bleecker, A.B. (2003). Canonical histidine kinase activity of the transmitter domain of the ETR1 ethylene receptor from Arabidopsis is not required for signal transmission. P Natl Acad Sci USA *100*, 352-357.

Wang, X., and Chory, J. (2006). Brassinosteroids regulate dissociation of BKI1, a negative regulator of BRI1 signaling, from the plasma membrane. Science *313*, 1118-1122.

Wang, X., Devaiah, S.P., Zhang, W., and Welti, R. (2006). Signaling functions of phosphatidic acid. Prog Lipid Res *45*, 250-278.

Wang, X., Kota, U., He, K., Blackburn, K., Li, J., Goshe, M.B., Huber, S.C., and Clouse, S.D. (2008a). Sequential transphosphorylation of the BRI1/BAK1 receptor kinase complex impacts early events in brassinosteroid signaling. Dev Cell *15*, 220-235.

Wang, X., Wang, Q., Han, Y.J., Liu, Q., Gu, L., Yang, Z., Su, J., Liu, B., Zuo, Z., He, W., *et al.* (2017). A CRY-BIC negative-feedback circuitry regulating blue light sensitivity of Arabidopsis. Plant J *92*, 426-436.

Wang, X., Wang, Q., Nguyen, P., and Lin, C. (2014). Cryptochrome-mediated light responses in plants. Enzymes *35*, 167-189.

Wang, X.F., Kota, U., He, K., Blackburn, K., Li, J., Goshe, M.B., Huber, S.C., and Clouse, S.D. (2008b). Sequential transphosphorylation of the BRI1/BAK1 receptor kinase complex impacts early events in brassinosteroid signaling. Developmental Cell *15*, 220-235.

Wang, Y.N., Li, K.X., Chen, L., Zou, Y.M., Liu, H.P., Tian, Y.P., Li, D.X., Wang, R., Zhao, F., Ferguson, B.J., *et al.* (2015). MicroRNA167-Directed Regulation of the Auxin Response Factors GmARF8a and GmARF8b Is Required for Soybean Nodulation and Lateral Root Development. Plant Physiology *168*, 101-+.

Wang, Y.S., Yao, H.Y., and Xue, H.W. (2016b). Lipidomic profiling analysis reveals the dynamics of phospholipid molecules in Arabidopsis thaliana seedling growth. J Integr Plant Biol *58*, 890-902.

Wang, Z., Meng, P., Zhang, X.Y., Ren, D.T., and Yang, S.H. (2011). BON1 interacts with the protein kinases BIR1 and BAK1 in modulation of temperature-dependent plant growth and cell death in Arabidopsis. Plant Journal *67*, 1081-1093.

Warnasooriya, S.N., and Montgomery, B.L. (2009). Detection of Spatial-Specific Phytochrome Responses Using Targeted Expression of Biliverdin Reductase in Arabidopsis. Plant Physiology *149*, 424-433.

References

Warnasooriya, S.N., Porter, K.J., and Montgomery, B.L. (2011). Tissue- and isoform-specific phytochrome regulation of light-dependent anthocyanin accumulation in Arabidopsis thaliana. Plant Signal Behav *6*, 624-631.

Wasternack, C., and Hause, B. (2013). Jasmonates: biosynthesis, perception, signal transduction and action in plant stress response, growth and development. An update to the 2007 review in Annals of Botany. Annals of Botany *111*, 1021-1058.

Wasternack, C., and Strnad, M. (2016). Jasmonate signaling in plant stress responses and development - active and inactive compounds. N Biotechnol *33*, 604-613.

Waszczak, C., Carmody, M., and Kangasjarvi, J. (2018). Reactive Oxygen Species in Plant Signaling. Annu Rev Plant Biol *69*, 209-236.

Waterhouse, A.M., Procter, J.B., Martin, D.M., Clamp, M., and Barton, G.J. (2009). Jalview Version 2--a multiple sequence alignment editor and analysis workbench. Bioinformatics *25*, 1189-1191.

Wei, Y.F., and Matthews, H.R. (1991). Identification of phosphohistidine in proteins and purification of protein-histidine kinases. Methods Enzymol *200*, 388-414.

Wen, X., Zhang, C.L., Ji, Y.S., Zhao, Q., He, W.R., An, F.Y., Jiang, L.W., and Guo, H.W. (2012). Activation of ethylene signaling is mediated by nuclear translocation of the cleaved EIN2 carboxyl terminus. Cell Res *22*, 1613-1616.

Wenden, B., Kozma-Bognar, L., Edwards, K.D., Hall, A.J.W., Locke, J.C.W., and Millar, A.J. (2011). Light inputs shape the Arabidopsis circadian system. Plant Journal *66*, 480-491.

Werner, J.E., and Finkelstein, R.R. (1995). Arabidopsis Mutants with Reduced Response to Nacl and Osmotic-Stress. Physiol Plantarum *93*, 659-666.

West, A.H., and Stock, A.M. (2001). Histidine kinases and response regulator proteins in two-component signaling systems. Trends in Biochemical Sciences *26*, 369-376.

Wewer, V., Dombrink, I., vom Dorp, K., and Dormann, P. (2011). Quantification of sterol lipids in plants by quadrupole time-of-flight mass spectrometry. J Lipid Res *52*, 1039-1054.

Wielandt, A.G., Pedersen, J.T., Falhof, J., Kemmer, G.C., Lund, A., Ekberg, K., Fuglsang, A.T., Pomorski, T.G., Buch-Pedersen, M.J., and Palmgren, M. (2015). Specific Activation of the Plant P-type Plasma Membrane H+-ATPase by Lysophospholipids Depends on the Autoinhibitory N- and C-terminal Domains. Journal of Biological Chemistry *290*, 16281-16291.

Wingler, A., Tijero, V., Muller, M., Yuan, B.Q., and Munne-Bosch, S. (2020). Interactions between sucrose and jasmonate signaling in the response to cold stress. BMC Plant Biol *20*, 13.

Wohlbach, D.J., Quirino, B.F., and Sussman, M.R. (2008). Analysis of the Arabidopsis histidine kinase ATHK1 reveals a connection between vegetative osmotic stress sensing and seed maturation. Plant Cell *20*, 1101-1117.

Wu, F., Chi, Y., Jiang, Z., Xu, Y., Xie, L., Huang, F., Wan, D., Ni, J., Yuan, F., Wu, X., *et al.* (2020). Hydrogen peroxide sensor HPCA1 is an LRR receptor kinase in Arabidopsis. Nature *578*, 577-581.

References

Wu, G., Wang, X., Li, X., Kamiya, Y., Otegui, M.S., and Chory, J. (2011). Methylation of a phosphatase specifies dephosphorylation and degradation of activated brassinosteroid receptors. Sci Signal *4*, ra29.

Wu, P., Gao, H.B., Zhang, L.L., Xue, H.W., and Lin, W.H. (2014). Phosphatidic acid regulates BZR1 activity and brassinosteroid signal of Arabidopsis. Mol Plant *7*, 445-447.

Wulfetange, K., Lomin, S.N., Romanov, G.A., Stolz, A., Heyl, A., and Schmülling, T. (2011). The cytokinin receptors of Arabidopsis are located mainly to the endoplasmic reticulum. Plant physiology *156*, 1808-1818.

Xiao, F., Goodwin, S.M., Xiao, Y., Sun, Z., Baker, D., Tang, X., Jenks, M.A., and Zhou, J.M. (2004). Arabidopsis CYP86A2 represses Pseudomonas syringae type III genes and is required for cuticle development. EMBO J *23*, 2903-2913.

Xiong, L.M., Ishitani, M., Lee, H., and Zhu, J.K. (2001). The Arabidopsis LOS5/ABA3 locus encodes a molybdenum cofactor sulfurase and modulates cold stress- and osmotic stress-responsive gene expression. Plant Cell *13*, 2063-2083.

Xu, Z., Mahmood, K., and Rothstein, S.J. (2017). ROS Induces Anthocyanin Production Via Late Biosynthetic Genes and Anthocyanin Deficiency Confers the Hypersensitivity to ROS-Generating Stresses in Arabidopsis. Plant Cell Physiol *58*, 1364-1377.

Yadav, A., Singh, D., Lingwan, M., Yadukrishnan, P., Masakapalli, S.K., and Datta, S. (2020). Light signaling and UV-B-mediated plant growth regulation. J Integr Plant Biol.

Yamada, H., Suzuki, T., Terada, K., Takei, K., Ishikawa, K., Miwa, K., Yamashino, T., and Mizuno, T. (2001). The Arabidopsis AHK4 Histidine Kinase is a Cytokinin-Binding Receptor that Transduces Cytokinin Signals Across the Membrane. Plant and Cell Physiology *42*, 1017-1023.

Yang, Y., Liang, T., Zhang, L., Shao, K., Gu, X., Shang, R., Shi, N., Li, X., Zhang, P., and Liu, H. (2018a). UVR8 interacts with WRKY36 to regulate HY5 transcription and hypocotyl elongation in Arabidopsis. Nat Plants *4*, 98-107.

Yang, Y., Yang, X., Jang, Z., Chen, Z., Ruo, X., Jin, W., Wu, Y., Shi, X., and Xu, M. (2018b). UV RESISTANCE LOCUS 8 From Chrysanthemum morifolium Ramat (CmUVR8) Plays Important Roles in UV-B Signal Transduction and UV-B-Induced Accumulation of Flavonoids. Front Plant Sci *9*.

Yanhui, C., Xiaoyuan, Y., Kun, H., Meihua, L., Jigang, L., Zhaofeng, G., Zhiqiang, L., Yunfei, Z., Xiaoxiao, W., Xiaoming, Q., *et al.* (2006). The MYB transcription factor superfamily of Arabidopsis: expression analysis and phylogenetic comparison with the rice MYB family. Plant Mol Biol *60*, 107-124.

Yao, H.Y., and Xue, H.W. (2018). Phosphatidic acid plays key roles regulating plant development and stress responses. J Integr Plant Biol *60*, 851-863.

Yoshida, T., Fujita, Y., Maruyama, K., Mogami, J., Todaka, D., Shinozaki, K., and Yamaguchi-Shinozaki, K. (2015). Four Arabidopsis AREB/ABF transcription factors function predominantly

in gene expression downstream of SnRK2 kinases in abscisic acid signaling in response to osmotic stress. Plant Cell Environ *38*, 35-49.

Yoshida, T., Fujita, Y., Sayama, H., Kidokoro, S., Maruyama, K., Mizoi, J., Shinozaki, K., and Yamaguchi-Shinozaki, K. (2010). AREB1, AREB2, and ABF3 are master transcription factors that cooperatively regulate ABRE-dependent ABA signaling involved in drought stress tolerance and require ABA for full activation. Plant Journal *61*, 672-685.

Yu, D.Y., Rupasinghe, T.W.T., Boughton, B.A., Natera, S.H.A., Hill, C.B., Tarazona, P., Feussner, I., and Roessner, U. (2018). A high-resolution HPLC-QqTOF platform using parallel reaction monitoring for in-depth lipid discovery and rapid profiling. Anal Chim Acta *1026*, 87-100,

Yu, L., Nie, J., Cao, C., Jin, Y., Yan, M., Wang, F., Liu, J., Xiao, Y., Liang, Y., and Zhang, W. (2010). Phosphatidic acid mediates salt stress response by regulation of MPK6 in Arabidopsis thaliana. New Phytol *188*, 762-773.

Yuan, W., Li, Y., Li, L.C., Siao, W., Zhang, Q., Zhang, Y.J., Liu, J.P., Xu, W.F., and Miao, R. (2018). BR-INSENSITIVE1 regulates hydrotropic response by interacting with plasma membrane H+-ATPases in Arabidopsis. Plant Signal Behav *13*.

Zahran, H.H. (1999). Rhizobium-legume symbiosis and nitrogen fixation under severe conditions and in an arid climate. Microbiol Mol Biol Rev *63*, 968-989, table of contents.

Zhang, Y., Wang, C., Xu, H., Shi, X., Zhen, W., Hu, Z., Huang, J., Zheng, Y., Huang, P., Zhang, K.X., *et al.* (2019). HY5 Contributes to Light-Regulated Root System Architecture Under a Root-Covered Culture System. Front Plant Sci *10*, 1490,

Zhang, Y., Zhu, H., Zhang, Q., Li, M., Yan, M., Wang, R., Wang, L., Welti, R., Zhang, W., and Wang, X. (2009). Phospholipase dalpha1 and phosphatidic acid regulate NADPH oxidase activity and production of reactive oxygen species in ABA-mediated stomatal closure in Arabidopsis. Plant Cell *21*, 2357-2377.

Zhang, Y.L., Cheng, Y.T., Qu, N., Zhao, Q.G., Bi, D.L., and Li, X. (2006). Negative regulation of defense responses in Arabidopsis by two NPR1 paralogs. Plant Journal *48*, 647-656.

Zhang, Y.L., Fan, W.H., Kinkema, M., Li, X., and Dong, X.N. (1999). Interaction of NPR1 with basic leucine zipper protein transcription factors that bind sequences required for salicylic acid induction of the PR-1 gene. P Natl Acad Sci USA *96*, 6523-6528.

Zhang, Z., and Hendrickson, W.A. (2010). Structural Characterization of the Predominant Family of Histidine Kinase Sensor Domains. Journal of Molecular Biology *400*, 335-353.

Zhao, J. (2015). Phospholipase D and phosphatidic acid in plant defence response: from protein-protein and lipid-protein interactions to hormone signaling. J Exp Bot *66*, 1721-1736.

Zhao, M., Liu, Q., Zhang, Y., Yang, N., Wu, G.F., Li, Q.X., and Wang, W. (2020). Alleviation of osmotic stress by H2S is related to regulated PLD alpha 1 and suppressed ROS in Arabidopsis thaliana. J Plant Res *133*, 393-407.

References

Zhao, X., Zhao, Q.P., Xu, C.Y., Wang, J., Zhu, J.D., Shang, B.S., and Zhang, X. (2018). Phot2-regulated relocation of NPH3 mediates phototropic response to high-intensity blue light in Arabidopsis thaliana. Journal of Integrative Plant Biology *60*, 562-577.

Zhao, Y., Qi, Z., and Berkowitz, G.A. (2013). Teaching an old hormone new tricks: cytosolic Ca2+ elevation involvement in plant brassinosteroid signal transduction cascades. Plant Physiol *163*, 555-565.

Zheng, Y., Zhan, Q., Shi, T., Liu, J., Zhao, K., and Gao, Y. (2020). The nuclear transporter SAD2 plays a role in calcium- and H2O2-mediated cell death in Arabidopsis. The Plant Journal *101*, 324-333.

Zhou, B., Wang, Y., Zhan, Y., Li, Y., and Kawabata, S. (2013). Chalcone synthase family genes have redundant roles in anthocyanin biosynthesis and in response to blue/UV-A light in turnip (Brassica rapa; Brassicaceae). Am J Bot *100*, 2458-2467.

Zhou, J.M., Trifa, Y., Silva, H., Pontier, D., Lam, E., Shah, J., and Klessig, D.F. (2000). NPR1 differentially interacts with members of the TGA/OBF family of transcription factors that bind an element of the PR-1 gene required for induction by salicylic acid. Mol Plant Microbe In *13*, 191-202.

Zhu, Y., Zuo, M., Liang, Y., Jiang, M., Zhang, J., Scheller, H.V., Tan, M., and Zhang, A. (2013). MAP65-1a positively regulates H2O2 amplification and enhances brassinosteroid-induced antioxidant defence in maize. J Exp Bot *64*, 3787-3802.

Zipfel, C., Robatzek, S., Navarro, L., Oakeley, E.J., Jones, J.D., Felix, G., and Boller, T. (2004). Bacterial disease resistance in Arabidopsis through flagellin perception. Nature *428*, 764-767.

Zoulias, N., Brown, J., Rowe, J., and Casson, S.A. (2019). HY5 is not integral to light mediated stomatal development in Arabidopsis. bioRxiv, 756221.

Zoulias, N., Brown, J., Rowe, J., and Casson, S.A. (2020). HY5 is not integral to light mediated stomatal development in Arabidopsis. PLoS One *15*, e0222480,

Zubo, Y.O., and Schaller, G.E. (2020). Role of the Cytokinin-Activated Type-B Response Regulators in Hormone Crosstalk. Plants (Basel) *9*.

Zuo, Z., Liu, H., Liu, B., Liu, X., and Lin, C. (2011). Blue light-dependent interaction of CRY2 with SPA1 regulates COP1 activity and floral initiation in Arabidopsis. Curr Biol *21*, 841-847.

Zwick, E. (2012). Analysen zur Funktion von PFT1, LAF1 und HY5 in der Lichtsignaltransduktion von *Arabidopsis thaliana* (Freiburg im Breisgau: Albert-Ludwigs-Universität), pp. 140,

6 Appendix

Figure 8-15: AHK1^{ED} ligand specification.
Phosphatidylinositol phosphate (PIP)-strip™ treated with MBP (left) and MBP-AHK1^{ED} (right). PIP strips contain 100 pM of lipid per spot.
First antibody: αMBP 1:4.000, secondary antibody: αmouse-HRP dilution 1:7.000, Detected with horseraddish peroxidase (HRP). Exposure time: 20 s and 3 min 20 sec
Abbreviations: IP3- inositol (1,4,5) triphosphate; PA- phosphatidic acid; LPA- LysoPA acyl transferase; PE- phosphatidylethanolamine; PI- phosphatidylinositol; PI4P- PI 4-phosphate; PI5P- PI 5-phosphate; PI(3,4,5)P_3- PI (3,4-5) trisphosphate; PI(4,5)P_2- PI (4-5) bisphosphate; PITPs- phosphatidylinositol transfer proteins; PS- synthase; PC- phospholipase C; PS- phosphatidylserine

Table 7-8: Results from the third repetition of ligand fishing with the LC-MS. Performed by Dr. Mark Stahl.

Compound	Neutral mass (Da)	m/z	Charge	Retention time (min)	Anova (p)	q Value	Max Fold Change	Highest Mean	Lowest Mean	Max. Abundance	Min.CV%	Normalized abundance MBP-AHK1+AWF 1	2	3	MBP+AWF 1	2	3
Negatively Charged																	
12,02_265,1471m/z		265,147096	1	12,02263333	0,00199079	0,00732248	1,339813177	MBP_AHK1+M	MBP+K	122846,6091	4,34	104710,067	121677,204	118549,366	91228,3957	83400,0784	100439,598
Positively Charged																	
12,49_267,1578m/z		267,157778	1	12,48861667	5,62E-05	5,09E-05	1,783632523	MBP_AHK1+M	MBP+M	1686079,064	3,43	1248353,77	1392776,09	1515128,04	1147762,36	1053856,47	1207368,51
12,17_239,1623m/z		**239,162265**	**1**	12,17405	0,00080262	0,00032477	1,94219756	MBP_AHK1+M	***MBP+M***	924996,8718	8,62	651129,426	726687,158	833776,74	605083,242	510068,18	670576,194
13,99_662,4465n	662,4464528	663,453729	1	13,99061667	0,00322096	0,00082922	2,195603378	MBP_AHK1+M	MBP+K	1815810,929	0,51	1563910,77	1825827,47	1731263,04	848027,076	791357,788	841679,267

	MBP-AHK1+AWF mannitol 1	2	3	MBP+AWF mannitol 1	2	3	Accepted Description	Adducts	Formula	Score	Fragmentation Score	Mass Error (ppm)	Isotope Similarity
98	119506,033	128990,878	120042,916	93705,4775	85221,8635	97149,1296	laurilsulfate	M-H	C12H26O4S	36,4	0	-3,041523955	85,60189115
51	1626931,6	1742419,48	1688886,12	1015965,94	873292,658	946660,308	Dodecyl sulfate	M+H	C12H26O4S	35,1	0	-17,57794146	93,19513986
94	848725,896	918508,463	1007756,26	523283,972	410301,302	495203,781	(S)-3-hydroxylauric acid	M+Na	C12H24O3	39	0	2,303199931	97,65628839
57	1820046,84	1805109,47	1822276,47	689006,179	576065,093	1355615,38	(1R,4S,5S,8R,9R,12S,13S,16S,19S)-19-Methoxy-8-[(2R,4E)-6-methoxy-6-methyl-4-hepten-2-yl]-5,9,17,17-tetramethyl-18-oxapentacyclo[10.5.2.0~1,13~.0~4,12~.0~5,9~]nonadec-2-en-16-yl beta-D-allopyranoside	M+H, M+Na	C38H62O9	54,1	83,4	10,65885744	98,42121513

6.1 Oligonucleotides

6.1.1 Genotyping of *A. thaliana* mutant lines

Genotype	Mutation/(Enzyme)	DNA-sequence
ahk1-3	T-DNA	CATTTTATAATAACGCTGCGGACATCTAC
gene-specific fwd		GACCTCTCTGGTATGACTCGGTATTATA
gene-specific rev		CACATCCAGTATCATCAACCTCAAACCA
ahk1-4	T-DNA	CATTTTATAATAACGCTGCGGACATCTAC
gene-specific fwd		AGGAAGGTGTTCGATAAAATGACTGAATG
gene-specific rev		CAAGTTCTTCTTGAGTTGTTGGCTTGTCA
ahk1-5	T-DNA	AACGTCCGCAATGTGTTATTAAGTTGTC
gene-specific fwd		TATTATTACAAACATATTCCTCTCTATA
gene-specific rev		GATCCCAAATCATAAACAAAGACACATA
ahk1-6	T-DNA	AACGTCCGCAATGTGTTATTAAGTTGTC
gene-specific fwd		TCTGGTATATTCTGTGATTACTCTACAG
gene-specific rev		GTTAAAAGCCCTATCAAAATTGCTAACA
bak1-1	T-DNA	CATTTTATAATAACGCTGCGGACATCTAC
gene-specific fwd		CTATTTGGCGACACTACTTTCTGAC
gene-specific rev		GGTGCTTCAAAGTTGGGATGC
bri1-5	EMS/ (HpyCH4V)	/
gene-specific fwd		TTTCATTTCAAGCTTCACCATCTCAG
gene-specific rev		AGAGATGTTCAACAACTTGAGCTCTG

6.1.2 Oligonucleotides for the detection of T-DNAs in stably transformed *Arabidopsis thaliana* lines

Insert	DNA-sequence (Fwd / Rev)
35S::AHK1-GFP	TATGGAAGTACAGCAAGAATGAT / TTACTTGTACAGCTCGTCCATGC
UBQ10::AHK1-GFP	TATGGAAGTACAGCAAGAATGAT / TTTGTATAGTTCATCCATGCCATGTG

6.2 Vectors provided for this PhD thesis

6.2.1 Entry vectors

Vector (source)	Selection	Purpose
pDONR207 (invitrogen)	Gent	Gateway^{TM}-cloning

6.2.2 Plant and *E. coli* vectors

Vector (source)	Selection (*E. coli* /plants)	Purpose
pB7-AHK1pro-mCherryNLS (Katharina Caesar)	Spec / Basta	test AHK1 promotor

pH7FWG2-AHK1 (Jakub Horak)	Spec / Hyg	35S::AHK1-GFP
pABind-AHK1-GFP	Spec / Hyg	lexA-4635S::AHK1-GFP
pB7-RD29Bpro-NLSmCherry (Manikandan Veerabagu)	Spec / Basta	RD29B::mCherry
pUC57-^{AHK1ED} (GenScript)	Amp	codon-optimized (c.o.) $AHK1^{ED}$
pDONR207-BRI1-S1172A	Gent	Gateway^{TM}-cloning
pDONR207-BRI1-S1172E	Gent	Gateway^{TM}-cloning

E. coli expression vectors (producer)	Selection	Purpose
pMH-HSsumo-$AHK1^{ED}$-6xhis	Amp	*E. coli* expression vector for $AHK1^{ED}$
pETM41-MBP-$AHK1^{ED}$-6xhis	Kan	*E. coli* expression vector for $AHK1^{ED}$

6.2.3 Vectors which have been generated during the Ph.D. thesis

Vector (source)	Selection	Purpose
pABind-BRI1-S1172A	Spec	Gateway^{TM}-cloning
pABind-BRI1-S1172E	Spec	Gateway^{TM}-cloning

Appendix

6.2.4 Vector maps

7 Erklärung

1.21.1- 1.21.2 Experimente wurden von mir an der Universität Freiburg, mithilfe der Geräte und Protokolle der AG Hiltbrunner, durchgeführt. Protokollansprechpartner: Philipp Schwenk.

1.21.3 Experimente wurden von mir durchgeführt, mithilfe der Geräte und Protokolle der AG Markmann. Protokollansprechpartner: Moritz Sexauer.

1.22.2 Massenspektronomie wurde von Dr. Mark Stahl durchgeführt

Eine Erklärung über den Rahmen der gemeinschaftlichen Arbeit, die Namen der Mitarbeiter und deren Anteil an dem Gesamtprojekt und die Bedeutung der eigenen Beiträge für die Gemeinschaftsarbeit.

8 Acknowledgements

I want to thank Prof. K. Harter for the opportunity to work in his group at the ZMBP and doing my PhD as well as for his time, continuous evaluation and support during this time. I am especially thankful for giving me the opportunity to discuss ideas with other scientists at conferences and to visit other laboratories to deepen my studies. Furthermore, I want to thank Prof. W. Schulze also for the PhD position as well as for both time and being my thesis advisors.

I also want to thank Prof. Dr. Claudia Oecking for evaluation and for the best Mett in Tübingen.

In addition, I want to thank Prof. Dr. K. Markmann and Prof. Dr. Andreas Hiltbrunner for their support by helping me with *Lotus japonicus* and light experiments. I also want to thank Prof. Dr. Hiltbrunner, Philipp Schwenk and the entire lab in Freiburg for the kind support and lively discussions. For this, I am also grateful to Üner and Klaus and Bay 6-8 for a great time with funny and extended card games next to your support in the lab.

Special thanks, to Dr. Mark Stahl for executing the mass spectrometry part of my experiments and to our gardeners at the ZMBP for their kind and caring support of my plants.

A big thank you to the ZMBP for a great time in which I learned a lot.

My deepest thank you to Moritz, having my back no matter how. For supporting and criticizing, whatever was needed. For discussing my work and listening to what I liked and what my problems where all the way through. Thank you for your love and encouragement. Thank you also to Gabi, Stefan and Franzi who also supported me in so many ways over the past years. I am also very grateful for Kathi and Pawel who have supported me for so many years. I thank them and Dani, Stefan, Caro, Dori, the „Tübinger“, and „Freiburger“ and “NRWler” for friendship, support and discussions which have always been encouraging. Didi, thank you also for your friendship, time, and criticism as well as your valuable thoughts from outside.

My deepest gratitude is for my father Ulrich and my grandparents Inge and Kurt who gave me the opportunity to study and their full support no matter how different we thought, for Maike, Markus, Fleur und Tessia, as well as Petra, Uwe, Marcel, Wiwi, Daniel and Celina for being my kindest and loveliest family who gave me all their positive support. Thank you, Susanne, for the most valuable support, without it I would have had a harder time to be experienced.

Pocahontas and Ygritte for their furry, fluffy and noisy help.

Acknowledgements